

LOCKHEED MARTIN ENERGY RESEARCH LIBRARIES



3 4456 0509837 3

ORNL/TM-5987

Fig. 103

LWR Fuel Reprocessing and Recycle Program Quarterly Report for Period April 1 to June 30, 1977

B. L. Vondra



OAK RIDGE NATIONAL LABORATORY
CENTRAL RESEARCH LIBRARY
DOCUMENT COLLECTION

LIBRARY LOAN COPY

DO NOT TRANSFER TO ANOTHER PERSON

If you wish someone else to see this
document, send in name with document
and the library will arrange a loan.

UCN-7969
13 3-671

OAK RIDGE NATIONAL LABORATORY

OPERATED BY UNION CARBIDE CORPORATION FOR THE ENERGY RESEARCH AND DEVELOPMENT ADMINISTRATION

This report was prepared as an account of work sponsored by the United States Government. Neither the United States nor the Energy Research and Development Administration/United States Nuclear Regulatory Commission, nor any of their employees, nor any of their contractors, subcontractors, or their employees, makes any warranty, express or implied, or assumes any legal liability or responsibility for the accuracy, completeness or usefulness of any information, apparatus, product or process disclosed, or represents that its use would not infringe privately owned rights.

Contract No. W-7405-eng-26

LWR FUEL REPROCESSING AND RECYCLE PROGRAM
QUARTERLY REPORT FOR PERIOD APRIL 1 TO JUNE 30, 1977

B. L. Vondra, Program Manager

Contributing Authors:

(ORNL)

W. D. Bond	J. C. Mailen
A. A. Brooks	L. Maya
D. O. Campbell	R. H. Rainey
J. H. Goode	H. C. Savage
W. S. Groenier	O. K. Tallent
D. W. Holladay	L. M. Toth
A. D. Kelmers	V. C. A. Vaughen
L. J. King	C. D. Watson
D. C. Kocher	M. E. Whatley
D. A. Lee	

(ORGDP)

J. H. Pashley
M. J. Stephenson

Date Published: August 1977

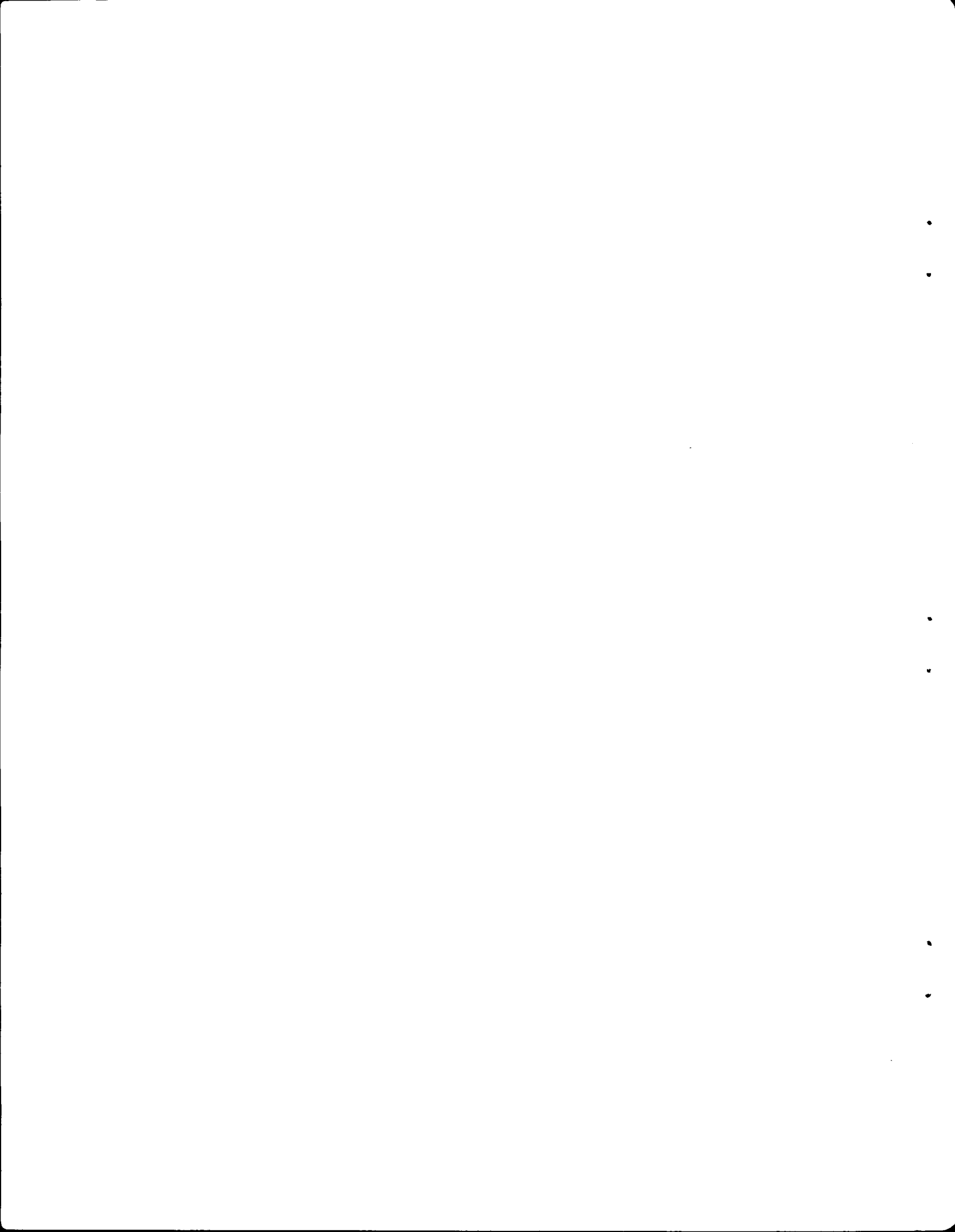
NOTICE This document contains information of a preliminary nature.
It is subject to revision or correction and therefore does not represent a
final report.

OAK RIDGE NATIONAL LABORATORY
Oak Ridge, Tennessee 37830
operated by
UNION CARBIDE CORPORATION
for the
ENERGY RESEARCH AND DEVELOPMENT ADMINISTRATION

LOCKHEED MARTIN ENERGY RESEARCH LIBRARIES



3 4456 0509837 3



CONTENTS

	<u>Page</u>
FOREWORD	ix
SUMMARY	xi
1. ASSISTANCE IN SHEAR DEVELOPMENT AND RELATED PROBLEMS	1-1
2. HEAD-END STUDIES: VOLOXIDATION AND DISSOLUTION	2-1
2.1 Voloxidation	2-1
2.1.1 Dimensional analysis of solid material transport effects in a rotary kiln	2-1
2.1.2 Rotary-kiln heat-transfer studies	2-5
2.1.3 Rotary-kiln, residence-time-distribution studies	2-8
2.1.4 Component development	2-11
2.1.5 Tritium retention from voloxidizer process off-gas	2-13
2.2 Hot-Cell Studies	2-15
2.2.1 Hot-cell dissolution	2-16
2.2.2 Radioactivity in off-gas	2-17
2.2.3 Dissolution residues	2-19
2.2.4 Solution stability	2-23
2.2.5 Solvent extraction	2-27
2.2.6 Waste concentration	2-31
2.2.7 Characterization methods	2-31
2.3 Building 4507 Hot-Cell Operations	2-32
2.3.1 Development of in-cell equipment	2-32
2.3.2 Building 4507 maintenance and improvements	2-33
2.3.3 Miscellaneous	2-33
2.3.4 Voloxidation studies	2-35
2.3.5 Dissolution studies	2-51
3. OFF-GASES - FLUOROCARBON ABSORPTION STUDIES	3-1
3.1 Fluorocarbon Absorption Process Development	3-1
3.1.1 Pilot-plant operation	3-1
3.1.2 Process application	3-5
3.2 Chemical Studies of Contaminants in LWR Off-Gas Processing	3-9
4. PUREX PROCESS STUDIES (SOLVENT EXTRACTION)	4-1
4.1 Laboratory Studies	4-1
4.1.1 Solvent cleanup	4-1
4.1.2 Ruthenium chemistry	4-6
4.1.3 Solvent extraction kinetics	4-16
4.1.4 Plutonium extraction studies	4-19
4.1.5 Analytical chemistry development	4-19
4.2 Cold Studies	4-20
4.2.1 Flowsheet studies using mixer-settlers	4-20
4.2.2 Batch countercurrent extractions	4-37
4.2.3 Component tests	4-39
4.3 Solvent Extraction Flowsheet Test Facility	4-43

	<u>Page</u>
5. URANIUM HEXAFLUORIDE CONVERSION	5-1
6. RADIOLOGICAL TECHNIQUES FOR ENVIRONMENTAL IMPACT ASSESSMENTS OF THE LWR FUEL CYCLE	6-1
7. CO ₂ REMOVAL FROM SIMULATED LWR FUEL REPROCESSING OFF-GAS	7-1
7.1 Introduction	7-1
7.2 Studies with 1068 ppm CO ₂ Feed	7-1
7.3 CO ₂ Removal from Air with the 27.3-cm-ID Contactor	7-2
7.4 Molecular Sieve Studies	7-2
7.5 CO ₂ Sorption with Solid Ba(OH) ₂ ·8H ₂ O	7-3
7.6 Analytical	7-5
8. LWR SUPPORT/STANDARD DATA INTERCHANGE FORMATS	8-1

LIST OF TABLES

	<u>Page</u>
Table 2.1. Dimensions of variables from the general case	2-3
Table 2.2. Configuration and conditions of RTD tests	2-10
Table 2.3. Tritium distribution during dissolution	2-18
Table 2.4. Carbon-14 distribution during dissolution	2-21
Table 2.5. Iodine-129 distribution during dissolution	2-22
Table 2.6. Material balance on voloxidation of UO ₂ (31,000 MWd/ton) (H. B. Robinson-2 reactor, rod G-10, assembly B05)	2-36
Table 2.7. Distribution of selected fission products remaining in the volox burner and off-gas system following voloxi- dation of H. B. Robinson fuel in air at 480°C (LWR-1)	2-47
Table 2.8. Fission product recoveries in the voloxidizer system following voloxidation of H. B. Robinson fuel in air at 480°C (LWR-1)	2-50
Table 2.9. Material balance on dissolution of UO ₂ or U ₃ O ₈ (H. B. Robinson-2 reactor, Zr-4 cladding, UO ₂ at about 31,000 MWd/ton)	2-54
Table 2.10. Uranium and plutonium dissolved in successive leaches	2-55
Table 2.11. Isotopic analyses of fuel solutions from H. B. Robinson rod No. G-10, Assembly B05	2-57
Table 2.12. Effect of dissolvent on amount of uranium and plutonium found in/on irradiated cladding	2-58
Table 2.13. Comparison of experimentally determined fission product content with calculated values (H. B. Robinson-2, rod G-10, assembly B05)	2-59
Table 2.14. Distribution of selected fission products during dissolution of H. B. Robinson-2 fuel in nitric acid (not oxidized)	2-61
Table 2.15. Distribution of selected fission products during dissolution of voloxidized H. B. Robinson-2 fuel in nitric acid	2-62
Table 2.16. Dissolution of fission products from cladding	2-65

	<u>Page</u>
Table 4.1. Ruthenium distribution (percent)	4-9
Table 4.2. Flowsheet conditions for Purex experiments in 16-stage mixer-settlers	4-21
Table 4.3. Operating parameters for Purex experimental runs in 16-stage mixer-settlers	4-23
Table 4.4. Operating conditions and uranium analyses of product and waste streams for Purex experimental runs in 16-stage mixer-settlers	4-27
Table 4.5. Uranium material balance and estimated overall stage efficiencies for Purex experimental runs in 16-stage mixer-settlers	4-30
Table 4.6. Batch countercurrent extraction of plutonium (feed:scrub:extractant = 1:0.66:3.33)	4-37
Table 4.7. Filtration of synthetic feed solution with a 1- μ m, pore-size, etched-disc filter and a 1- μ m Millipore filter	4-41
Table 7.1. Removal of CO ₂ from air in the 27.3-cm-ID stirred tank contactor-detection by gas chromatography	7-4

LIST OF FIGURES

<u>Figure</u>		<u>Page</u>
2.1	Effect of dispersion on the temperature profile in the cooling zone of a voloxidizer.	2-6
2.2	Filtered dissolver residue - 9D6 F.	2-24
2.3	Filtered dissolver residue -9D6 F.	2-25
2.4	Silica gel and type 4A molecular sieve tritium traps.	2-34
2.5	Voloxidation off-gas control and monitoring system, Building 4507.	2-38
2.6	Rotary voloxidizer and deposition tubing inserts.	2-39
2.7	Release of ^{85}Kr and oxygen consumption during voloxidation of H. B. Robinson Zircaloy-clad UO_2 (rod G-10) in air at 480°C (run LWR-1).	2-41
2.8	Release of ^{85}Kr and oxygen consumption during voloxidation of H. B. Robinson Zircaloy-clad UO_2 (rod G-10) in air at 480°C (run LWR-2).	2-42
2.9	Conversion of Zircaloy-clad UO_2 to U_3O_8 during voloxidation in air at 480°C (run LWR-2).	2-43
2.10	Release of tritium and oxygen consumption during voloxidation of Zircaloy-clad UO_2 in air at 480°C (run LWR-2).	2-45
2.11	Fission product deposition from voloxidizer off-gas (run LWR-2).	2-48
2.12	Zircaloy-clad UO_2 before and after voloxidation.	2-52
3.1	Fractionator column concentration profile during internal column concentration test.	3-3
3.2	Schematic of the fluorocarbon process based on a combination absorber-fractionator-stripper column.	3-6
3.3	Required control instrumentation for combination column.	3-8
3.4	CO_2 distribution coefficients.	3-10
3.5	Mole fraction of I_2 in R-12.	3-12

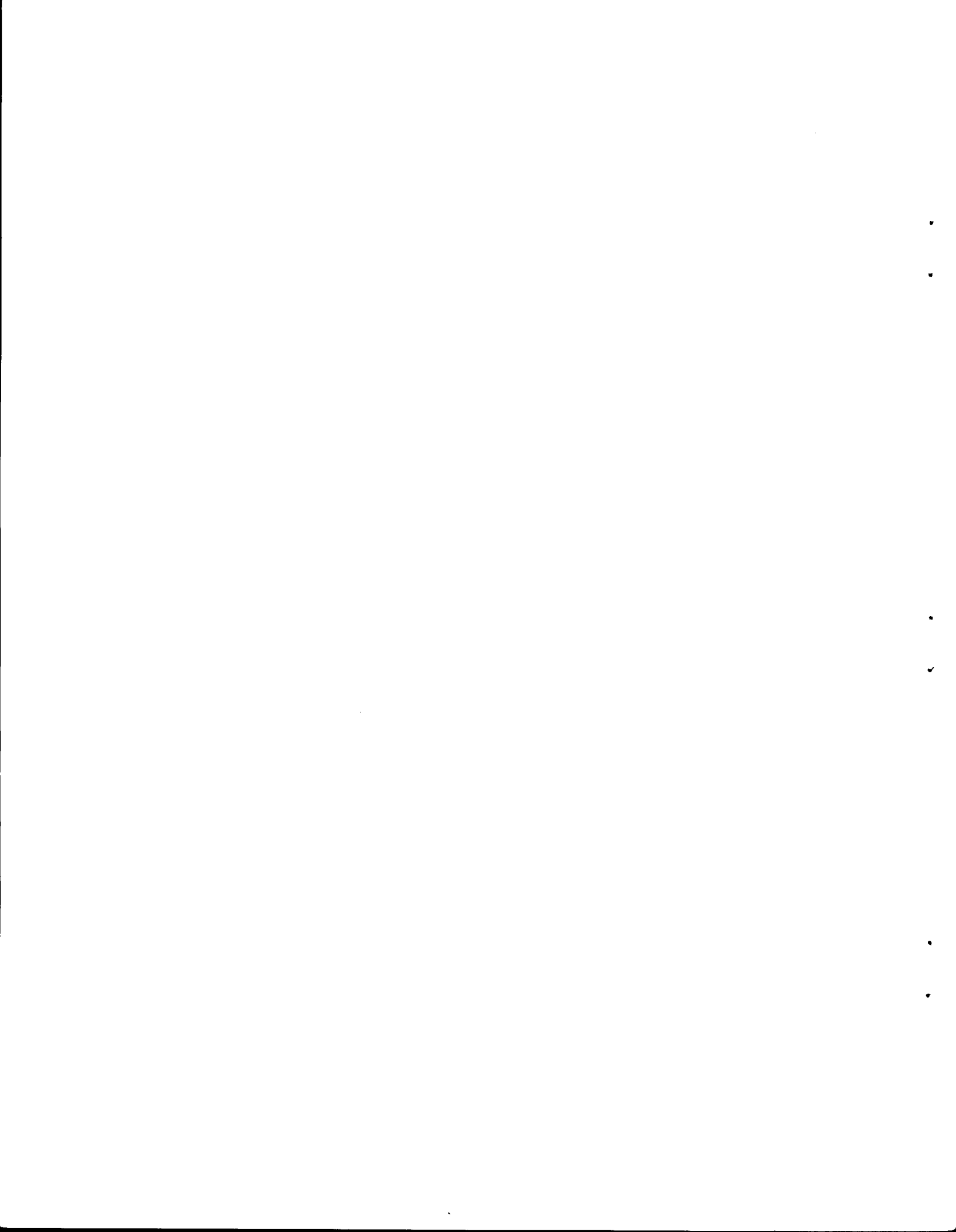
<u>Figure</u>	<u>Page</u>
4.1 Degradation of A-29 macroreticular resin in 30% TBP-70% dodecane: (a) original, (b) unstirred 5 hr, (c) stirred 1 hr, and (d) stirred 5 hr.	4-3
4.2 Effect of A-29 macroreticular resin on 30% TBP-70% dodecane IR spectra: (a) uncontacted solvent, (b) after 5-hr contact with unstirred resin, (c) after 5-hr contact with stirred resin.	4-5
4.3 Ruthenium species in nitric acid and their conversions.	4-7
4.4 Kinetics of the photodecomposition of $\text{RuNO}(\text{NO}_3)_x$ by uv light.	4-11
4.5 Flowsheet for experimental Purex runs in 16-stage mixer-settlers.	4-22
4.6 Operating regions of mixer-settlers.	4-23
4.7 Agitators used in experimental Purex runs.	4-25
4.8 End-stream uranium concentrations vs operating time during run 1.	4-29
4.9 McCabe-Thiele diagram for extraction (stages 25 through 32) section, A bank, Purex experimental run 3.	4-32
4.10 McCabe-Thiele diagram for stripping (stages 1 through 16) in C bank, Purex experimental run 1.	4-33
4.11 Experimentally determined operating parameters of mixer-settlers.	4-35
4.12 Uranium concentrations in the aqueous and organic phases in the stripping bowls with solid- and split-bladed agitators.	4-36
4.13 Distribution of plutonium in batch countercurrent extraction run X, Table 4.6.	4-38

FOREWORD

Eight tasks under the Light-Water Reactor (LWR) Fuel Reprocessing and Recycle Program have been assigned to UCC-ND, with major efforts centered at the Oak Ridge National Laboratory. Because of the close relationship of the reprocessing activities with the ongoing Advanced Fuel Recycle (AFR) Program at ORNL, these tasks are managed within a combined AFR/LWR Program under the direction of W. D. Burch. B. L. Vondra, as LWR Program Manager, is coordinating all activities reported here. The responsibility for the coordination and collation of reports of all work at Oak Ridge was assigned to ORNL by Savannah River Operations-Savannah River Laboratory (SRO/SRL), the office designated as the lead organization for the LWR Fuel Recycle Program.

Projects for which budget and work plans have been established are as follows:

- F-OR-02-001 SRO/LWR: Assistance in Shear Development and Related Problems
- F-OR-02-002 SRO/LWR: Head-End Studies: Voloxidation and Dissolution
- F-OR-02-003 SRO/LWR: Off-Gases Fluorocarbon Absorption Studies
- F-OR-02-004 SRO/LWR: Purex Process Studies (Solvent Extraction)
- F-OR-02-006 SRO/LWR: Uranium Hexafluoride Conversion
- F-OR-02-008 SRO/LWR: Radiological Techniques for Environmental Assessments of the LWR Fuel Cycle
- F-OR-02-009 SRO/LWR: Off-Gases - The Experimental Investigation of the Fixation of ^{14}C
- F-OR-02-010 SRO/LWR: LWR Support/Standard Data Interchange Formats



SUMMARY

This is the sixth quarterly report issued on the LWR Fuel Reprocessing and Recycle Program at ORNL as part of the national program administered by Savannah River Operations—Savannah River Laboratory.

Experimental and modeling studies on the applicability of rotary kilns to the voloxidation process continued. Efforts are directed toward residence-time-distribution and heat-transfer studies, toward the procurement of a 0.5-ton/day unit for study and testing, and toward the evaluation of a process for isolating tritium as water from the process off-gas.

In tests with irradiated LWR fuel samples, the time required to achieve essentially complete dissolution of uranium and plutonium from sheared fuel rods was greatly increased when the length of the fuel segments was increased from 2 to 4.5 in. Photos of the dissolver residues showed that particle sizes extend down to much less than 1 μ . The clarified dissolver solution is subject to postprecipitation of noble metals, which extends for about three weeks. Solvent extraction tests with 30% tributyl phosphate (TBP) again showed no apparent presence of significant unextractable plutonium (>99.99% recovery).

Several voloxidation runs were made with H. B. Robinson reactor fuel. Volatilization of tritium from the fuel in 4 hr at 480°C was in the range of 97 to more than 99%. In subsequent dissolution tests, the weight of the residue was about a factor of 3 higher for voloxidized samples than for a sample that was not given the voloxidation treatment. Also, losses of uranium and plutonium to the residues were higher [although still low (<0.04%)] for the voloxidized samples.

Pilot-plant tests and studies of the krypton absorption system have revealed a possible practical application of the fractionator pinch-point phenomenon, which enables the three operations of absorption, fractionation, and stripping to occur in a single unit. The success of such a process simplification will depend upon effective process instrumentation and control; one possible control method was identified.

Macroreticular resins, which have been considered for solvent cleanup, were found to be degraded by exposure to 30% TBP-normal dodecane.

A photolytic method was discovered for converting extractable ruthenium species to inextractable forms.

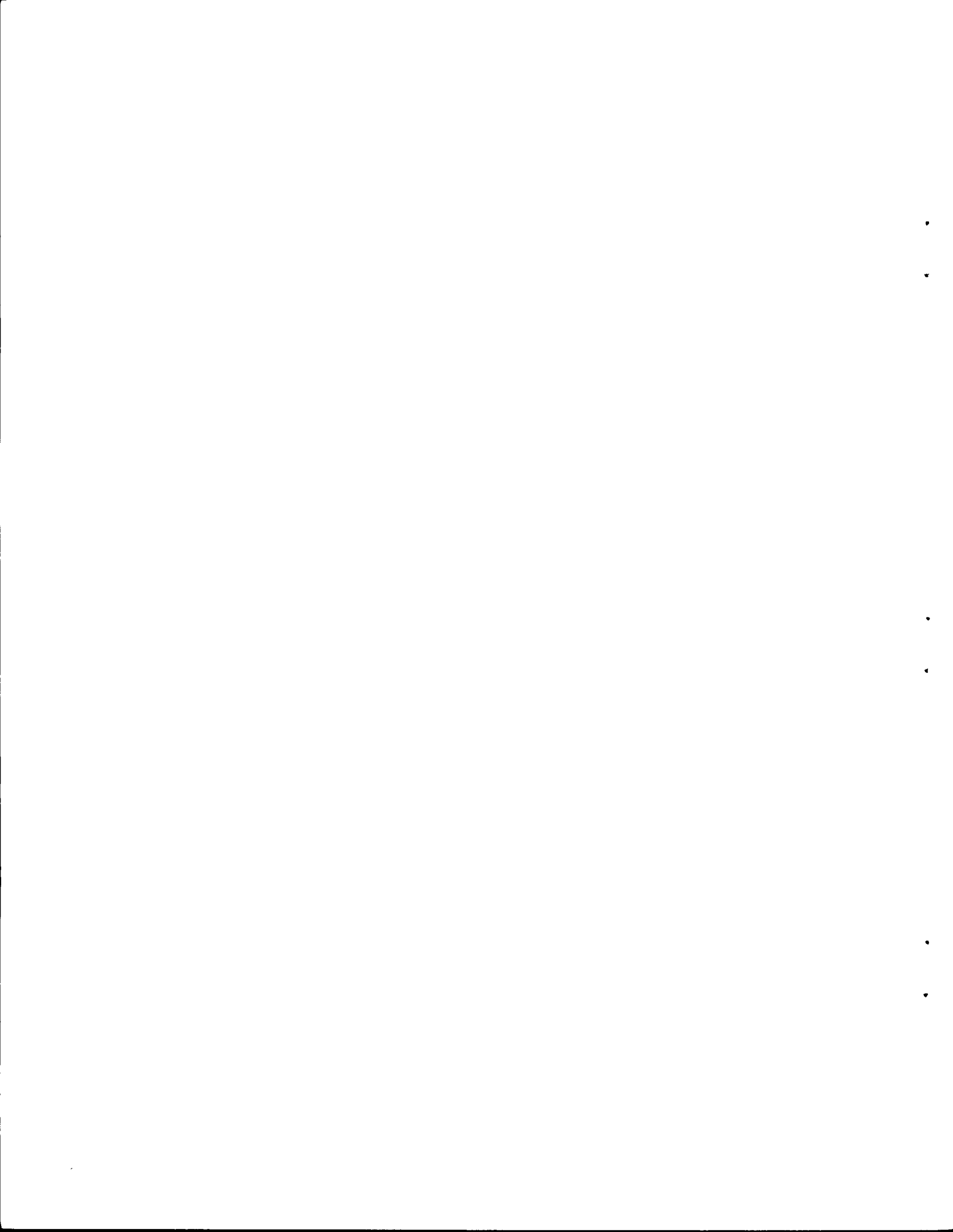
The fission products zirconium, niobium, cerium, and ruthenium were found to transfer more slowly than uranium from the aqueous to the organic phase but more rapidly than uranium from the organic to the aqueous phase.

A series of cold runs of uranium extraction and stripping in mixer-settler banks was made to define suitable operating parameters for these units.

Work was authorized and is in progress for equipment and instrumentation design, fabrication, and installation of the Solvent Extraction Flowsheet Facility at the Transuranium Processing Plant. Design of the facility is about 50% complete.

A modification of the computer code for calculating the effects of building structures on internal dose from inhaled radionuclides and external photon dose from airborne and surface-deposited radionuclides was completed.

In studies of $^{14}\text{CO}_2$ removal from air, decontamination factors higher than 100 were obtained with a molecular sieve bed and with beds of solid $\text{Ba}(\text{OH})_2 \cdot 8\text{H}_2\text{O}$.



1. ASSISTANCE IN SHEAR DEVELOPMENT AND RELATED PROBLEMS

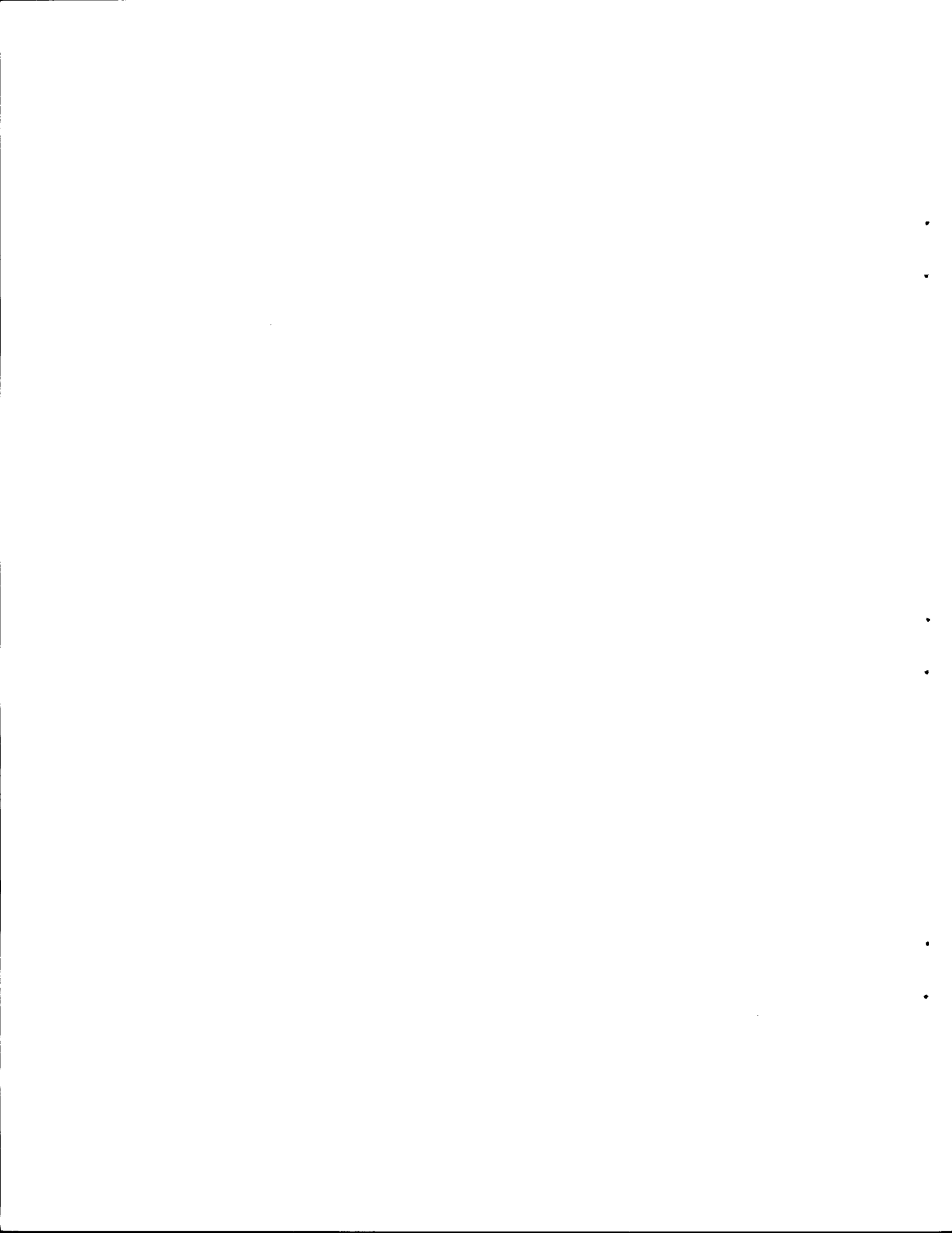
C. D. Watson (Chemical Technology Division, ORNL)

Westinghouse (Waltz Mill, Pennsylvania) completed the loading of 173⁴ Zr-4 reject tubing sections (12.5 ft long) with Steatite. These dummy fuel rods are to be shipped to Columbia, South Carolina, for final assembly into grids consisting of six 17 x 17 dummy pressurized water reactor (PWR) fuel assemblies.

Some old LWR shear tooling has been reworked in the ORNL machine shops and is being installed in the ORNL 250-ton shear for tests with the in-house fabricated 17 x 17 dummy PWR assembly.

It has been reported that a commercial shredding device has been used successfully to break up a dummy PWR assembly into short pieces, in a manner similar to the shearing method. However, recent highly unsuccessful tests with a shredder in which LMFBR fuels were used has raised serious doubts concerning its applicability because of tube closure, high holdup in the machine, and the production of metallic fines. A joint ORNL/SRL/SRP test using dummy PWR fuel is being planned to further evaluate this machine.

Recently, some cutting tests using electric-arc saws were made at Retech, Inc., Upland, California, with dummy LMFBR assembly sections. For comparison, four plunge cuts (two in water and two in air) were made on an unfilled dummy PWR (17 x 17 array). The cuts were made in a matter of seconds; the underwater cuts were very clean and shiny, compared with severe oxidation in the first air cut and ignition of the bundle in the second cut. It is apparent that Zircaloy can only be sawed by electric arc while safely submerged in a water spray or in an argon atmosphere.



2. HEAD-END STUDIES: VOLOXIDATION AND DISSOLUTION

2.1 Voloxidation

M. E. Whatley (Chemical Technology Division, ORNL)

The voloxidation process is being developed as a head-end method for removing tritium from fuel prior to aqueous processing. Based on experimental work, it appears that this objective can be met by reacting the oxide fuel with oxygen or air in a temperature range of 450 to 650°C. The release of tritium and, to a lesser extent, some of the other fission products occurs when UO_2 is restructured during oxidation to U_3O_8 . The early removal of tritium from the fuel into a relatively small volume is desirable to avoid mixing the tritium as water with aqueous streams in subsequent process steps.

During this report period, the investigation of the applicability of rotary kilns to the voloxidation process was continued by performing tests that extend residence-time-distribution (RTD) studies to include variations in flight design. Modeling studies of rotary-kiln RTD and heat transfer were continued. Efforts to procure a larger-scale voloxidizer for study and testing are also described in this report.

2.1.1 Dimensional analysis of solid material transport effects in a rotary kiln

M. E. Whatley (Chemical Technology Division, ORNL)

To organize the data being obtained in the experimental program to measure the dispersion coefficient for material in rotating kilns, a dimensional analysis was performed using all of the variables now thought to be relevant.¹ The incentive for this study was to provide insight into

the performance of rotary kilns as applied to the voloxidation process. In the analysis of the system as a chemical reactor and in the analysis of heat transfer to solids, the dispersion coefficient is an important term. This coefficient is a steady-state property of the system - a function of system design and operating variables - and although it is probably not a function of position, it is defined at any point along the length of the kiln.

The task of explaining or correlating the dispersion coefficient as a steady-state system property is not to be confused with the task of measuring it. The most convenient method for measuring the dispersion coefficient is a transient method requiring concentration data on the effluent stream from an operating kiln subjected to an input change. It was expected, therefore, that different dimensionless groups would be indicated. In addition to identifying the important dimensionless groups, dimensional analysis also identifies the degrees of freedom in an experimental system. Dimensional analysis yields sets of dimensionless groups, each set being sufficient to express all functional relationships.

Solids transport in a rotary kiln was analyzed by the Buckingham Pi method using a computer program. The dimensions included were mass (M), length (L), and time (T). The variables are discussed below:

- Diameter refers to the inside diameter of the kiln and is used as the reference length variable where possible.
- Length refers to the length of the kiln in which solids are found.
- Flight size is twice the protrusion of a flight inside the kiln (to properly relate to kiln diameter). Flights are assumed as parallel with

the axis of the kiln and simple in structure. The number of flights is itself a dimensionless number that should be considered.

- Feed size is a characteristic dimension of the feed particles. The feed actually has a size distribution that could be important, but for simple analysis a single number could be used.
- Feed rate is the mass rate of feed to the kiln, which is the rate of mass progression through the kiln at steady state.
- Rotation is the revolutions of the kiln per unit time.
- Velocity is the linear rate of progression of material through the kiln.
- Bulk density is the mass-per-unit volume of settled solids in the kiln.
- Holdup is the mass of solids per unit of length of kiln.
- Dispersion refers to the dispersion coefficient used to characterize axial mixing.

Since this is a steady-state analysis, time is not a variable. The operating slope of the kiln is a dimensionless group in itself. The variables and their dimensions are summarized in Table 2.1

Table 2.1. Dimensions of variables from the general case

Variable	Mass	Length	Time
Diameter	0	1	0
Length	0	1	0
Holdup	1	-1	0
Feed rate	1	0	-1
Rotation	0	0	-1
Feed size	0	1	0
Dispersion	0	2	-1
Velocity	0	1	-1
Bulk density	1	-3	0
Flight size	0	1	0

By simple inspection, it is possible to identify the set of dimensionless groups (in addition to the kiln operating slope and the number of flights) comprised of ratios of variables with length as the only dimension. Beyond these dimensionless groups, many other groups were found, among which the most interesting were:

$$\text{Dispersion number} = \frac{\text{Dispersion coefficient}}{(\text{Kiln length}) (\text{Velocity})} \quad (2.1)$$

$$\text{Modified dispersion number} = \frac{\text{Dispersion coefficient}}{(\text{Kiln diameter}) (\text{Velocity})} \quad (2.2)$$

$$\text{Watt number} = \frac{\text{Dispersion coefficient}}{(\text{Rotation rate}) (\text{Diameter})^2} \quad (2.3)$$

$$\text{Velocity number} = \frac{\text{Velocity}}{(\text{Rotation rate}) (\text{Diameter})} \quad (2.4)$$

$$\text{Holdup number} = \frac{\text{Holdup}}{(\text{Density}) (\text{Diameter})^2} \quad (2.5)$$

$$\text{Flow identity} = \frac{(\text{Holdup}) (\text{Velocity})}{\text{Feed rate}} \quad (2.6)$$

The last of this group can be ignored since it is simply a statement of a mass balance and is always unity. The analysis indicated that a set sufficient for correlation would consist of the holdup number, the velocity number, and one of the remaining three. The dispersion number, so useful in interpreting transient data, is of no use in this analysis since it involves the kiln length. Either the modified dispersion number or the Watt number would satisfy the theoretical criteria and serve as an expression for the dispersion coefficient; however, the modified dispersion number uses the velocity number, which is a second dependent variable, whereas the Watt number uses only independent variables as additional factors.

Without destroying the elegance of the treatment, the holdup number can be modified by multiplying by $4/\pi$ to convert it to fraction full, and the velocity number can be combined with the operating slope to convert it to a dimensionless number (UNUM) previously used in the program,

$$\text{UNUM} = \frac{\text{Velocity}}{2\pi (\text{Rotation rate}) (\text{Diameter}) (\text{Slope})} \cdot \quad (2.7)$$

It is possible to conclude from this study that the Watt number can be expressed as a function of UNUM, the fraction full, and the set of dimensionless groups that define the feed size and the geometrical configuration of the kiln. Even this simple statement may be further simplified. There is some experimental evidence that the Watt number and UNUM are in fact independent, and the fraction full imposes only second-order effects.

2.1.2 Rotary-kiln heat-transfer studies

B. B. Spencer and M. E. Whatley (Chemical Technology Division, ORNL)

Heat-transfer studies were continued using a computer model to predict the temperature profile in a rotary kiln. Parametric studies were performed to determine the effect of the dispersion of flowing sheared prototype fuel on the temperature profile in the cooling zone of a voloxidizer. This effect is shown in Fig. 2.1 as the Watt number (N_{WAT}), a measure of the extent of dispersion (dispersion increases as the Watt number increases). For the case shown in Fig. 2.1, all variables except N_{WAT} were held constant. These variables and their values are as follows:

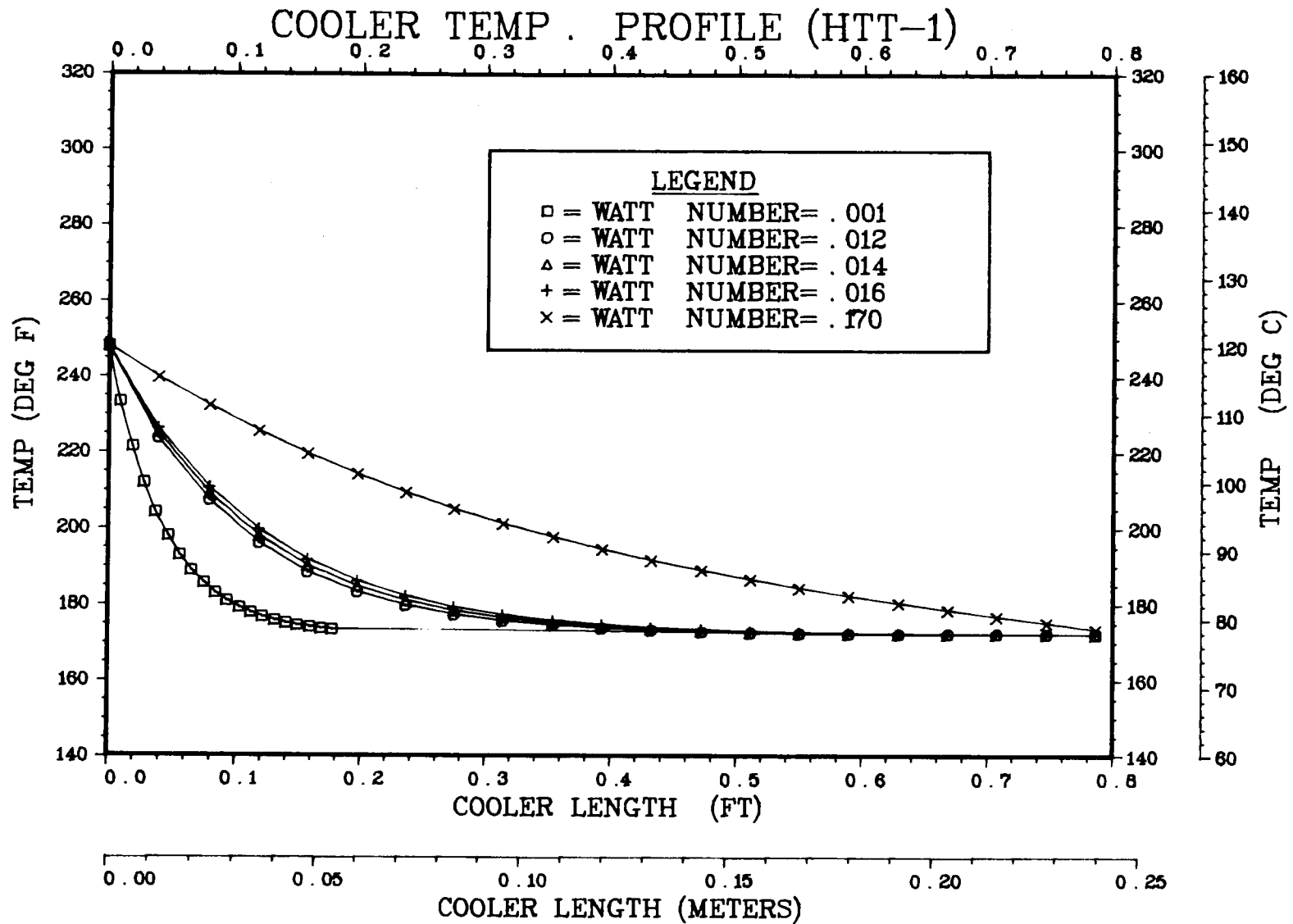


Fig. 2.1. Effect of dispersion on the temperature profile in the cooling zone of a voloxidizer.

radius of kiln = 0.267 ft	(0.0814 m)
kiln wall temperature = 172°F	(77.78°C)
feed temperature = 248°F	(120.0°C)
kiln slope = 0.00521 ft/ft	(0.00521 m/m)
cooler length = 0.786 ft	(0.2396 m)
rotational rate = 8.0 rpm	(0.8378 rad/sec)
feed rate = 11.57 lb/hr	(0.00146 kg/sec)
heat capacity of prototype fuel = 0.20 Btu lb ⁻¹ °F ⁻¹	(837.4 J kg ⁻¹ °C ⁻¹)
density of prototype fuel = 92.7 lb/ft ³	(1485 kg/m ³)
thermal conductivity of prototype fuel = 0.20 Btu ft ⁻¹ hr ⁻¹ °F ⁻¹	(0.328 x 10 ⁻³ W m ⁻¹ °C ⁻¹)
emissivity of prototype fuel (estimate) = 0.80	
decay and reaction heat generation rate = 0 Btu ft ⁻³ hr ⁻¹	(0 W m ⁻³ hr ⁻¹)

The effects of the gas phase in the voloxidizer were neglected.

The temperature of the solids is seen to rapidly approach the kiln wall temperature for small values of N_{WAT} and flow rate. For values of N_{WAT} approaching zero, the solids temperature approaches the plug-flow solution. As the value of N_{WAT} increases, there is more axial mixing, and the bed temperature approaches the wall temperature less rapidly. Information from RTD studies² indicates that the Watt number is in the range of 0.012 to 0.016.

The Watt number is a dimensionless number used to correlate the dispersion coefficient for geometrically similar kilns and is a constant

for such a set of kilns. The definition of the Watt number and its relation to the dispersion coefficient and dispersion number is discussed in Sect. 2.1.1.

Infrared pyrometers have been obtained for test and evaluation in the voloxidizer development program. They will be used to obtain new temperature data for comparison with the computer model. A periscope is being fabricated to be used with the pyrometers to view specific points within the operating kiln.

A second type of temperature measurement system has been ordered. This system, which will be evaluated for kiln-temperature measurements, features thermocouples and the use of telemetry to transmit the resultant signals to a receiver coupled to a console recorder. The telemetry device will handle up to 15 thermocouple signals concurrently.

Heat-transfer tests will be continued next quarter to determine the emissivity of sheared prototype fuel and to obtain temperature profiles of the operating kiln.

2.1.3 Rotary-kiln, residence-time-distribution studies

T. D. Welch (Chemical Technology Division, ORNL)

The influence of kiln diameter, slope, feed rate, and feed size on the RTD of rotary kilns has been determined. The effects of varying the flight configuration are now under study. Initial runs with a smaller flight-width-to-diameter ratio show a definite decrease in the RTD spread.

The RTD of the process material in the kiln is necessary to accurately predict kiln performance for design purposes. All particles do not have

the same residence time. The amount of tritium removed from sheared fuel by the voloxidation process will depend upon the RTD in the kiln, as well as the reaction rate.

The experimental equipment and method have been described previously.³ New flights have been installed in the 0.4572-m-diam unit with a width-to-diameter ratio of 1:18 replacing the 1:6 flights. A summary of the kiln configurations and operating conditions used thus far is presented in Table 2.2.

The effect of diameter, slope, and rotational rate was discussed in a previous report.² Recent work has included six runs using a 0.305-m-diam kiln to further study the effect of diameter, and also the initiation of tests with a 0.457-m-diam kiln with small (0.0254-m) flights. These latest runs have been carried out at slopes more characteristic of a real system, namely, 0.005 m/m. The small flight tests have involved feeds of both sheared hulls and fines.

Initial data indicate that the dispersion number decreases with flight size. For example, at a slope of 0.021 m/m, a rotational rate of 4 rpm, and a feed rate of 0.9 kg/min of sheared prototype fuel, the larger flight design produced a dispersion number $(D/uL)^*$ of 0.018. For the smaller flight design, the dispersion number was 0.014 in runs made under similar operating conditions. For all conditions tested to date, the dispersion number has been in the range of 0.001 for fines in a 0.152-m kiln to 0.03 for sheared hulls in a 0.457-m kiln.

*D = dispersion coefficient, m^2/min .

u = particle linear velocity, m/min.

L = kiln length, m.

Table 2.2. Configuration and conditions of RTD tests

Diameter (m)	Length (m)	Ratio of flight width to diameter	Number of flights	Rotation rate (rpm)	Slope (m/m)	Feed rate (kg/min)
0.152	2.134	1:6	6	2-8	0.0208-0.005	0.1-0.2
0.305	2.134	1:6	6	2-4	0.0208-0.005	0.4-0.8
0.457	2.134	1:6-1:18	6	0.66-4	0.0208-0.005	0.3-4.0

2.1.4 Component development

M. E. Whatley (Chemical Technology Division, ORNL)

A rotary-kiln voloxidizer is being purchased for study and testing from C. E. Raymond/Bartlett-Snow, who is the principal manufacturer of small experimental kilns in the United States. This unit is sized to handle 0.5 metric ton of fuel per day and will be sufficiently flexible, both in construction and in heating capability, to provide the latitude in operation and in modification necessary for development. This unit will not be prototypical, in that it will not be remotely maintainable and will have some features that are not compatible with the operation in a radiochemical plant. Insofar as possible, however, the major mechanical features, the materials of construction, and the lubricants will conform to radiochemical plant requirements.

Layout design drawings were received from the vendor for review and comment. These showed the drum to be 18 in. in diameter by 24 ft, 8 in. long. All major components of the unit, including the drum, end breeching sections, seals, rollers, gears, and structural features, were acceptable. The changes requested were primarily concerned with details in design and were easily resolved. An exception was the design of the flight cartridge, which was deferred until we can provide the vendor with drawings that more clearly indicate what is desired. The unit design provides for changing and replacing the flight cartridge during the development work; hence, the cartridge supplied with the kiln is only the first of a series.

We intend to use this unit to obtain certain necessary process performance information on full-scale equipment, such as solids progression,

axial mixing, and heat transfer. The performance of the nonconforming mechanical features will provide a point of departure for the development of suitable designs.

The auxiliaries for this unit are being provided by ORNL. These include a feeding station, solids sampling stations both before and after the kiln, isolation valves before and after the kiln, a filter assembly, and a product receiving station. In order to provide feed to the voloxidizer with the proper distribution of hulls, powder, and shroud pieces, the feeding station will screen large batches into three fractions and will meter each fraction separately. The isolation valves to control the gas flow through the solids transfer lines will not be prototypical since these valves are being developed under another task. We will use less-expensive, commercially available valves as stand-ins. The solids sampling stations will be used only in the development program and will be of simple design. The filter assembly is being developed for pilot-plant use and is innovative in principle. Filter cartridges will be inserted in a manifold structure such that seals are effected by an interference fit. After several blow-back cycles when the filter medium loses porosity, new cartridges can be inserted in such a way that the old cartridges are displaced into the voloxidizer and then proceed with the fuel into the dissolver. A test unit embodying this principle has been fabricated and is being studied. The design for the auxiliaries is proceeding on schedule, so that when the kiln is delivered the site will be prepared and installation should go smoothly.

2.1.5 Tritium retention from voloxidizer process off-gas

W. D. Holland (Tennessee Technological University)

The purpose of this activity is to determine the effect of iodine on the operation of a water vapor removal system for the treatment of voloxidizer off-gases. A series of experiments will be conducted on a small-scale molecular sieve drying system operated at conditions expected to prevail in a full-scale voloxidizer off-gas drying system in a 5-ton/day reprocessing plant. A 2-in.-diam by 30-in.-long bed of 1/16-in.-diam molecular sieve pellets will be used to remove the water vapor from an air stream containing iodine vapor.

Experiments are planned to determine (1) the amount of iodine retained in the drying bed during the drying cycle, (2) the effect of retained iodine on bed performance, (3) the effect of absorbed iodine on regeneration characteristics of the bed, and (4) the behavior of iodine in the regeneration gas condenser.

The system will be operated through enough drying and bed regeneration cycles to obtain a reasonable estimate of long-term system performance. Nonradioactive water vapor and iodine will be used in place of titrated water and radioactive iodine, which will be present in the full-scale reprocessing system.

The system consists of:

1. An inlet-gas makeup section including a humidifier, an iodine vapor generator, and a heater to supply 1.75 cfm to the molecular sieve bed containing 0.01 g/liter of water vapor and 0.0015 g/liter of iodine vapor. For a drying cycle time of 3.2 hr, water and iodine input per cycle should be 106 g and 14.3 g respectively.

2. A 2-in.-diam by 30-in.-long bed of Linde 3A molecular sieves equipped with electrical heaters and cooling coil.
3. A regeneration gas condenser and condensate receiver designed to cool the regeneration gas to about 0°C.
4. Auxiliary systems to provide 300°C dry air for bed regeneration and cooling fluid for the condenser.
5. Sampling devices and instrumentation, including an aluminum oxide hygrometer for dew-point measurements, thermocouples at various key locations, and flowmeters.

The design is based on a bed loading of 10% water and a 20% iodine retention. The chiller-condenser should receive about 2.8 g of iodine during the regeneration cycle. Outlet-gas dew points are expected to vary from -80°F to -40°F during a run; these values are within the range of the available instrument.

Progress to date includes the complete installation and checkout of experiment components and the performance of preliminary runs. A corrosion problem developed with the hygrometer probes when exposed to iodine and water vapor; new Teflon-coated probes are now on order. Modifications are being made to protect these probes during periods when actual runs are not being conducted. A "validator" is being purchased to check probe calibration on a periodic basis.

This work is being performed by subcontract (UCNC No. 7164) and is scheduled for completion in November 1977.

2.2 Hot-Cell Studies

D. O. Campbell, S. R. Buxton, and W. L. Pattison
(Chemical Technology Division, ORNL)

An experimental program centered around hot-cell tests of fuel reprocessing operations was initiated in January 1976. Although a variety of LWR fuels will be used as they can be acquired, most work to date has been done with fully irradiated PWR fuel cooled two to three years. The work is supported by "cold" experiments with synthetic process solutions that are similar in chemical composition to true process solutions.

Two fuel dissolutions were carried out during the report period, and experimental work on run 9 was largely completed. Run 10 was made with clad first-cycle fuel from the Oconee-1 reactor, operated by Duke Power Company. Run 11 was made with clad Robinson reactor fuel cut into much longer lengths than for prior runs.

Two areas of investigation have received primary attention, namely (1) solutions stability, clarification, and study of solids, and (2) solvent extraction and stripping from representative process solutions. Other studies have continued with less emphasis, including the distribution of ^3H , ^{14}C , and ^{129}I during dissolution, radioactivity associated with cladding, and acid loss during air sparging of waste solutions.

Excellent photos were obtained for the dissolver residue, which indicate that particle sizes must extend down to much less than $0.1\ \mu$. No defined particles or interstitial voids could be observed even at 3000X.

Additional tests support the observation that there is postprecipitation of noble metals, in addition to the noble metal fraction that is initially insoluble when the fuel is dissolved. This precipitate appears slowly for about three weeks after dissolution and consists of extremely small particles that contribute to the interfacial crud problem.

Extensive batch extraction and stripping tests were completed with 30% TBP and clarified dissolver solution from both the Robinson and Oconee-1 reactors. The results provide additional confirmation of the observations reported previously. Plutonium is extracted to the extent that the aqueous raffinate contains at most a few thousandths of 1%. Co-stripping with 0.25 to 0.35 M HNO_3 successfully recovers both uranium and plutonium, but plutonium strips somewhat more slowly after about 99.9% has been stripped.

2.2.1 Hot-cell dissolution

The dissolution of Run 10 was made routinely using 353.5 g of clad fuel from the Oconee-1 reactor (292.7 g of fuel plus 60.8 g of cladding). This fuel is from the first irradiation cycle and has a relatively low burnup, about 14,000 MWD/MTU. The fuel was cut into nine pieces about 2 in. long using a single-rod shear. The ends of the pieces were flattened somewhat, but all were open enough for ready dissolution.

The dissolution proceeded similarly to the procedure used for Robinson reactor fuel and appeared to be complete after only 0.6 hr at 90 to 92°C. Dissolution was continued for a total time of 1 hr; the solution was then

transferred from the dissolver. The cladding was rinsed twice and transferred from the dissolver. For analysis, four pieces of cladding were dissolved in hydrofluoric acid containing some nitric acid.

The dissolver solution was clarified by centrifugation followed by filtration through Millipore filters (Sects. 2.2.3 and 2.2.4); a portion of the solution was used for solvent extraction studies (Sect. 2.2.5).

The dissolution for run 11 was made with clad Robinson reactor fuel; this time, however, the fuel was cut with a tubing cutter into four pieces each about 4.5 in. long. All prior work had used 2-in.-long sections. It had been observed that the dissolution time required for 2-in. pieces was only slightly longer than for fuel fragments; one purpose of this run was to determine the effect of fuel pieces that were substantially longer than 2 in.

The dissolution was much slower; after 7 hr at 90 to 92°C, an examination of three pieces of cladding showed that one still contained fuel and two were clean. After standing overnight, the dissolver was heated to 90°C for an additional hour, and the solution was transferred from the dissolver. It was subsequently observed that one piece of cladding still contained a small amount of solids and that collectively, these fuel pieces were too long.

The dissolver solution was centrifuged and then filtered several times through Millipore filters (Sects. 2.2.3 and 2.2.4).

2.2.2 Radioactivity in off-gas

The data for tritium, ^{14}C , and ^{129}I for the first nine runs have been reexamined; updated results are reported in Tables 2.3, 2.4, and 2.5. There are some discrepancies in the results for runs 10 and 11; some analyses are not yet complete, therefore these runs are not reported.

Table 2.3. Tritium distribution during dissolution

Run	Ci/MTU	Found	Percent of total found in -				
		Percent of ORIGEN	Dissolver	Condensate	Scrub 1	Scrub 2	Scrub 3 ^a
1	138	46 ^b	98.3	1.22	0.047	0.0009	
2	264	53	98.6	1.29	0.11	0.0003	
3	201	63 ^b	99.0	0.95	0.04	0.006	
4	312	61	96.6	2.75	0.17		0.47
5	373	73	96.8	2.81	0.12		0.25
6	310	61	59.0	40.4	0.26		0.29
8	261	53	97.6	2.00	0.11	0.003	0.46
9	295	59	99.2	0.35	0.12	0.002	0.12

^aAfter hot CuO bed.

^bValues are approximations because of uncertain irradiation history.

We are continuing to attempt to obtain direct analyses for nitrogen and ^{14}C in the irradiated fuel, as well as for tritium and ^{129}I in some cases, using small samples of the same batch of fuel used for the dissolution experiments. The Oconee-1 fuel is reported to contain substantially more nitrogen than the Robinson fuel, therefore a measurable effect is expected. The irradiation level is only about half that of the Robinson fuel, however, and calculated (ORIGEN) values are subject to major uncertainties, since reactor conditions are significantly different during the first and second irradiation cycles than during subsequent cycles for which ORIGEN is optimized.

Samples of dissolver solution from runs 9 and 10 were analyzed for ^{14}C and ^{129}I using wet oxidation to destroy any possible organic constituents in the solution. The results generally confirm that the dissolver solutions contain very little of these isotopes. There was no detectable iodine, and the ^{14}C value represents not more than 2% of the total ^{14}C present.

2.2.3 Dissolution residues

A large number of solids samples from runs 9, 10, and 11 have been submitted for analysis and scanning electron microscope (SEM) and microscope characterization. Nearly all samples were obtained by filtration using 0.1- μ pore-size Millipore filters. Much of the data are not yet complete, and results to date should not be considered definitive. The preparation of samples for analyses and characterization is still presenting some problems.

Emission spectrographic analyses for the dissolver residue from run 9 indicate the following qualitative composition: Ru-Tc > Mo-Pd > Rh > Zr, with very little zirconium and no other fission products detected. This method is not sensitive to a number of fission product elements. Spark-source mass spectrometry (SSMS) and microprobe results are not yet available. No results have been received for runs 10 or 11.

Many of the filtered samples show appreciable amounts of uranium; it is not clear whether the uranium is a constituent of the solids or a contaminant on the filter material. When only a few milligrams of solids are collected, contamination by a few microliters of dissolver solution would contribute a major amount of uranium. Because of the arrangement of the Millipore filter, an annular ring of the filter may be saturated with the solution being filtered and may subsequently be largely bypassed by wash solutions. We are attempting to remove such soluble contaminants by placing the filters on blotter paper saturated with 3 M HNO₃; however, the effectiveness of this procedure is not clear. Some filters have a visible yellow ring surrounding the black circle of filtered solids.

Filtration of the run 10 dissolver solution proved quite difficult, perhaps even more so than for run 9. The total quantity of solids collected was less (as expected) because of the low fuel burnup; solids collected in the initial clarification constituted only 0.092% of the weight of UO₂. In contrast, less difficulty was encountered in filtering the run 11 solution. Run 11 differed from others in that the dissolution lasted much longer, thereby possibly dissolving some fine particles. The initial solids recovered constituted 0.18% of the weight of fuel. Both these solutions were centrifuged before filtering.

Table 2.4. Carbon-14 distribution during dissolution

Run	Found (Ci/MTU)	Calculated nitrogen ^b (ppm)	Dissolver	Percent of total found in -			
				Condensate	Scrub 1	Scrub 2	Scrub 3 ^a
1	0.14	~3.6	<<	<<	99.5	0.5	
2	0.27	7.3	<<	0.44	97.5	2.1	
3	0.15	6.5	<<	0.65	97.5	1.85	
4	0.24	5.6	<<	0.41	58.7		40.9
5	0.29	8.2	<<	0.16	83.2		16.8
6	0.42	14.5	<<	<<	94.4		5.6
8	0.37	11.9	<<	0.04	94.1	3.7	1.7
9	0.32	10	<<	0.82	89.9	6.1	2.5

^aAfter hot CuO bed.

^bBased on ¹⁴C found, corrected for (n,α) on ¹⁷O.

Table 2.5. Iodine-129 distribution during dissolution

Run	Found		Percent of total found in -				
	g/MTU	Percent of ORIGEN	Dissolver	Condensate	Scrub 1	Scrub 2	Scrub 3 ^a
1	118	82	0.52	0.14	99.3	0.08	
2	157	84	0.97	1.08	97.4	0.57	
3	45	41	0.50	0.90	98.3	0.30	
4 ^b	149	80	0.20	0.01	98.9		0.80
5 ^b	169	84	0.23	0.23	99.4		0.18
6	141	76	0.98	2.89	94.6		1.57
8	120	64	0.35	0.26	99.2	0.18	0.015
9	132	70	0.99	0.01	98.5	0.47	0.02

^aAfter hot CuO bed.

^bAir sparged following dissolution.

A number of samples of solids have been submitted for characterization by SEM and microprobe, but only a few SEM photos have been obtained. Figures 2.2 and 2.3 show photos of the dissolver residue (initial filtration) from run 9. These samples are far too radioactive for microprobe analyses with equipment available here. Figure 2.2 is a view looking down on fragments of filter cake at four different magnifications. Even at 3000X, no defined particles or interparticle voids are visible, although some rounded particles are attached to the cake. An unexpected observation is especially apparent in the 3000X photo, where particles on the surface appear to flow or melt into the filter cake.

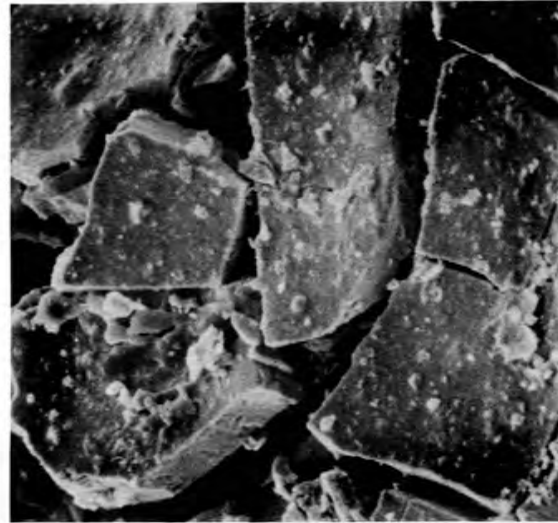
Figure 2.3 is a view of the edge of the filter fragments and filter cake. The 3000X photo is a reference view of the filter material; the 0.1 μ pores are plainly visible. The 1000X photo shows the filter cake with filter material below it. It is obvious that no particles or interparticle voids are visible, in contrast to the Millipore filter material; therefore, much of the solid must be well below 0.1 μ in size. From this photo, the thickness of the filter cake is estimated to be 25 to 30 μ . If this thickness is reasonably uniform over the 9.6 cm² filter, the density of the cake is approximately 7. This observation is consistent with the suggestion that the residue consists of metal particles (such as ruthenium-molybdenum, etc., alloys) rather than oxides or compounds.

2.2.4 Solution stability

We are continuing to study the apparent postprecipitation of noble metals from dissolver solution. This study involves primarily filtration or centrifugation of solutions and attempts to characterize the small



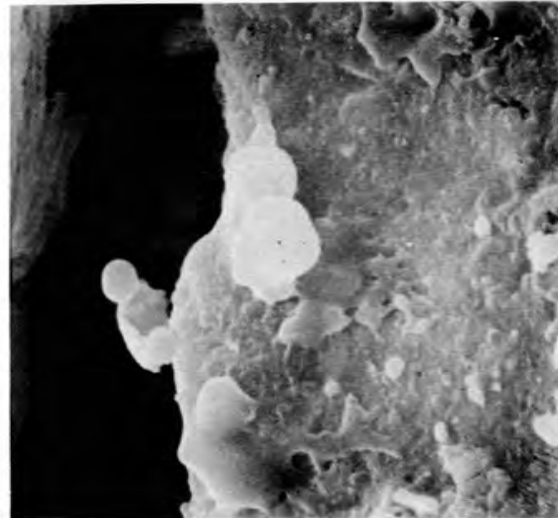
100 X



300 X



1000 X



3000 X

Fig. 2.2. Filtered dissolver residue - 9D6 F.



300 X

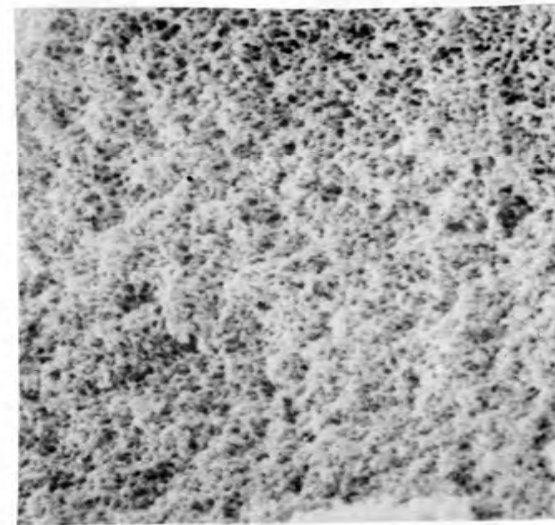


100 X



10 μ

1000 X



10 μ

FILTER

3000X

Fig. 2.3. Filtered dissolver residue - 9D6 F.

amounts of solids collected. Several samples of solids from run 9 were examined by emission spectrography; these samples contained comparable amounts of palladium, molybdenum, and ruthenium, and possibly technetium, with palladium probably dominant. This characterization is somewhat different than the composition of the dissolution residue; however, there is considerable uncertainty in these results. The problem mentioned in the previous section, relating to uranium contamination of the filters, is especially important for these samples because of the small amount of solids.

Similar studies are being carried out for the dissolver solution from runs 10 and 11, and a large number of samples have been submitted for SEM, microprobe, emission spectrographic, and SSMS analyses. Sample preparation is extremely difficult for these materials.

In the run 10 dissolver solution, successive filtrations were very slow because the flow rate decreased rapidly. About 100 ml could be filtered in a day, most of it within the first hour, and the amount of solids collected was quite small. The precipitate formed was of a size that effectively plugged the filter pores. If the filtrate was immediately refiltered the flow rate did not decrease markedly; however, after aging one or a few days the filtration rate would again drop drastically. Typical flow rates were around $0.5 \text{ ml min}^{-1} \text{ cm}^{-2}$ initially and twenty times less after one to a few hours.

Filtration characteristics of the run 11 dissolver solution were much better, and it was possible to filter the entire solution (600 to 700 ml) in a few hours. The long dissolution time for run 11 may have

affected the noble metals in some way such that they either did not precipitate in such large amounts or the particle sizes were different.

In the three series of filtration tests (runs 9, 10, and 11), it was observed that postprecipitation essentially ceases after about three weeks. Subsequent to this time, there is little decrease in flow rate during the filtration, although very small amounts of solids are still collected. The reason for this is not known.

It has also been observed that, in solvent extraction tests made with dissolver solution that had been repeatedly filtered and had aged beyond this time during which solids continue to form, there was very much less, if any, interfacial crud. It is not clear whether interfacial crud was present, or whether it was merely less visible because of the absence of these black solids which, if present, associate with the crud.

2.2.5 Solvent extraction

Data for the solvent extraction tests made with run 9 dissolver solution were completed, and a much more extensive series of extractions with TBP and co-stripping tests with dilute nitric acid were made with run 10 dissolver solution. In general, information reported previously was confirmed. In several cases, stripping tests indicated that the plutonium distribution coefficient (DC) increased (plutonium was harder to strip) after about 99.9% of the plutonium was stripped; however, the remainder continued to strip. In only one case, involving an aged solvent and unusual conditions, about half the plutonium could not be stripped into dilute nitric acid.

Final data for the extraction and stripping tests with di(2-ethylhexyl) sulfoxide generally confirmed the earlier conclusions. It was determined that ruthenium extracts to a significant extent, the DC organic-aqueous (O:A) increasing from 0.0066 at high uranium loading to 0.12 after most of the uranium had been removed. This ruthenium did not readily strip into 0.25 M HNO_3 , the DC being about 200. The decontamination factor for the total process, extraction plus stripping, was about 10^4 . The behavior of ruthenium in a continuous countercurrent system cannot be predicted from this procedure.

All other isotopes, including americium, curium, cesium, cerium, and europium, extracted to a much smaller extent than with TBP. This extractant is clearly an interesting one that will receive additional study when a supply has been obtained. The apparent associated problems relate to the irreversible extraction of noble metals, especially palladium and ruthenium. Solvent cleanup for recycle requires study.

Run 10 dissolver solution (Ocone-1 fuel) was used for an extensive set of solvent extraction tests. The dissolver solution was first extracted ten times with equal volumes of 30% TBP; the phases were mixed for 10 min and allowed to separate for a few minutes. The first and second organic extracts (both essentially saturated with uranium) were stripped with 0.26 and 0.38 M HNO_3 respectively. The fourth organic, about 10% saturated, was stripped with 0.26 M HNO_3 . For comparison, a separate portion of dissolver solution was extracted with TBP for a 6-hr contact time; the first organic extract was stripped identically to that from the 10-min contact. In all cases, ten successive strips were made with a volume ratio (O:A) of 1 to 2, and phases were contacted for 10 min.

Extraction results were generally very good. Both uranium and plutonium were reduced to very low concentrations in the aqueous, near $10^{-3}\%$ of the feed. However, the concentrations in the organic phase tended to level off in the last three stages at a few thousandths of 1% of the feed. This leveling off suggests that there may be small amounts of uranium and plutonium not contained in either phase, perhaps material precipitated with or absorbed on the interfacial crud, part of which sticks to the sides of the separatory funnel.

Stripping tests with the first and second organic extracts were also good. After ten strips the uranium was reduced to 0.01% of the initial concentration, and there was no indication of any change in the DC. Plutonium behavior was significantly different. The plutonium DC was constant for about five stages and then increased significantly (about a factor of 5) for the remaining stages. Plutonium was effectively stripped throughout; however, after about 99.9% stripped with the expected DC, the remainder stripped more slowly.

It is significant that the stripping behavior of the organic that received the 6-hr extraction contact was essentially identical to that which received a 10-min contact. The long extraction time caused a noticeable increase in interfacial crud, and various degradation products would be expected to be present in appreciable amounts. However, stripping tests with the clear organic showed no effects. Thus, it appears that any problems from radiation exposure followed the aqueous phase or the interfacial crud but not the clarified organic phase.

The one test that did not show good behavior was the strip of the fourth organic extract. Although uranium stripped normally, about half

the plutonium was not stripped (DC about 150). This was not a small amount of plutonium; the initial concentration was within a factor of 10 of that of the other experiments. The final concentration was a factor of 100 or more higher. The reason for this behavior is not known. However, there is an additional variable that was inadvertently introduced, that being aging time. This experiment was done nine days after the extraction, whereas the others were done between one and seven days after the extraction. The other difference with this experiment is the low loading, which is an equilibrium condition in a batch extraction but only a transient condition in a countercurrent system.

Fission product analyses are not yet complete; however, it is clear that some fission products extracted to a much greater extent after the 6-hr contact. Ruthenium was about 100 times greater and it did not readily strip; there was also substantial amounts of cerium europium, niobium, and probably zirconium, most of which did strip. As expected, the organic from the fourth extraction, with a low uranium loading, contained a high concentration of ruthenium, about 10^3 higher than the first organic (saturated in uranium) and it also extracted a significant amount of cerium and europium.

In all these tests there has been no problem with the co-stripping of uranium and plutonium. Plutonium strips more readily than uranium. The minimum acid concentration that will avoid any problems due to plutonium hydrolysis or polymer formation is not known; however, good results seem to be obtained with nitric acid concentrations of about

0.3 M. Distribution coefficients are not especially favorable, and more than ten stages would be required with an aqueous to organic flow ratio of 2.

2.2.6 Waste concentration

The experiment involving prolonged air sparging of the waste concentrate from run 8 was continued through most of the present report period before it was terminated. The data from this test have not yet been calculated; however, it is clear that there was a substantial decrease in acidity during the several months that the experiment continued.

2.2.7 Characterization methods

Certain analytical problems were better identified and partially resolved. It was found that all radioactivity determinations made with the GeLi detector (gamma scans) have been in error for the indefinite past. This affects nearly all fission product analyses, with the discrepancy being about 25% for low-energy gammas, such as ^{144}Ce , and 15% for higher-energy gammas, which include all other isotopes (^{106}Ru , $^{134-137}\text{Cs}$, ^{154}Eu , ^{60}Co , ^{54}Mn , and a few others). Reported results have been low.

We have noted frequent discrepancies of a few percent for uranium analyses run at different times and for uranium material balances. Recently, several samples were run by isotopic dilution and mass analysis, as well as the conventional hot-cell methods. The isotopic dilution method nearly always gave higher results, in some cases by 10% or more. Part of the problem has been shown to be incomplete extraction of uranium for the hot-cell determinations with high-level samples; a TBP extraction

has been used to separate uranium from the gamma activity. A modified procedure has been developed using a tri-n-octyl phosphine oxide extraction; however, it is not clear that that is the only problem. It has not yet been demonstrated that different analytical methods agree to within the expected experimental error in the case of samples such as dissolver solution, which contains large amounts of fission product elements and radioactivity.

2.3 Building 4507 Hot-Cell Operations

V. C. A. Vaughen, J. H. Goode, R. G. Stacy, G. K. Ford, E. C. Hendren, J. R. Travis, and C. S. Webster (Chemical Technology Division, ORNL)

2.3.1 Development of in-cell equipment

Continuous tritium monitor. Samples of off-gas from voloxidizer runs with irradiated H. B. Robinson-2 UO_2 in Building 4507 were brought to the Building 4500N development laboratory. The samples, which contained air, 3H_2O , ^{14}C , and ^{85}Kr radionuclides, were displaced with air from the sample bulbs into the continuous tritium monitor (an absorption-single-channel scintillation counting system). Aliquots of the scintillation liquid being discharged from the flow-through counter were collected as samples for a more sophisticated, multichannel scintillation counter. The single-channel counter showed only the growth and elimination of a massive peak of radioactivity (up to 5×10^6 counts/min total) that represented the sum of 3H_2 , ^{14}C , and traces of ^{85}Kr present in the off-gas sample. Analysts using the multichannel scintillation counter were able to differentiate between the various radionuclides by counting the aliquots, comparing them to known standards, and solving simultaneous equations for the individual components. It is clear that our simple

electronics system must be upgraded before a true in-line tritium monitor can be put into service. Until that time, we are obtaining some estimate of release rates with a series of silica gel and type 4A molecular sieve tritium traps that can be valved sequentially into the off-gas stream on a predetermined schedule (Fig. 2.4).

2.3.2 Building 4507 maintenance and improvements

New telescoping intercell transfer conveyors were remotely installed in the existing openings between cells 2 and 3 and cells 3 and 4. This improvement permits easier transfer of fuel containers, samples, and waste into and out of the hot cells in Building 4507. A new equipment maintenance glove box was designed and approved for construction on top of cells 3 and 4. The glove box allows access to the cells within a contained environment for the installation, removal, or maintenance of equipment, and the handling of alpha-contaminated articles, etc. The remaining part of the CRF (cell 4) is being outfitted initially for short-term physical property studies under the HTGR program.

2.3.3 Miscellaneous

Quad Cities-1 mixed oxide fuel was packaged and shipped to SRL for their use. Requests for quotations have been sent to Babcock and Wilcox for delivery of samples of the second core of the Oconee-1 reactor and to Westinghouse Electric for samples of Point Beach-1 fuel having two densities and two levels of burnup. We are awaiting a proposal from General Electric for specimens from various boiling water reactors and from Battelle-Columbus Laboratories for other types of fuel.

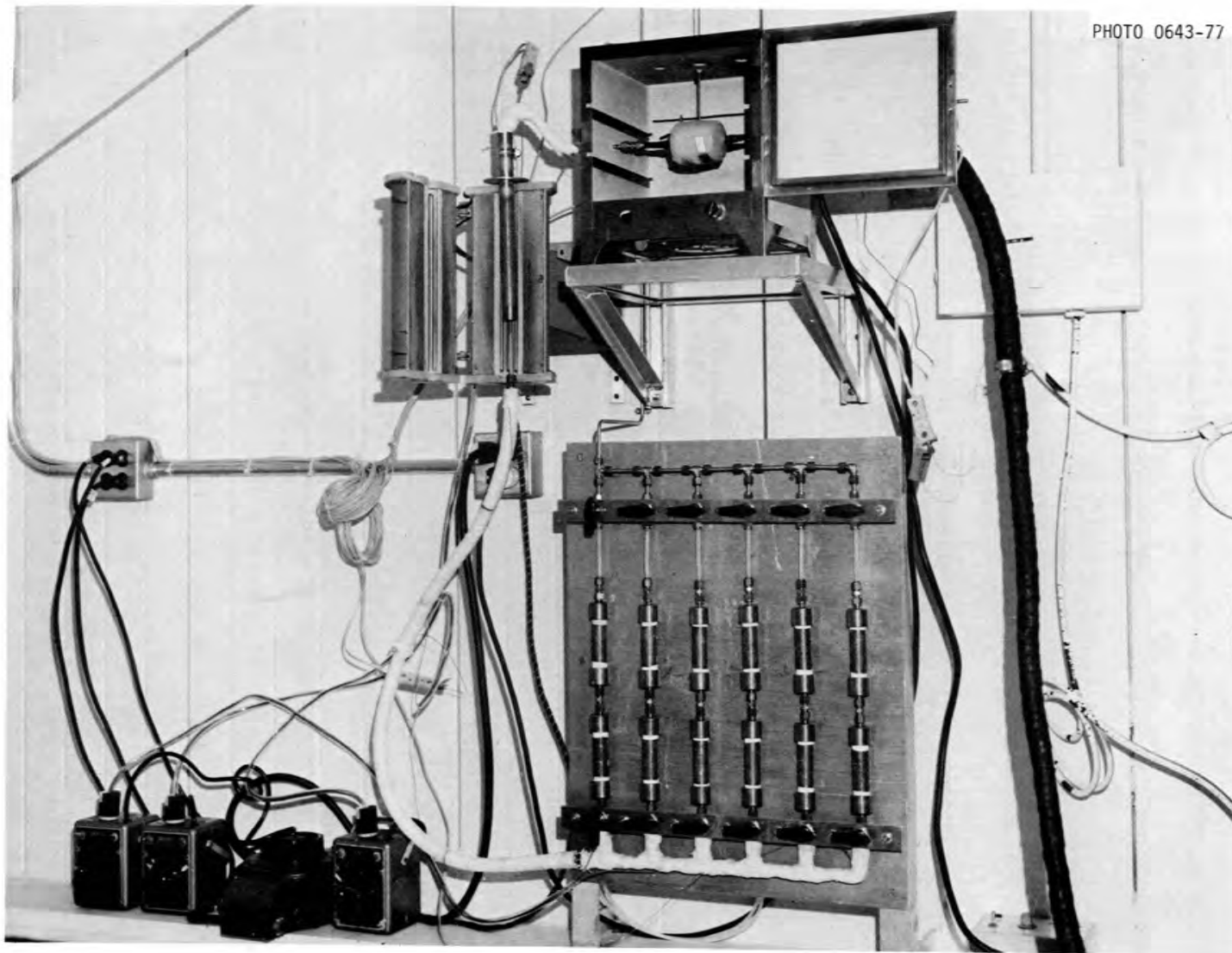


Fig. 2.4. Silica gel and type 4A molecular sieve tritium traps.

2.3.4 Voloxidation studies

Last quarter we reported that a base-line voloxidation experiment had been run on a mixture of clad and unclad UO_2 (31,000 MWd/metric ton) discharged from the H. B. Robinson-2 reactor. Preliminary results from that experiment and subsequent runs indicate that the voloxidation apparatus and the off-gas monitoring system are performing satisfactorily. A replicate voloxidation has been run to enlarge the data matrix for characteristic gaseous releases and fission product distributions at base-line operating conditions (4 hr in air at 480°C). The reduction of data from the initial LWR series is essentially completed. Dissolutions of oxidized and nonoxidized Robinson fuel and Zircaloy-4 cladding have been made in conjunction with these voloxidation studies for the determination of heavy-metal, fission-product, and tritium contents. Analytical results from those tests are reported in Sect. 2.3.5. In addition, a single voloxidation experiment was performed on an unclad charge of Robinson UO_2 for the determination of cladding effects during treatment. Data evaluation for that run is currently in progress. As a stock supply for future reprocessing studies, including examination of alternative voloxidation processes (vacuum and inert roasting, etc.), several hundred grams of H. B. Robinson fuel have been sheared, declad, and characterized with respect to the size distribution.

Qualitative shear data for cuts made on mid-portion segments of H. B. Robinson rod G-10, assembly B05, were reported earlier.⁴ Products from that operation were used in the three voloxidation experiments shown in Table 2.6. For runs 1 and 2, the rotary voloxidizer was loaded with a mixture of loose UO_2 and UO_2 clad in 1-in. hulls. The ratio of

Table 2.6. Material balance on voloxidation of UO_2 (31,000 Mwd/ton)
 (H. B. Robinson-2 reactor, rod G-10, assembly B05)

	Run		
	LWR-1	LWR-2	LWR-3
<u>Inputs, g</u>			
UO_2 (clad)	92.5	82.5	
UO_2 (fines)	20.1	15.2	72.7
Cladding	23.3	22.9	
Total	135.9	120.6	72.7
<u>Outputs, g</u>			
U_3O_8 ^a	116.3	101.8	75.2
Cladding	23.3	22.9	
Total	139.6	124.7	75.2
Weight gain, g	3.7	4.1	2.5
Oxide conversion, ^b %	83.0	106	87.0

^aIncludes unconverted UO_2 if present.

^bAssuming minimal zirconium oxidation.

loose fuel to clad fuel in each experiment was proportionate to the amount dislodged from the hulls during shearing. Treatment conditions for the two replicate runs were as follows:

Time: 4.0 to 4.5 hr

Temperature: 480°C

Atmosphere: air fed at 200 to 300 cm³/min

Agitation: rotation at 12 rpm

For run 3, the voloxidizer was charged with loose oxide only, and all conditions remained the same as above except that the time at temperature was shortened to 3.0 hours. To ensure completeness of the reaction at these conditions, each experiment was run beyond the point at which oxygen was being consumed and the ⁸⁵Kr levels in the off-gas returned to near background levels.

The voloxidation apparatus, the gas flow system, and the operating and sampling procedures employed in this experimental series were described last quarter.⁴ The entire system is diagrammed in Fig. 2.5. Voloxidation off-gases are sent to the penthouse area above the cell where they are sequentially trapped for ³H₂O content, continuously analyzed for ⁸⁵Kr and O₂ content, and finally collected for accumulative measurements on ⁸⁵Kr and ¹⁴C release. The system is sampled for particulates and semivolatile species in the following manner:

1. Sheet specimens and coupons inside the voloxidizer to check for fission product deposition and scouring by hulls;
2. Following a 35-μ metal frit in the exit end (cooling zone) of the burner are stainless steel deposition tubing inserts and steel wool packing (Fig. 2.6);

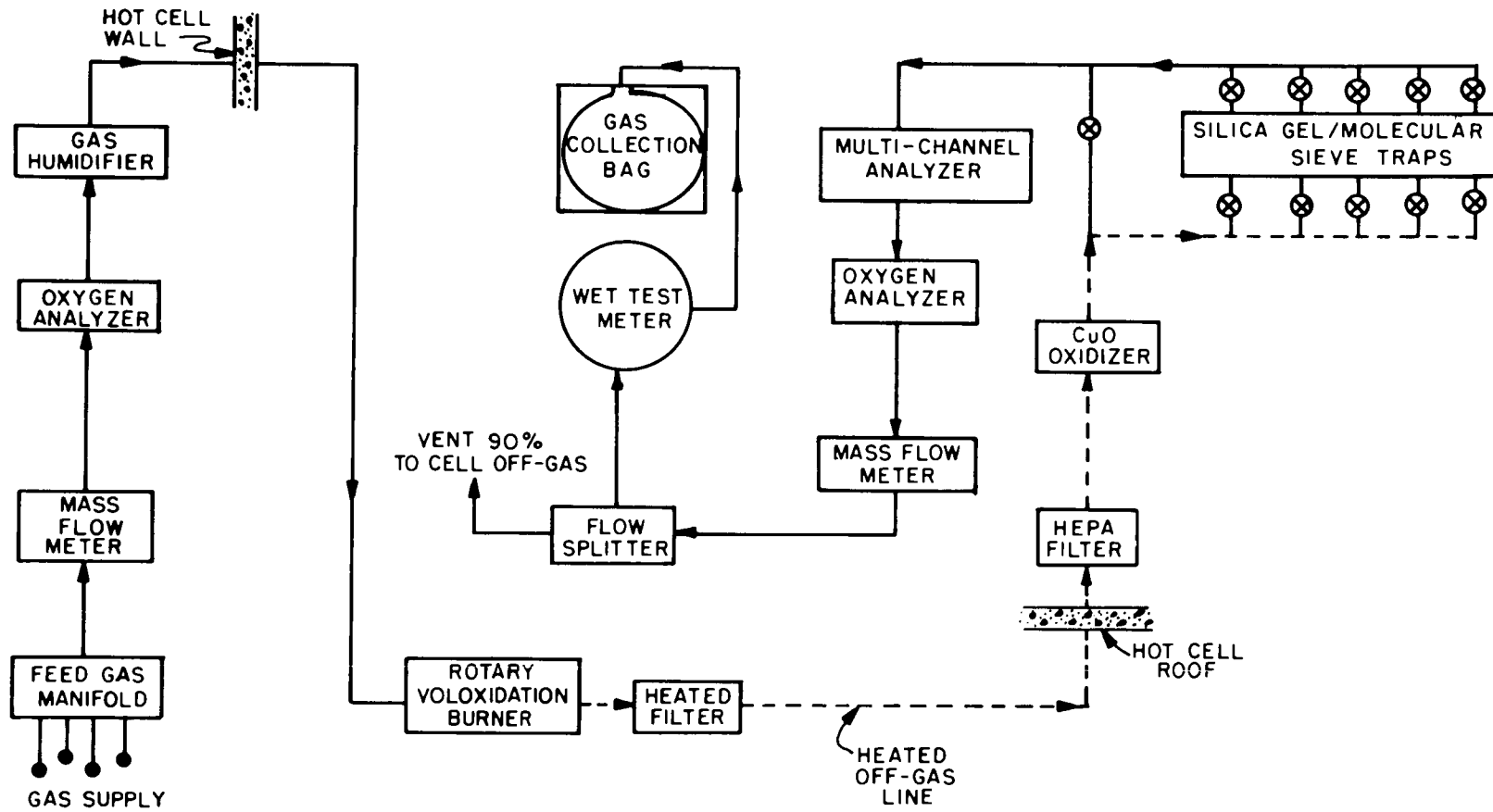


Fig. 2.5. Voloxidation off-gas control and monitoring system, Building 4507.

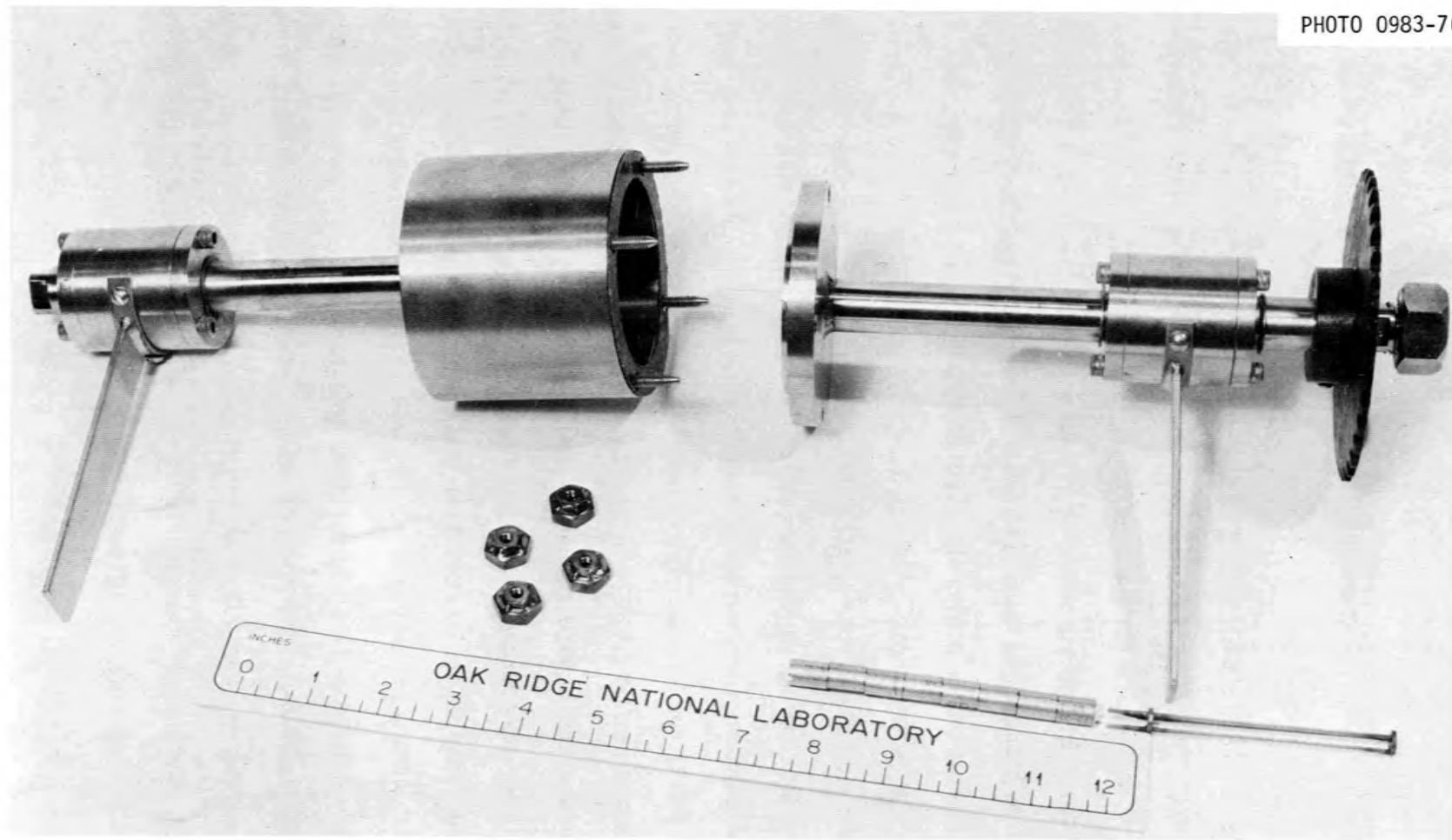


Fig. 2.6. Rotary voloxidizer and deposition tubing inserts.

3. A heated filter pack containing metal frits, graded filter papers, and charcoal granules;
4. A HEPA filter is located immediately outside the cell for secondary particulate removal.

Oxide conversion and gas evolution. Krypton evolution rate curves obtained with multichannel analyzer counts on the gas stream are shown for each of the replicate runs in Figs. 2.7 and 2.8. The corresponding oxygen content in the voloxidizer off-gas is also seen as a function of run time. Accumulative consumption of oxygen during the voloxidation is presented as an oxide conversion profile for the second experiment (Fig. 2.9).

During run LWR-2, the UO_2 gradually began reacting (percent of O_2 in off-gas decreased) as the temperature of the charge rose above $400^\circ C$. Oxygen consumption then markedly increased during approximately the first 30 min at $480^\circ C$ until a generally uniform conversion rate was attained for the next 90 to 100 min. Only slight variation in the rate of oxide conversion was noticeable for this period (Fig. 2.9), even though the off-gas oxygen percentage briefly increased prior to a second rise in consumption (Fig. 2.8). After less than 2.5 hr at temperature, 80% of the UO_2 had undergone conversion. Oxygen utilization then slowly dropped back to zero (the oxygen in the off-gas equaled the feed air concentration, 20.9%). In run LWR-2, the conversion was completed with >99% of the oxide being released from the hulls as fine powder (99% < 325 mesh). The same powdering behavior was observed for the LWR-1 product, even though the measured oxide conversion was less (83%).

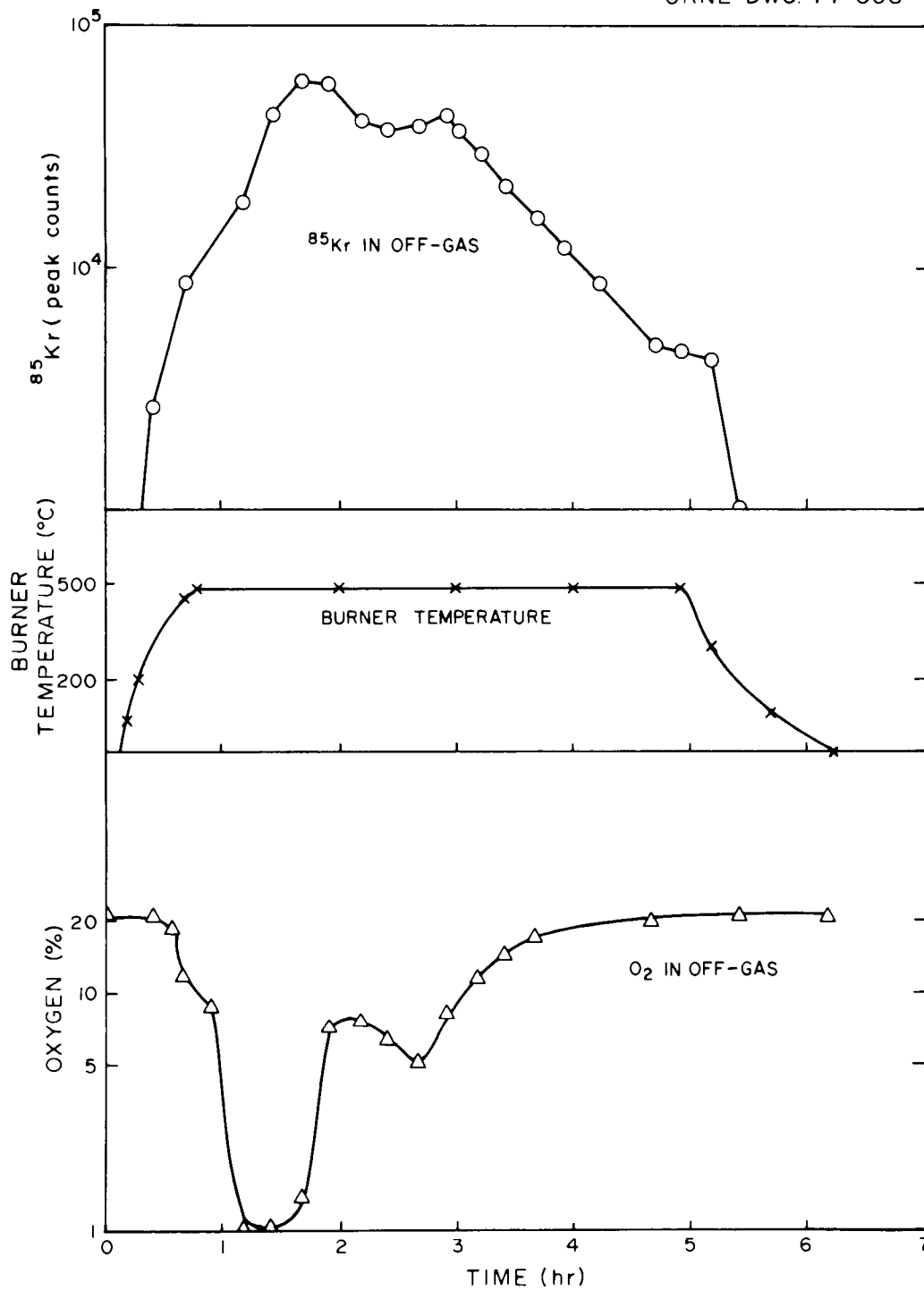


Fig. 2.7. Release of ^{85}Kr and oxygen consumption during voloxidation of H. B. Robinson Zircaloy-clad UO_2 (rod G-10) in air at 480°C (run LWR-1).

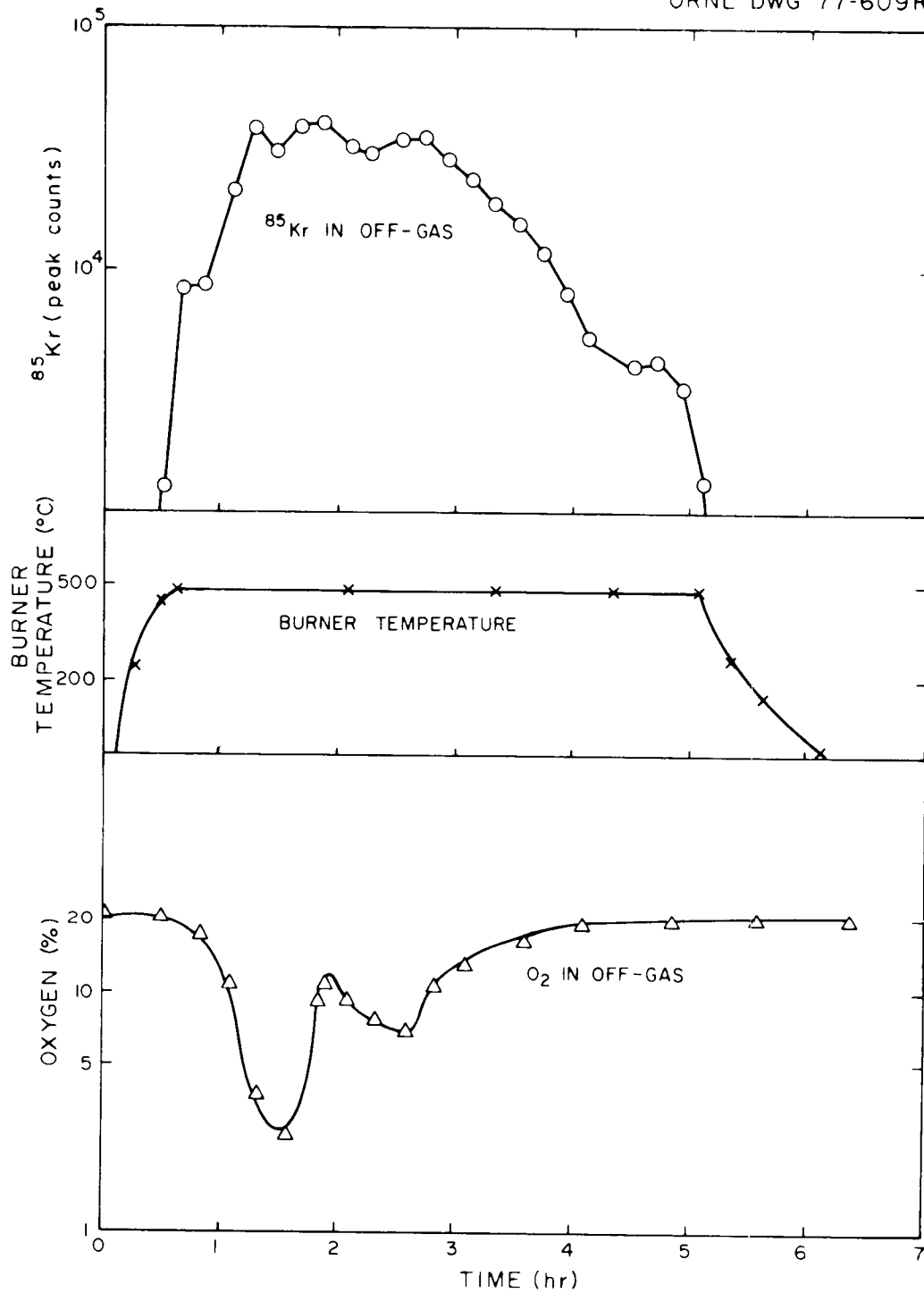


Fig. 2.8. Release of ^{85}Kr and oxygen consumption during voloxidation of H. B. Robinson Zircaloy-clad UO_2 (rod G-10) in air at 480°C (run LWR-2).

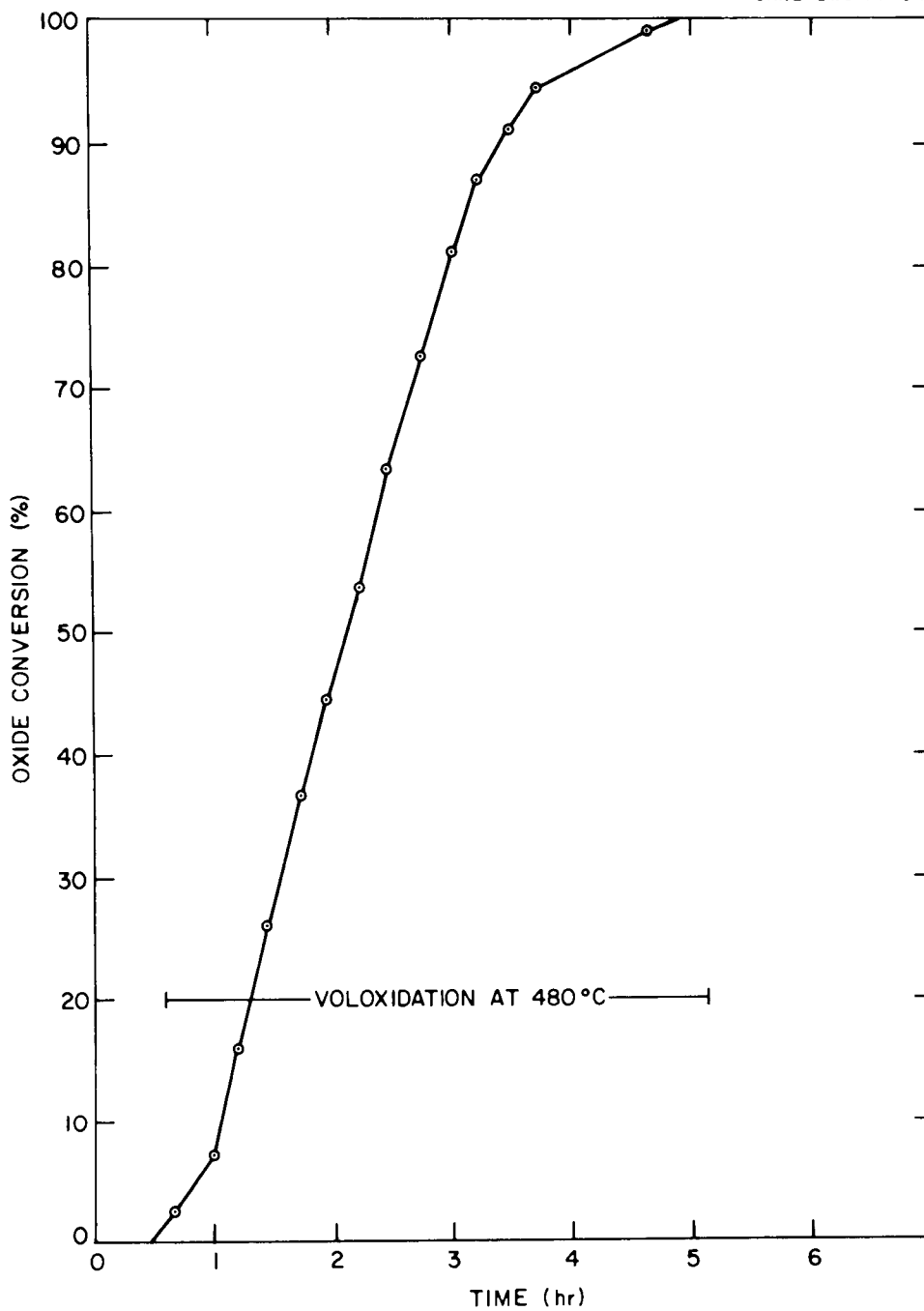


Fig. 2.9. Conversion of Zircaloy-clad UO_2 to U_3O_8 during voloxidation in air at $480^\circ C$ (run LWR-2).

The double peaking observed for oxygen consumption during voloxidation of clad-unclad mixes of H. B. Robinson fuel is also visible to some degree for the release of ^{85}Kr , though apparently delayed by 20 to 30 min. Similar behavior for ^3H release is evident from the evolution rate data shown in Fig. 2.10; however, the time lags are more of the order of 40 to 60 min behind the O_2 -usage peaks. Regardless of the inherent delayed release patterns, the 4.5-hr treatment at 480°C during LWR-2 was sufficient to release 98.9% of the tritium. (Dissolution of the voloxidized fuel showed that the residual ^3H concentration was about 1.1% of the initial inventory.)

The variation in oxygen consumption (Figs. 2.7 and 2.8) is probably related to a number of factors. Because the charge is a mixture of loose and clad oxide, it would seem reasonable that the loose fuel oxidizes almost immediately, followed by a second wave of reaction as the remaining material becomes dislodged from the cladding. However, during the LWR-3 voloxidation of unclad Robinson oxide, a pronounced, though distinctly different, type of double-peaking effect for the oxygen consumption was again present. This would indicate that particle size also has a noticeable effect on the oxygen depletion curve. In all three experiments the loose oxide charged to the burner was in the following fractional split: 35 mesh \leq 64%; 100 mesh \leq 23% < 35 mesh; and 13% < 100 mesh.

Additional LWR voloxidations will be used to further investigate the variations in oxide conversion rate and the accompanying effects upon gaseous radionuclide release. In two as yet unreported voloxidations at 650°C performed on Nuclear Materials and Equipment Company (NUMEC) mechanically blended mixed oxides, no double peak was visible either for the

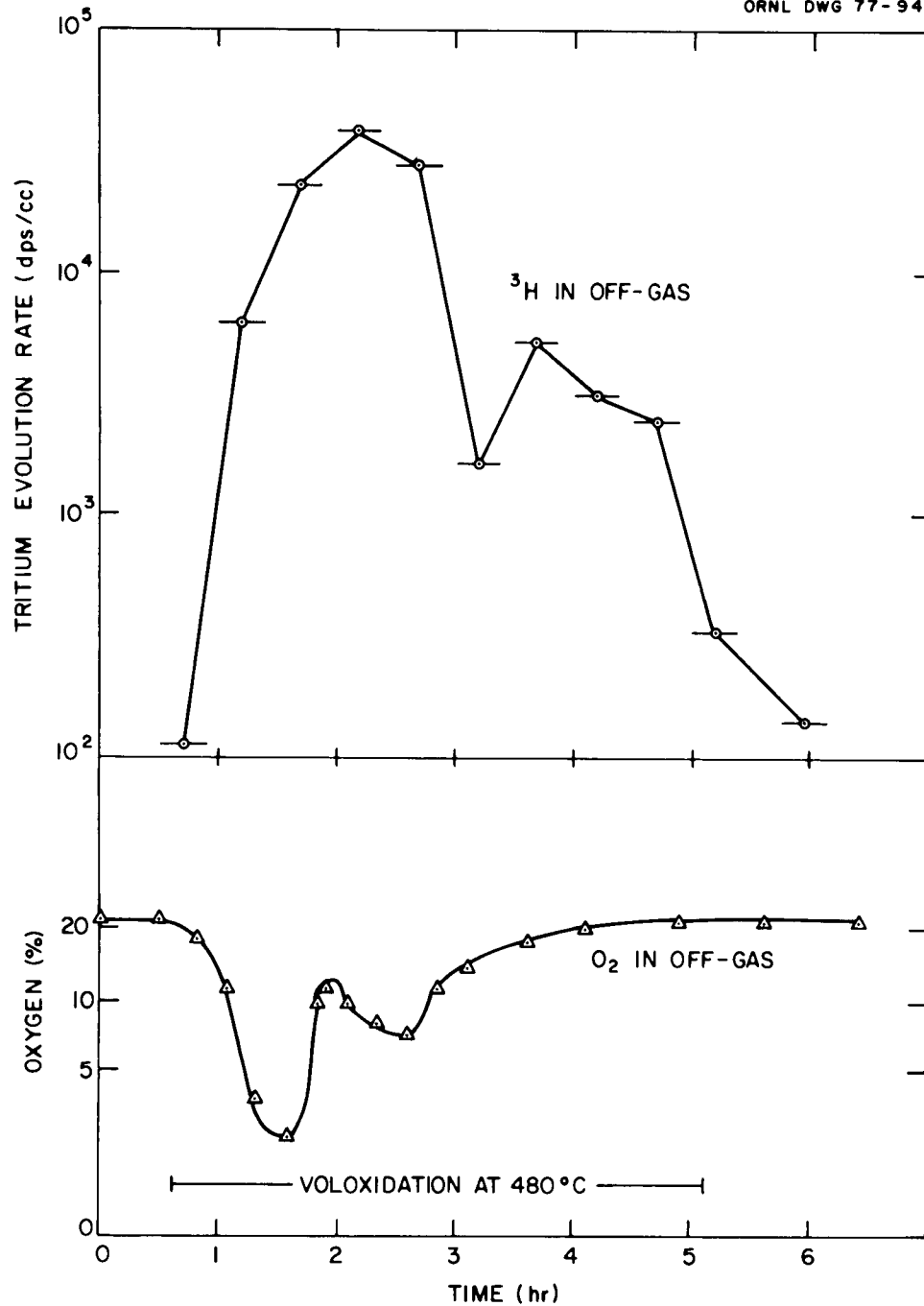


Fig. 2.10. Release of tritium and oxygen consumption during voloxidation of Zircaloy-clad UO_2 in air at 480°C (run LWR-2).

oxygen consumption or for the krypton release; however, the tritium evolution pattern showed two distinct peaks as the run progressed.

Fission product distribution. Following voloxidation of mixtures of clad and unclad Robinson fuel at 480°C, a number of fission products were found deposited on system surfaces and entrained in the heated filter network. Table 2.7 shows a distribution of the relative amounts remaining in the system after LWR-1. Distribution for the replicate run was nearly identical.

The largest portion of activity found remained attached to inner surfaces of the voloxidizer (on sample specimens inside the reaction chamber). Decontamination factors of 100 or more for ^{106}Ru , ^{134}Cs , ^{137}Cs , and ^{144}Ce were obtained as the off-gas passed through the 35- μ sintered steel frit into the cooling end of the burner. The next largest concentration deposited from the rapidly cooling gas onto the tubing insert specimens. A profile of the deposition in this region as a function of temperature can be seen in Fig. 2.11 for the second voloxidation experiment. The presence of steel wool packing in the tubing end segments increased fission product collection by a factor of 8 or 9. One point to notice is that the relative depositions of ^{106}Ru , ^{137}Cs , and ^{144}Ce do not differ greatly in relation to each other as the off-gas cools from above 400°C to near 100°C. Activation analysis of the tubing sections showed very little ^{129}I plated out in this region; most of it was absorbed by the heated charcoal bed. Of the entrained activity in the graded filters, most of it was associated with particulates sized between 5 and 10 μ .

Table 2.7. Distribution of selected fission products remaining in the volox burner and off-gas system following voloxidation of H. B. Robinson fuel in air at 480°C (LWR-1)

Nuclide	System distribution (Percent found in -)						Total found (dis sec ⁻¹ g ⁻¹ of uranium)
	Burner walls	Deposition specimens	Graded filters ≤ 10 μ	Charcoal	HEPA filter 0.3 μ	Adsorption traps	
³ H						100.0	7.28 x 10 ⁶
¹⁴ C							4.59 x 10 ³
⁸⁵ Kr							2.10 x 10 ⁷
¹⁰⁶ Ru	98.9	0.80	0.27	a	a		1.75 x 10 ⁵
¹³⁴ Cs	99.5	0.32	0.12	a	a		3.01 x 10 ⁵
¹³⁷ Cs	99.6	0.27	0.10	a	a		6.62 x 10 ⁵
¹⁴⁴ Ce	99.5	0.34	0.10	a			3.48 x 10 ⁵
¹²⁹ I	26.6	0.7	16.5	56.2			1.36 (μg/g of uranium)

^aTrace quantities.

ORNL DWG 77-943

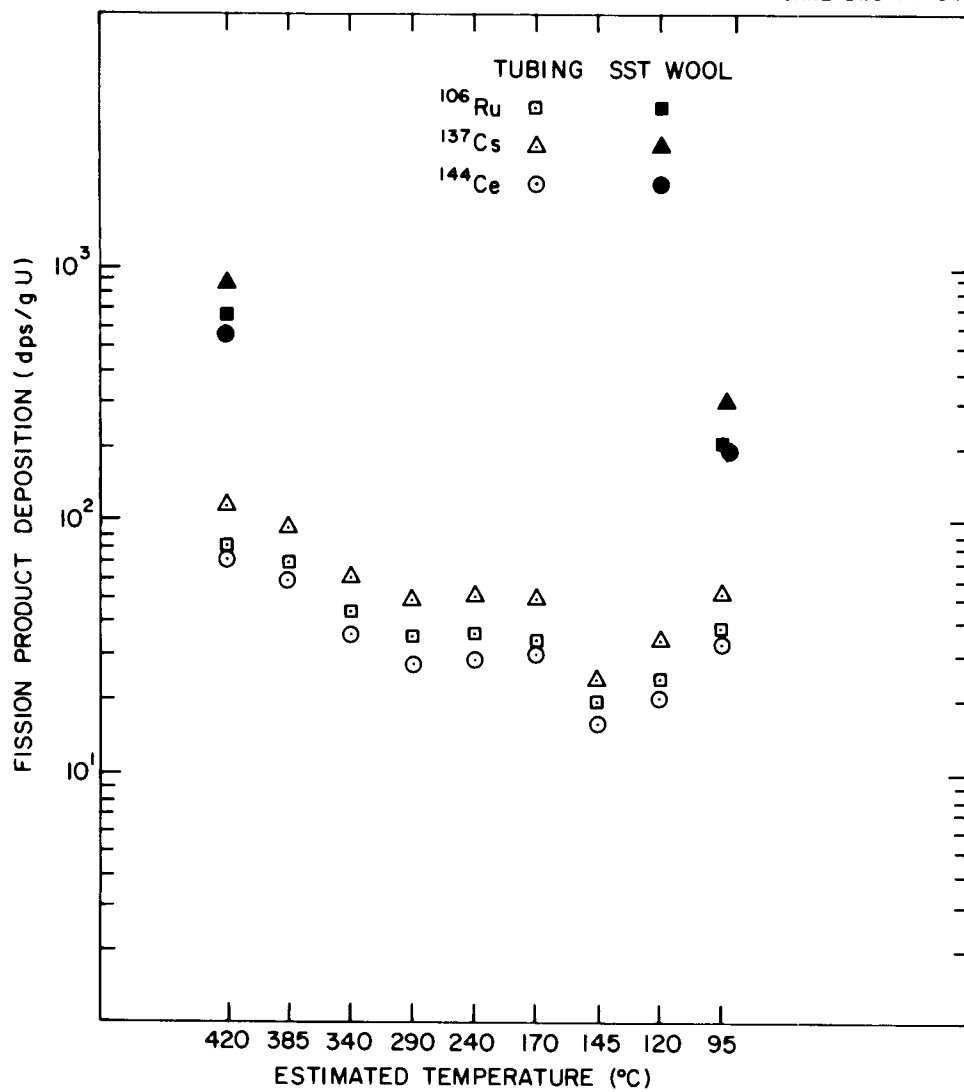


Fig. 2.11. Fission product deposition from voloxidizer off-gas (run LWR-2).

The fission product recoveries in the voloxidizer system are listed as a percent of the initial contents into the burner (Table 2.8). Agreement between the replicate experiments is good except for ^{14}C release; we have been experiencing some sampling and analysis problems. At this time, the higher value of 38.6% of total released would seem to be more correct. Results from the third voloxidation run tend to verify this fact. Typically low ^{85}Kr releases (~6.0% of total) have been the case for each run; these low releases are in general agreement with anticipated values based on earlier voloxidations of LWR fuels.⁵

Recoveries of tritium ($^3\text{H}_2\text{O}$ vapor) in the voloxidizer system have been consistently within the 70 to 75% range. Dissolution of the oxidized product from the first three runs and analysis of the dissolver solution for tritium indicates the effectiveness of tritium release by voloxidation: LWR-1, 97%; LWR-2, 98.9%; and LWR-3, >99% of total.

The net amounts of ruthenium, cesium, and cerium activity associated with the burner walls and the immediate downstream gas system were each less than 0.02% of the total. The preliminary ^{129}I results indicate less than 1.0% volatilization; however, the exactness of this figure is questionable until difficulties with iodine analyses in dissolver solutions are resolved.

Though no direct effort was made to look for the alpha activity distribution in the downstream system, analyses from the first NUMEC fast reactor fuel voloxidation have shown that only small quantities of gross alpha activity were present in the deposition tubing and in the steel wool specimens. Even less would be expected in the voloxidation of LWR fuels.

Table 2.8. Fission product recoveries in the voloxidizer system following voloxidation of H. B. Robinson fuel in air at 480°C (LWR-1)

Nuclide	Initial contents ^a (dis sec ⁻¹ g ⁻¹ of uranium)	Found in volox system	
		(dis sec ⁻¹ g ⁻¹ of uranium)	Percent of initial
³ H	9.80 x 10 ⁶	7.28 x 10 ⁶	74.3 ^c
¹⁴ C	1.95 x 10 ^{4b}	4.59 x 10 ³	23.5 ^d
⁸⁵ Kr	3.23 x 10 ⁸	2.10 x 10 ⁷	6.5
¹⁰⁶ Ru	2.53 x 10 ⁹	1.75 x 10 ⁵	0.007
¹³⁴ Cs	1.83 x 10 ⁹	3.01 x 10 ⁵	0.017
¹³⁷ Cs	3.52 x 10 ⁹	6.62 x 10 ⁵	0.019
¹⁴⁴ Ce	2.66 x 10 ⁹	3.48 x 10 ⁵	0.013
¹²⁹ I	152 ^b (μg/g of uranium)	1.36 (μg/g of uranium)	0.89

^aDetermined from LWR-1A dissolution of nonoxidized fuel (Sect. 2.3.5).

^bBased on average values from D. O. Campbell's dissolutions.

^cDissolution of oxidized fuel indicates 97.0% tritium was released during the LWR-1 voloxidation and 98.9% was released during the LWR-2 voloxidation.

^dValue from LWR-2 voloxidation indicates ¹⁴C release at 38.6%.

A report covering the head-end reprocessing of H. B. Robinson fuels is now in progress.

2.3.5 Dissolution studies

Recovery of fissile values. Dissolutions of oxidized and nonoxidized UO_2 from the H. B. Robinson-2 reactor (Fig. 2.12) were made in conjunction with the voloxidation studies in the previous section. The general procedure was as follows:

1st leach: 7 M HNO_3 , 92-95°C, 2 hr

2nd leach: 3 M HNO_3 , 92-95°C, 2 hr

3rd leach: 7 M HNO_3 , 92-95°C, 2 hr

4th leach: 8 M HNO_3 - 0.05 M HF, 92-95°C, 2 hr

The successive leaches with nitric acid simulated fresh dissolvent, spent dissolvent, and fresh dissolvent contacting the leached hulls. The fourth leach (HF) was to dissolve PuO_2 from the residue for material balance purposes (in absence of Zircaloy). The insoluble residues were submitted for complete analysis after drying and weighing.

In most casts the first leach was conducted in Pyrex flasks (125- to 1000-ml volume) fitted with a purge gas inlet, reflux condenser, connecting tubing, an empty Pyrex trap to collect entrained moisture, a fritted glass gas dispersion tube in a caustic scrubber bottle, a 600°C copper oxide trap, and a second trap and caustic scrubber. The off-gases were then passed through a HEPA filter and into a ^{85}Kr monitor and collection system. The first leach solution was separated from the washed cladding and then centrifuged. The insoluble residue was washed with dilute nitric



Fig. 2.12. Zircaloy-clad UO₂ before and after voloxidation.

acid. The cladding and residue were usually given further treatment in parallel operations in smaller vessels, for example, centrifuge cones, small bottles, etc.

Some dissolutions were made with the UO_2 or U_3O_8 alone, while the Zircaloy-4 cladding was present in the other (Table 2.9).

Run 1A was made with sheared fuel only, and runs 1B, 1C, 2A, and 3A were made with voloxidized fuel. Segments of leached Zircaloy-4 cladding from two experiments were dissolved in 10 M HF-0.05 M HNO_3 (as per Sect. 2.2) or in 6 M NH_4F -1 M NH_4NO_3 (Zirflex reagent) for the determination of the heavy metal, fission product, and tritium contents.

The principal point to notice in Table 2.9 is that voloxidation increased the weight of insoluble residue by factors of about 2 to 3, that is, from about 0.2 wt % to about 0.6 wt %. The quantities of undissolved uranium and plutonium in the residues also increased (Table 2.10).

Plutonium weights were calculated on the basis of a specific activity of 4.14×10^8 alpha counts $min^{-1} mg^{-1}$ of plutonium. This value was derived from an earlier plutonium isotopic analysis and the specific activity of each isotope:

$$^{238}Pu \ 1.56\% \times 1.97 \times 10^{10} \text{ counts } min^{-1} \ mg^{-1} = 3.073 \times 10^8 \text{ counts } min^{-1} \ mg^{-1}$$

$$^{239}Pu \ 55.79\% \times 6.95 \times 10^7 \text{ counts } min^{-1} \ mg^{-1} = 3.877 \times 10^7 \text{ counts } min^{-1} \ mg^{-1}$$

$$^{240}Pu \ 24.91\% \times 2.70 \times 10^8 \text{ counts } min^{-1} \ mg^{-1} = 6.726 \times 10^7 \text{ counts } min^{-1} \ mg^{-1}$$

$$^{241}Pu \ 12.29\% \times \text{no alpha}$$

$$^{242}Pu \ 5.45\% \times 4.41 \times 10^6 \text{ counts } min^{-1} \ mg^{-1} = \frac{2.404 \times 10^5 \text{ counts } min^{-1} \ mg^{-1}}{4.136 \times 10^8 \text{ counts } min^{-1} \ mg^{-1}}$$

Isotopic analyses were later performed on the first leach solutions from two dissolutions of the H. B. Robinson fuel from Rod No. G-10

Table 2.9. Material balance on dissolution of UO_2 or U_3O_8
 (H. B. Robinson-2 reactor, Zr-4 cladding, UO_2 at about 31,000 MWd/ton)

	Run				
	1A	1B ^b	1C ^b	2A ^b	3A ^b
<u>Inputs, g</u>					
U_3O_8 , measured	0.00	18.5	97.8	19.0	75.2
UO_2	29.75	17.81 ^a	94.14 ^a	18.29 ^a	72.38 ^a
Cladding	<u>6.75</u>	<u>0.00</u>	<u>23.30</u>	<u>0.19</u>	<u>0.00</u>
Total, as UO_2	36.50	17.81	117.44	18.48	72.38
<u>Outputs, g</u>					
UO_2	29.46	17.68	93.19	18.53	73.38
Residue	0.05	0.11	0.42	0.11	0.53
Cladding	<u>6.75</u>	<u>0.00</u>	<u>23.30</u>	<u>0.19</u>	<u>0.00</u>
Total	36.26	17.79	116.91	18.83	73.91
Recovery, %	99.3	99.9	99.6	101.9	102.1
Residue, wt % of fuel	0.18	0.60	0.45	0.57	0.72

$${}^aUO_2 = U_3O_8 \times 0.963.$$

^bVoloxidized at 480°C in air.

Table 2.10. Uranium and plutonium dissolved in successive leaches

Leach	HNO ₃ (M) ³	HF (M)	Time (hr)	Amount dissolved each leach - Percent of total									
				Run 1A ^a		Run 1B		Run 1C		Run 2A		Run 3A	
				U	Pu	U	Pu	U	Pu	U	Pu	U	Pu
1	7	0	2	99.99	99.99	99.98	99.96	99.93	99.72	99.99	99.97	99.98	99.97
2	3	0	2					0.05	0.14				
3	7	0	2					0.001	0.02				
4	8	0.05	2					<0.001	0.003				
Residue				0.001	0.004	0.010	0.038	0.004	0.009	0.012	0.017	0.018	0.026

^aNot oxidized before dissolution.

(Table 2.11) and result in a specific activity of 4.359×10^8 counts $\text{min}^{-1} \text{mg}^{-1}$. These slightly different values would make about a 5% decrease in the calculated weights of plutonium in these experiments, and would be uniformly distributed across all samples.

More residual uranium and plutonium were found when the leached cladding segments were dissolved with Zirflex reagent (6 M NH_4F -1.0 M NH_4NO_3) than when dissolved with 10 M HF -0.05 M HNO_3 (Table 2.12). Further tests are indicated, since the 2.05×10^5 plutonium alpha counts $\text{min}^{-1} \text{g}^{-1}$ of Zr-4 in run 1A is equivalent to about 92 $\mu\text{Ci}/\text{kg}$ of Zr-4, or about ten times the limit of 10 $\mu\text{Ci}/\text{kg}$ for consideration as alpha-free waste. (Note: these values are typical of unpublished hot-cell results from earlier experiments on leaching irradiated PWR-1 blanket rods when cross-contamination was suspected. When that leached cladding was removed from the cell and dissolved in a laboratory hood to minimize cross-contamination, we found about 10 to 16 $\mu\text{Ci}/\text{kg}$ of Zr-2.)

Fission product distribution in dissolution. Fission products present in the mid-portion of rod G-10 used in these tests were determined by radiochemical analysis and by gamma spectroscopy on leach solutions and residues. Concentrations were also calculated using the ORIGEN code for comparison. Table 2.13 summarizes analytical data received thus far. There appears to be reasonable agreement between the different experimenters at ORNL and at SRL for the major nuclides. Results for ^{137}Cs and ^{144}Ce have the poorest agreement. The experimental values do not agree as well with some of the ORIGEN estimates. Some of the ORIGEN input data may be

Table 2.11. Isotopic analyses of fuel solutions from H. B. Robinson rod
No. G-10, Assembly B05

Mass	Atom percent	
	Run IWR-1	Run IWR-2
^{233}U	≤ 0.001	≤ 0.001
^{234}U	0.013	0.015
^{235}U	0.629	0.628
^{236}U	0.354	0.354
^{238}U	99.00	99.00
^{238}Pu	1.66	1.63
^{239}Pu	54.62	55.00
^{240}Pu	26.18	26.20
^{241}Pu	11.69	11.30
^{242}Pu	5.85	5.87

Table 2.12. Effect of dissolvent on amount of uranium and plutonium found in/on irradiated cladding

Run	Uranium (milligrams per gram of Zr-4)		Plutonium (alpha counts min ⁻¹ g ⁻¹ of Zr-4)	
	10 M HF-0.05 M HNO ₃ dissolvent	6 M NH ₄ F-1 M NH ₄ NO ₃ dissolvent	10 M HF-0.05 M HNO ₃ dissolvent	6 M NH ₄ F-1 M NH ₄ NO ₃ dissolvent
1A	0.006	0.071	4.00 x 10 ⁴	2.05 x 10 ⁵
1Ca	0.003	0.095	4.18 x 10 ⁴	7.60 x 10 ⁵
1Cb	0.015		5.00 x 10 ⁴	

Table 2.13. Comparison of experimentally determined fission product content with calculated values (H. B. Robinson-2, rod G-10, assembly B05)

Nuclide	SRL ^a	ORNL ^b	ORIGEN ^c	ORNL/ORIGEN (%)
	(dis sec ⁻¹ g ⁻¹ of uranium)	(dis sec ⁻¹ g ⁻¹ of uranium, av)	(dis sec ⁻¹ g ⁻¹ of uranium)	
³ H ₂	9.06E06	(8.50 ± 2.01)E06 ^d	1.76E07	48 ± 11
¹⁴ C	NR	(1.50 ± 0.95)E04	1.97E04	76 ± 48
⁸⁵ Kr	NR	(3.18 ± 0.63)E08	2.66E08	120 ± 24
⁹⁹ Tc ^e	NR	NA	7.10E02 ^e	NA
¹⁰⁶ Ru	2.53E09	(2.16 ± 0.46)E09	3.08E09	73 ± 12
¹²⁵ Sb	NR	(7.64 ± 3.16)E07	1.92E08	40 ± 16
¹²⁹ I ^e	164.5 ^d	152 ^{e, f}	1.87E02 ^e	81
¹³⁴ Cs	1.52E09	(1.74 ± 0.20)E09	3.10E09	54 ± 7
¹³⁷ Cs	2.71E09	(3.39 ± 0.29)E09	3.62E09	93 ± 5
¹⁴⁴ Ce	3.65E09	(2.47 ± 0.44)E09	3.13E09	80 ± 8

^aDPST/LWR-76-1-3.

^bResults of this section and those of Sect. 2.2 of this report are averaged together.

^cComputer run made for 4-1-77 decay data.

^dDoes not include tritium associated with the cladding.

^eMicrograms per gram of uranium.

^fCampbell only.

NR = not reported.

NA = not available yet.

incorrect. We found more ^{85}Kr than calculated and less ^{99}Tc , ^{106}Ru , ^{125}Sb , and ^{134}Cs . The analysis for ^{99}Tc in the presence of ^{106}Ru -Rh is also giving problems.

Table 2.14 summarizes the distribution of selected fission products in the dissolver off-gas system for the base-line run with nonoxidized fuel. Most of the fission products were contained in the dissolver solution and residue. Only traces of tritium and ^{14}C were found in the traps and scrubbers; however, greater than 95% of the ^{129}I carried by the purge gas stream was found in the first caustic scrubber. Table 2.15 summarizes two dissolutions of voloxidized H. B. Robinson fuel in nitric acid. Only traces of tritium and other fission products were volatilized, except for ^{14}C and ^{129}I , which reported to the first scrubber.

Fission products in dissolution residues. The composition of the dissolution residue has been well established as a mixture of molybdenum, technetium, the noble metals, and small amounts of zirconium.⁶ Analyses by SSMS and emission spectroscopy (ES) of the residues from three of these runs, LWR-1A, LWR-1B, and LWR-1C, were in fair agreement:

Element	Residue composition, wt %			
	LWR-1A	LWR-1B	LWR-1C	
	SSMS	SSMS	SSMS	ES
Tc	~2.0	2.0	3.0	8.0
Pd	6.0	7.0	10.0	10.0
Ru	35.0	40.0	30.0	45.0
Rh	0.25	0.20	1.0	5.0
Mo	15.0	13.0	10.0	30.0
Zr	6.0	5.0	<1.0	1.0
Sr	<1.0	1.0	<1.0	

Table 2.14. Distribution of selected fission products during dissolution of H. B. Robinson-2 fuel in nitric acid (not oxidized)

Nuclide	Percent of total found in -				
	Dissolver and residue	Condenser, tubing, and spray trap	First scrubber	Second trap	Second scrubber
α	99.99	0.001	0.006	<0.001	<0.001
$^3\text{H}_2$	99.24	0.09	0.34	0.03	0.03
^{14}C	99.99 ^a	<0.001	<0.001	<0.001	<0.001
^{106}Ru	99.98	0.001	0.005	0.001	0.001
^{129}I	4.6	<0.001	95.4	<0.001	<0.001
^{137}Cs	99.99	<0.002	0.004	0.002	0.002
^{144}Ce	99.99	<0.002	0.001	0.002	0.002

^aThis may be an anomalous result since it is in complete disagreement with results of other tests in which essentially all of the ^{14}C was evolved during dissolution (see Table 2.4).

Table 2.15. Distribution of selected fission products during dissolution of voloxidized
H. B. Robinson-1 fuel in nitric acid

Nuclide	Percent of total found in --				
	Dissolver and residue	Condenser, tubing, and spray trap	First scrubber	Second trap	Second scrubber
γ	99.98-99.99	<0.001-0.002	<0.001-0.015	<0.001-0.002	<0.001-0.002
$^3\text{H}_2$	99.78-99.99 ^a	<0.01-0.13	<0.001-0.02	<0.001-0.07	0.001
^{14}C	1.21-1.37	<0.001	92.52-98.79	<0.001	<0.001-4.89
^{106}Ru	99.98-99.99	<0.001-0.002	<0.001-0.015	<0.001-0.004	0.001-0.002
^{129}I	0.37-94.8	<0.03-0.13	4.94-99.50	<0.001	<0.001
^{137}Cs	99.98-99.99	<0.001-0.002	<0.001-0.005	<0.001-0.006	<0.001-0.003
^{144}Ce	99.98-99.99	<0.001-0.002	<0.001	<0.001-0.009	<0.001-0.002

^aPercent of total tritium found; 97% of original tritium in fuel released by voloxidation in Run LWR-1.

Calculations, based on the ^{106}Ru content of each of the residues above, on the specific activity of ^{106}Ru (2.95×10^{-4} g/ci), and on the isotopic fraction of ^{106}Ru to total ruthenium (0.01031), indicated a slightly lower, but similar, ruthenium content in each of the residues:

Run	Total Ru-106 (dis/sec)	Calculated ruthenium weight (mg)	Residue weight (mg)	Ruthenium in residue (wt %)
LWR-1A	1.74×10^{10}	13.5	53.0	25.5
LWR-1B	3.17×10^{10}	24.6	106.5	23.1
LWR-1C	1.30×10^{11}	100.6	421.0	24.1

Voloxidation appeared to make more of the total ruthenium insoluble for example, from 27 to 83%, thus contributing to the overall increase in the weight of the residue. Oxidation had little effect on the cesium and rare earths; data for technetium are incomplete.

Run	Oxidized at 480°C	Percent of total isotope found in residue			
		^{99}Tc	^{106}Ru	^{137}Cs	^{144}Ce
LWR-1A	No	95.4	26.8	1.0	<1.0
LWR-1B	Yes	9.8	83.6	<1.0	<1.0
LWR-1C	Yes	29.9	83.8	<1.0	<1.0
LWR-2A	Yes	*	31.1	<1.0	<1.0
LWR-3A	Yes	*	86.8	<1.0	<1.0

*Analyses incomplete.

Fission products in cladding. Segments of leached cladding were dissolved in 10 M HF-0.005 M HNO₃ or in 6 M NH₄F-1 M NH₄NO₃ to determine the residual uranium and plutonium (reported above) and fission products. We found, using the two reagents, little difference in the amounts of fission products associated with the cladding (Table 2.16).

Using the average values for residual fission products from run LWR-1C (above), the weight of cladding and of the uranium in the fuel, we calculated the levels of contamination on the cladding to be:

Nuclide	dis sec ⁻¹ g ⁻¹ of uranium	Ci/MTU	Ci/MTU ^a
¹⁰⁶ Ru	3.12 x 10 ⁶	84	185 ± 39
¹²⁵ Sb	1.46 x 10 ⁷	395	400 ± 29
¹³⁴ Cs	2.38 x 10 ⁶	64	92 ± 11
¹³⁷ Cs	4.88 x 10 ⁶	132	125 ± 9
¹⁴⁴ Ce	Very low	Very low	143 ± 180

^aContamination levels reported by Campbell in ORNL/TM-3760, p. 22.

Based on the weight of leached Zircaloy-4 alone, the amounts associated with waste cladding would be a factor of 3.5 times greater. The differences are probably due to experimental technique.

Tritium in cladding. Analyses of the dissolver solutions by us, by Campbell, and by SRL (Table 2.13) have consistently shown around 50 to 60% of the amount of tritium estimated by ORIGEN. We suspected that the "missing" tritium might be in the Zircaloy cladding. We therefore installed a 600°C copper oxide unit, two traps, and two scrubbers in the off-gas lines from the Zirflex dissolution of cladding segments from

Table 2.16. Dissolution of fission products from cladding

Run	Nuclide, dis sec ⁻¹ g ⁻¹ of Zr-4							
	¹⁰⁶ Ru		¹²⁵ Sb		¹³⁷ Cs		Gross gamma ^a	
	10 M HF	Zirflex	10 M HF	Zirflex	10 M HF	Zirflex	10 M HF	Zirflex
LWR-1A ^b	1.62 x 10 ⁷	2.59 x 10 ⁷	6.64 x 10 ⁷	6.18 x 10 ⁷	2.56 x 10 ⁷	1.19 x 10 ⁷	1.89 x 10 ⁷	2.38 x 10 ⁷
LWR-1C ^c (a)	1.22 x 10 ⁷	9.14 x 10 ⁶	5.13 x 10 ⁷	5.13 x 10 ⁷	1.69 x 10 ⁷	7.53 x 10 ⁶	1.42 x 10 ⁷	1.07 x 10 ⁷
(b)	1.16 x 10 ⁷		5.16 x 10 ⁷		1.74 x 10 ⁷		1.59 x 10 ⁷	
\bar{X} =	1.19 x 10 ⁷	9.14 x 10 ⁶	5.15 x 10 ⁷	5.13 x 10 ⁷	1.72 x 10 ⁷	7.53 x 10 ⁶	1.51 x 10 ⁷	1.07 x 10 ⁷

^aCounts per gram of Zr-4.

^bOne 2-hr leach with 8 M HNO₃.

^cThree 2-hr leaches as per procedure.

runs 1A and 1C. All of the solutions, including the $\text{NH}_4\text{F}-\text{NH}_4\text{NO}_3$ Zirflex reagent and trap rinsings, were analyzed for tritium. We found considerable tritium in the cladding, the amounts found being 70 to 84% of the amounts found in the fuel itself.

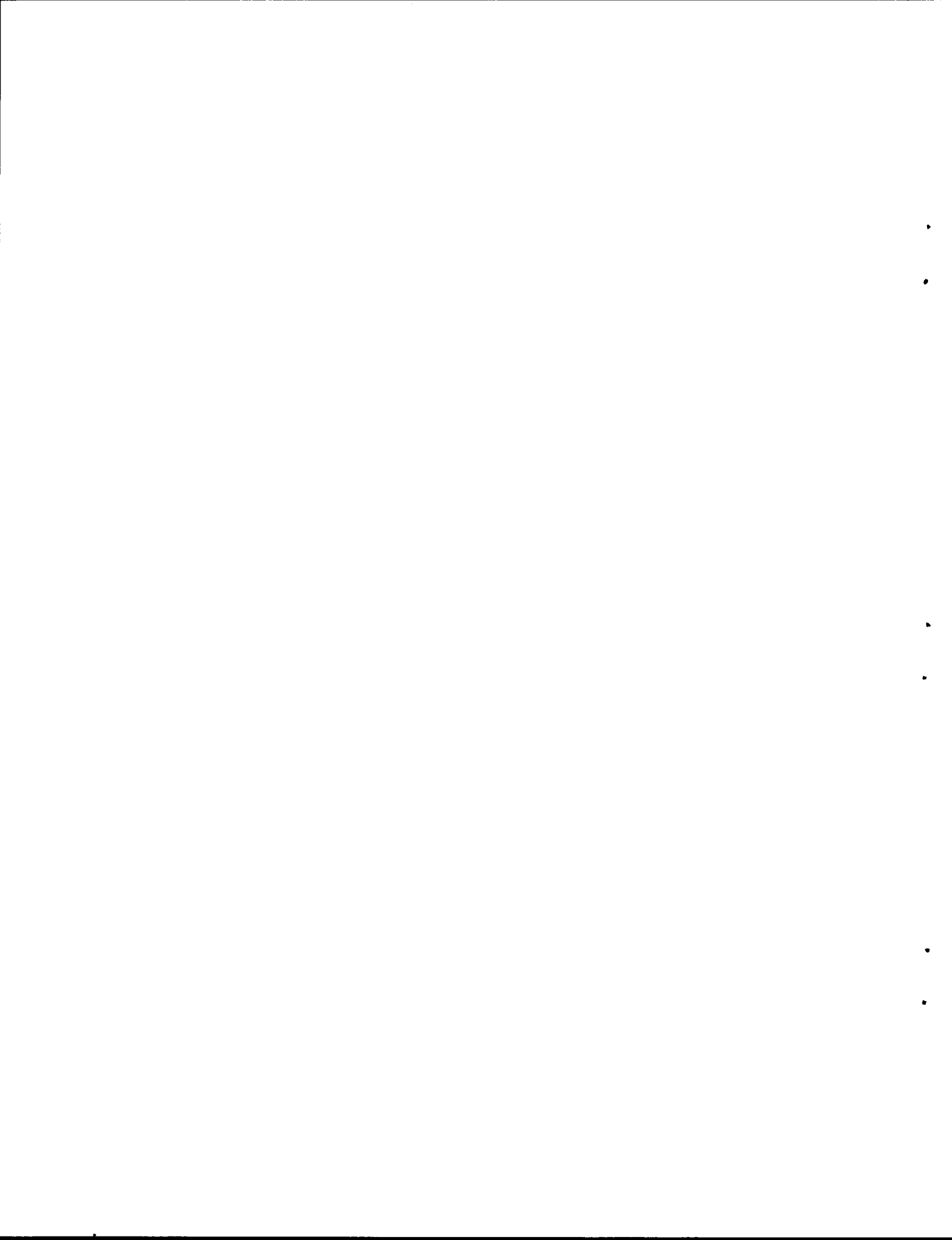
Run	Fuel (total dis/sec)	Cladding (total dis/sec)	dis sec ⁻¹ g ⁻¹ of uranium	ORIGEN dis sec ⁻¹ g ⁻¹ of uranium
LWR-1A	2.54×10^8	2.14×10^8	1.81×10^7	1.76×10^7
LWR-1C ^a	7.51×10^8	5.25×10^8	1.29×10^7	1.76×10^7

^aVoloxidized at 480°C in air. Some tritium was not recovered in trap system.

REFERENCES FOR SECTION 2

1. M. E. Whatley, A Dimensional Analysis of Solids Transport and Dispersion in a Rotary Kiln, ORNL/TM-5898 (in progress).
2. B. L. Vondra, LWR Fuel Reprocessing and Recycle Program Quarterly Report for Period January 1 to March 31, 1977, ORNL/TM-5864 (May 1977).
3. B. L. Vondra, LWR Fuel Reprocessing and Recycle Program Quarterly Report for Period July 1 to September 30, 1976, ORNL/TM-5660, (November 1976).
4. B. L. Vondra, LWR Fuel Reprocessing and Recycle Program Quarterly Report for Period January 1 to March 31, 1977, ORNL/TM-5864 (May 1977).
5. J. H. Goode, Voloxidation-Removal of Volatile Fission Products from Spent LMFBF Fuels, ORNL/TM-3723 (January 1973).

6. B. L. Vondra, LWR Fuel Reprocessing and Recycle Program Quarterly Report for Period October 1 to December 31, 1976, ORNL/TM-5760 (February 1977), pp. 32-33.



3. OFF-GASES - FLUOROCARBON ABSORPTION STUDIES*

M. J. Stephenson (ORGDP)

This task is concerned with the development of the krypton absorption process on an accelerated basis. Funding is provided for the expansion of pilot-plant development, for initiating plant engineering design criteria, for performing a system reliability analysis, and for a study of the chemical effects of impurities in the fluorocarbon solvent on the process and equipment.

3.1 Fluorocarbon Absorption Process Development

M. J. Stephenson (ORGDP)

3.1.1 Pilot-plant operation

B. E. Kanak, R. S. Eby, V. C. Huffstetler, and J. L. Patton (ORGDP)

Pilot-plant tests to further investigate the process behavior of various feed gas components are continuing. The current test series is part of campaign 4. Fractionator column concentration profiles were presented in the last progress report to show the quantitative effect of solvent flow rate and column pressure on the fractionator operation. An interesting krypton-85 concentration peak was measured in each case using an external gamma scintillation scanning device. It was determined that the internal krypton buildup was brought about by a complex sorption-desorption phenomenon centered about a soluble gas pinch point. Additional tests demonstrated that the location of the pinch point could be manipulated

*Jointly funded by LWR Fuel Reprocessing and Recycle Program and the Advanced Fuel Recycle Program.

within the column and subsequently forced to locate at any interior point simply by adjusting relative heat contents of the two phases. It was found that when the pinch point was raised high in the column, enough stripping stages became available to effectively strip all of the dissolved gases from the solvent. If sufficient contact stages were provided both below and above the pinch point, the more soluble components could be greatly concentrated within the column because of the repeated sorption-desorption activity. In fact, during tests with krypton, fractionator internal concentration buildups in excess of 10,000 were measured. Figure 3.1 shows a typical column concentration profile established during one such test. Specifically, this figure presents the concentration ratio of krypton at various places within the column to the amount of krypton at the top or inlet section of the column. It is of significance to point out that the concentration peak always occurred precisely where the column temperature gradient was maintained. Furthermore, in one test, the temperature gradient was established at a section of the column where a gas sampling point was located, and the highly concentrated krypton product was withdrawn from the system to demonstrate the feasibility of pulling the captured fission gas from the system as a side-stream product.

Preliminary tests have been completed to evaluate the effectiveness of the feed gas cooler as a batch cold trap for water removal from a saturated process feed. The introduction of water into the fluorocarbon process is of particular interest as a result of its limited solubility in refrigerant-12. The initial phase of testing was conducted over a continuous 4-day period in which 15.3 scfm of air containing 12,500 ppm (by volume) water was first compressed to an absorber pressure of 150 psig

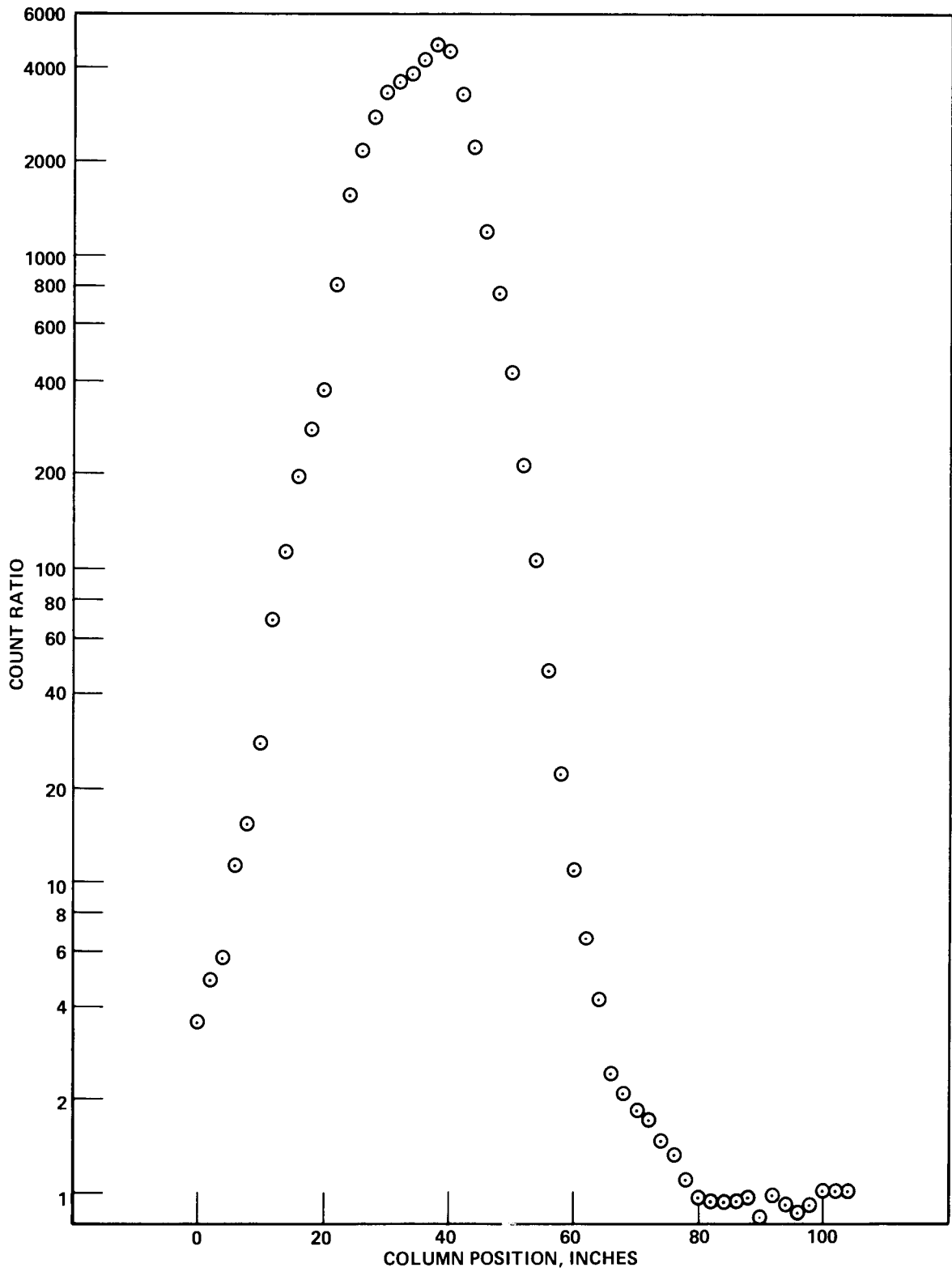


Fig. 3.1. Fractionator column concentration profile during internal column concentration test.

and then fed through the feed gas cooler. By cooling the gas stream down to an outlet temperature of near -20°F the water content was reduced to a level of 55 ppm, which is equivalent to a removal efficiency of 99.6%. This resulting gas stream concentration was approximately one-third the maximum allowable concentration needed to saturate the absorber solvent. It is important to point out that a large quantity of water was condensed in the intermediate and final compressor receiver tanks, indicating a potential need for at least some feed gas pretreatment or else allow the compressor to run hotter, with little or no interstage or afterstage cooling. Additional water removal tests have been conducted and are presently under analysis. These tests support the earlier results by showing that even over a broad range of operating conditions, the water content of the gas leaving the feed gas cooler will remain below the process solvent saturation limits.

Currently, plant tests are being conducted with nitrogen dioxide. Preliminary results indicate that significantly better solvent cleanup can be achieved in the modified solvent still with improved reflux capability. While maintaining a moderate distillate-to-reflux ratio of 0.75 and a nitrogen dioxide feed concentration of 2000 ppm, only 30 ppm was detected in the process off-gas. The current series of tests will continue for approximately one month and will be summarized in the next progress report.

Recurring intermediate hydraulic and liquid flow check-valve problems forced premature replacement of the solvent metering pump with a more reliable regenerative turbine pump. Unlike the metering pump, however, the new unit requires external pressure and flow controls. Approximately

500 hr have been logged on the new pump without incident. Compared with the diaphragm type, the regenerative pump is easier to start-up and maintain because the impeller is the only moving part. A mechanical shaft seal is used and, consequently, will have to be carefully evaluated. Other modifications to the pilot plant include the installation of a mini-absorber and product cold trap. The mini-absorber will allow the evaluation of packed-column diameter and height parameters on overall performance and a comparison of different types of packings. The product cold trap will give the plant sufficient capability to effect a krypton-xenon-carbon dioxide product separation.

3.1.2 Process application

R. S. Eby and M. J. Stephenson (ORGDP)

One of the objectives of this work is to identify flowsheet options and simplifications that lead to a more economical and/or reliable process. Recently, a new process flowsheet based on a combination absorber-fractionator was proposed. The intrinsic operating and economic advantages of this particular flowsheet were obvious. Figure 3.2 is a schematic of a greatly simplified process based on a combination absorber-fractionator-stripper column. This flowsheet is well founded upon fractionator data taken to quantify the unusual pinch-point phenomenon, and also exploits the internal column concentration buildup behavior shown in Fig. 3.1. Unlike its predecessor, the new process contains only a single packed column within which to conduct the necessary process functions of absorption, fractionation, and stripping. A solvent purification still is needed if the feed gas contains significant amounts of high boiling components such as water, nitrogen dioxide, and iodine.

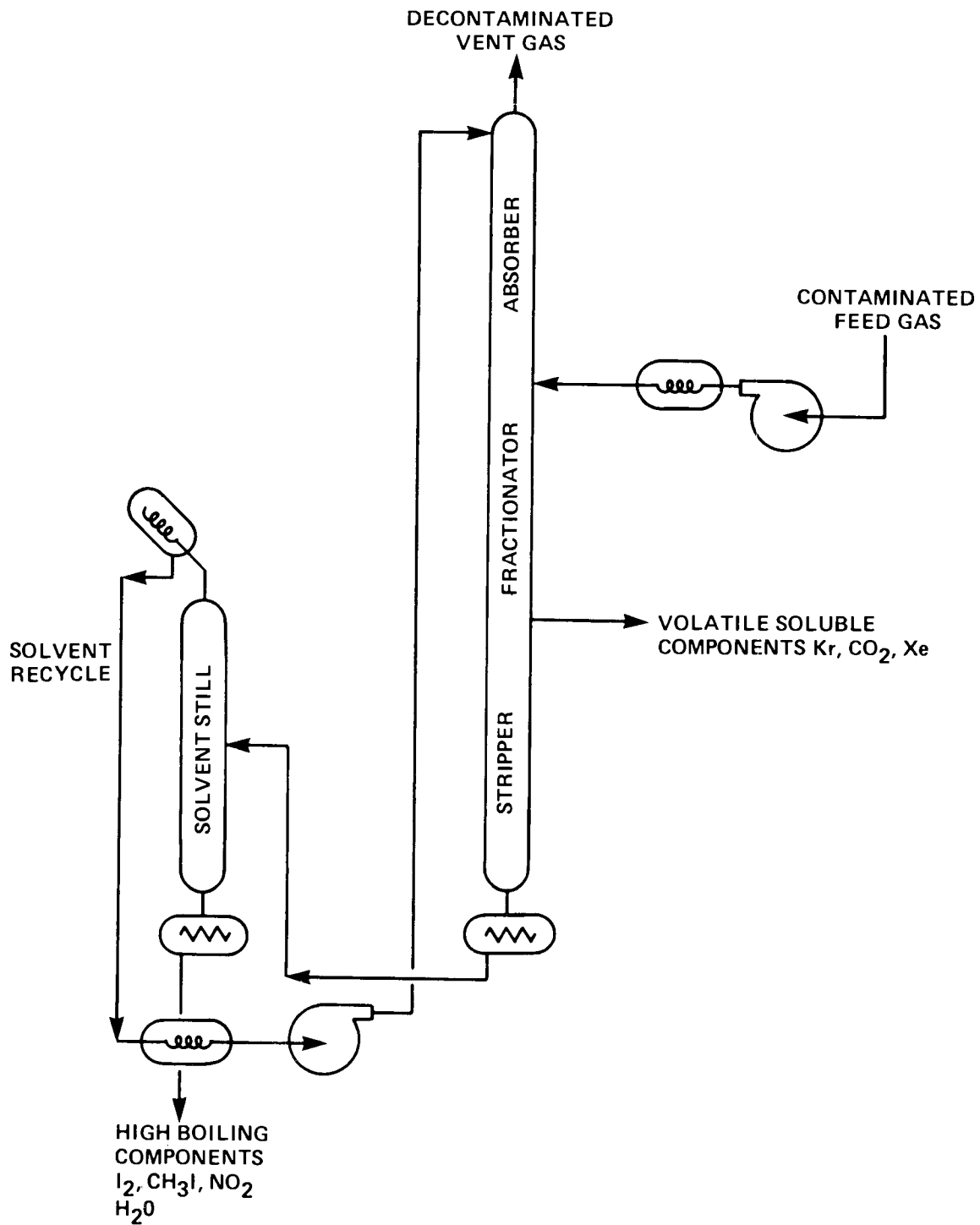


Fig. 3.2. Schematic of the fluorocarbon process based on a combination absorber-fractionator-stripper column.

Decontaminated off-gas flows from the top of the combination column and regenerated solvent flows from the bottom, while the fission product gases are collected as a side stream. The top part of the column, that is, that part above the feed gas point, is the absorption section of the process. The middle section, that is, that part of the column between the product takeoff and the gas feed point, serves as the fractionator. The bottom section, including the reboiler, makes up the stripper. Figure 3.3 shows a possible instrumentation scheme that might be employed for column control. Like the conventional process, the individual sections of the modified plant operate at different solvent-to-gas flow-rate ratios. In fact, in the absence of a pressure gradient, the modified process relies even more heavily upon varying liquid-to-gas (L:G) ratios to achieve the three-regime operation. The dependency of the equilibrium distribution coefficient with temperature also contributes to the success of the combined operation. The absorber L:G is established by the solvent flow rate that is needed to achieve the desired removal of fission products from the feed gas. The fractionator L:G is fixed primarily by the temperature of the downflowing solvent and total pressure of the system. The stripping section L:G is established by the boilup rate required to strip the dissolved gases from the solvent. Product is withdrawn at a column position near the pinch point. An inline column condenser can be added as part of the combination column between the stripper and fractionator zones, as shown in Fig. 3.3, to give the process a greater operating flexibility when the heat content of the required stripping vapor flow is greater than the heat content of the cold downflowing solvent. Specifically, when higher process removals of very soluble components such as

DWG. NO. G-77-243
(U)

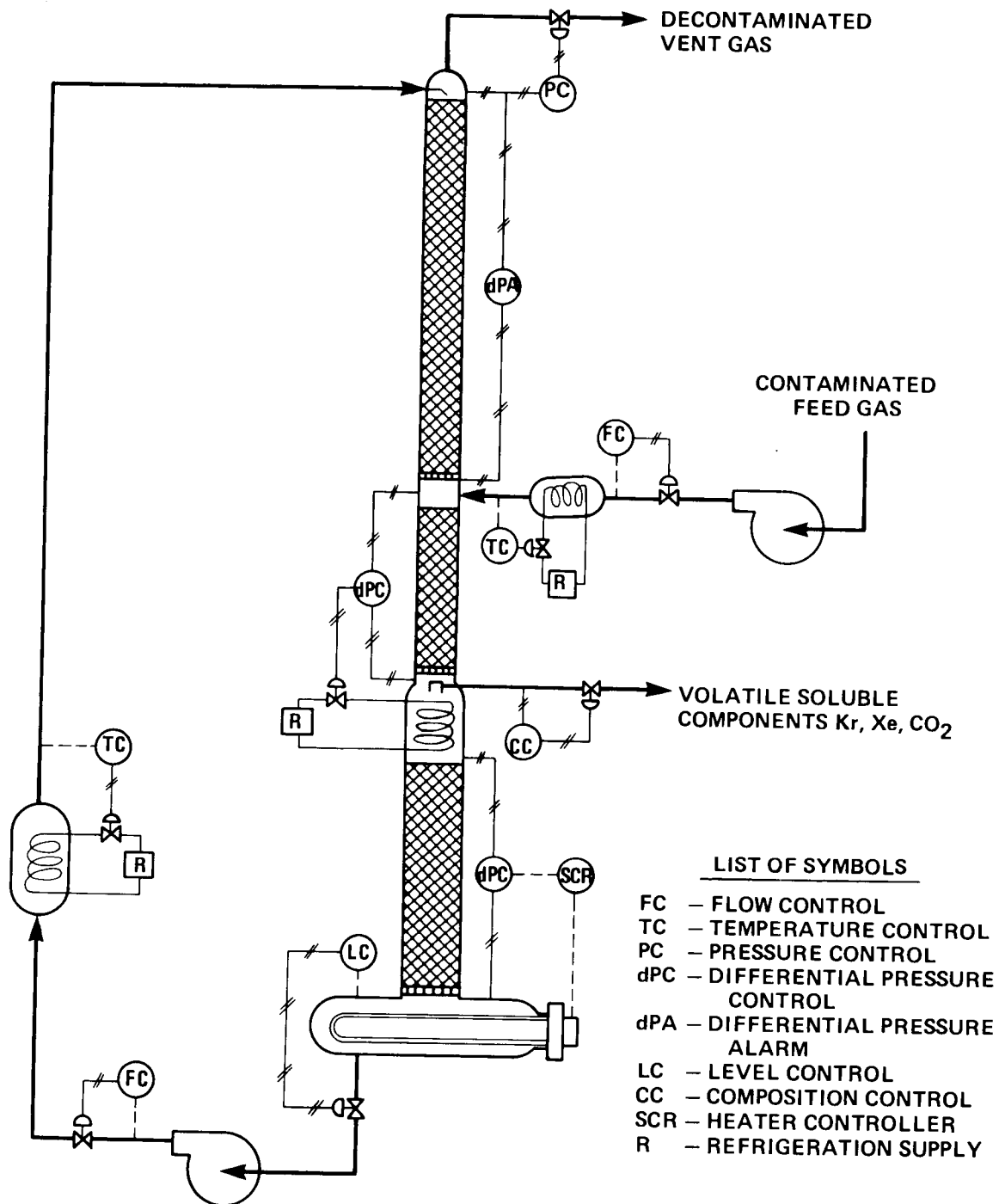


Fig. 3.3. Required control instrumentation for combination column.

xenon and carbon dioxide are needed, it might become necessary to use a higher boilup rate in the stripper to get a more complete cleanup of the recycle solvent.

The new selective absorption process will require substantially less equipment and control instrumentation than the standard version, and because it is a simpler process, one can easily assume that the simplified process will be more economical, easier to control, and more reliable. Also, the simplified plant will obviously occupy less space.

3.2 Chemical Studies of Contaminants in LWR Off-Gas Processing

L. M. Toth and D. W. Fuller (Chemistry Division, ORNL)

Carbon dioxide distribution coefficients in the R-12 gas-liquid system have been analyzed as a function of temperature for CO₂ concentrations of ≤ 4 mole %. The distribution coefficient, $D = X^L/X^V$ (where X is the mole fraction in the liquid (L) and vapor (V) phases respectively), has been fit by least-squares to

$$\log_{10} D = -0.4397 - 174.1/T \quad (T \text{ is degrees Kelvin}) \quad (3.1)$$

These data are shown in Fig. 3.4. The standard error of each term in the above expression is 0.0486 and 12.77 respectively. Distribution data have also been obtained for higher CO₂ concentrations (up to $X_{CO_2}^L \approx 0.9$); however, because these solutions are considerably removed from the dilute solution limits, the corresponding R-12 concentration in each phase must be known before a distribution coefficient expression similar to the one given above can be determined. These R-12 concentration data will be obtained during the coming month.

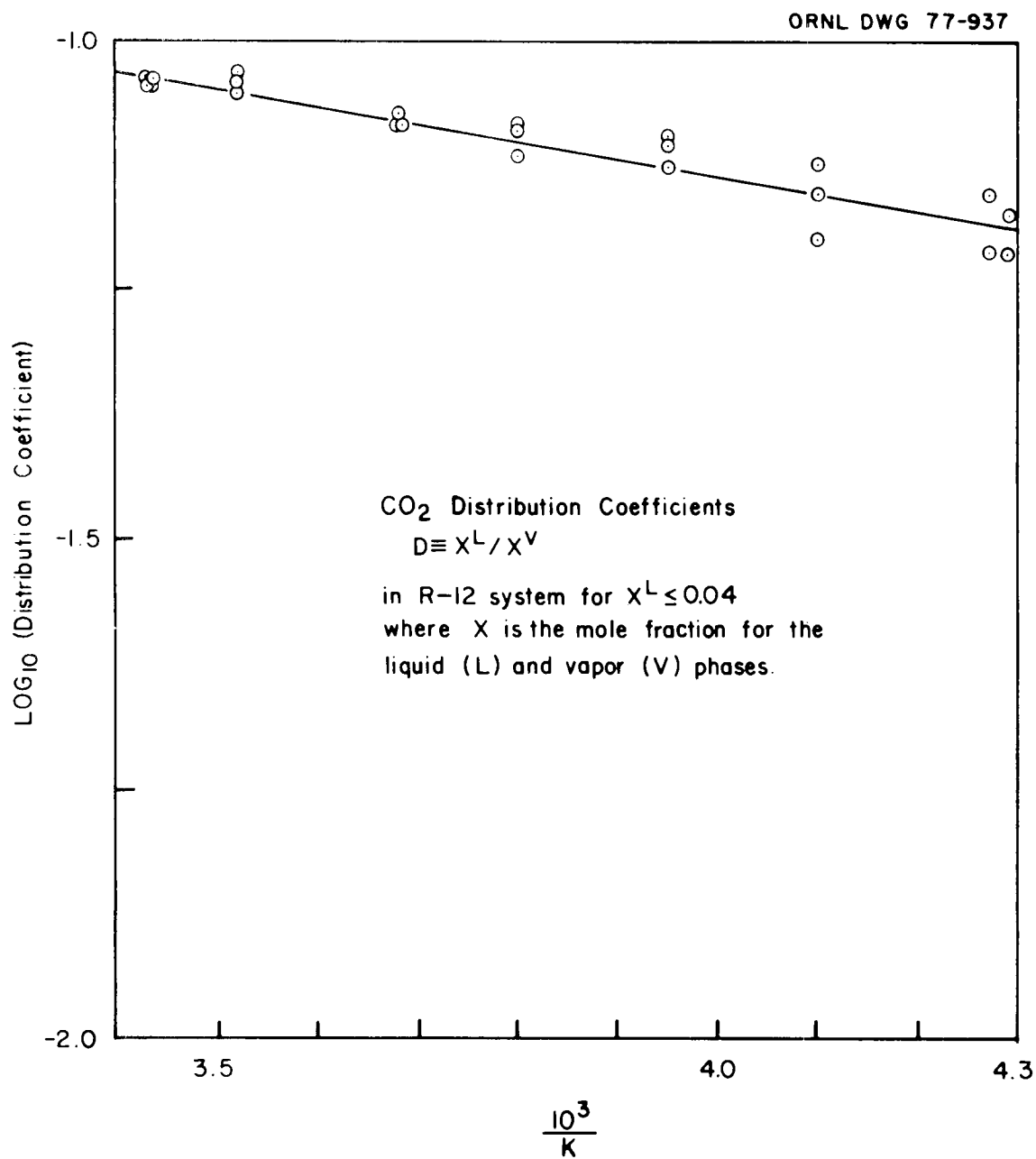
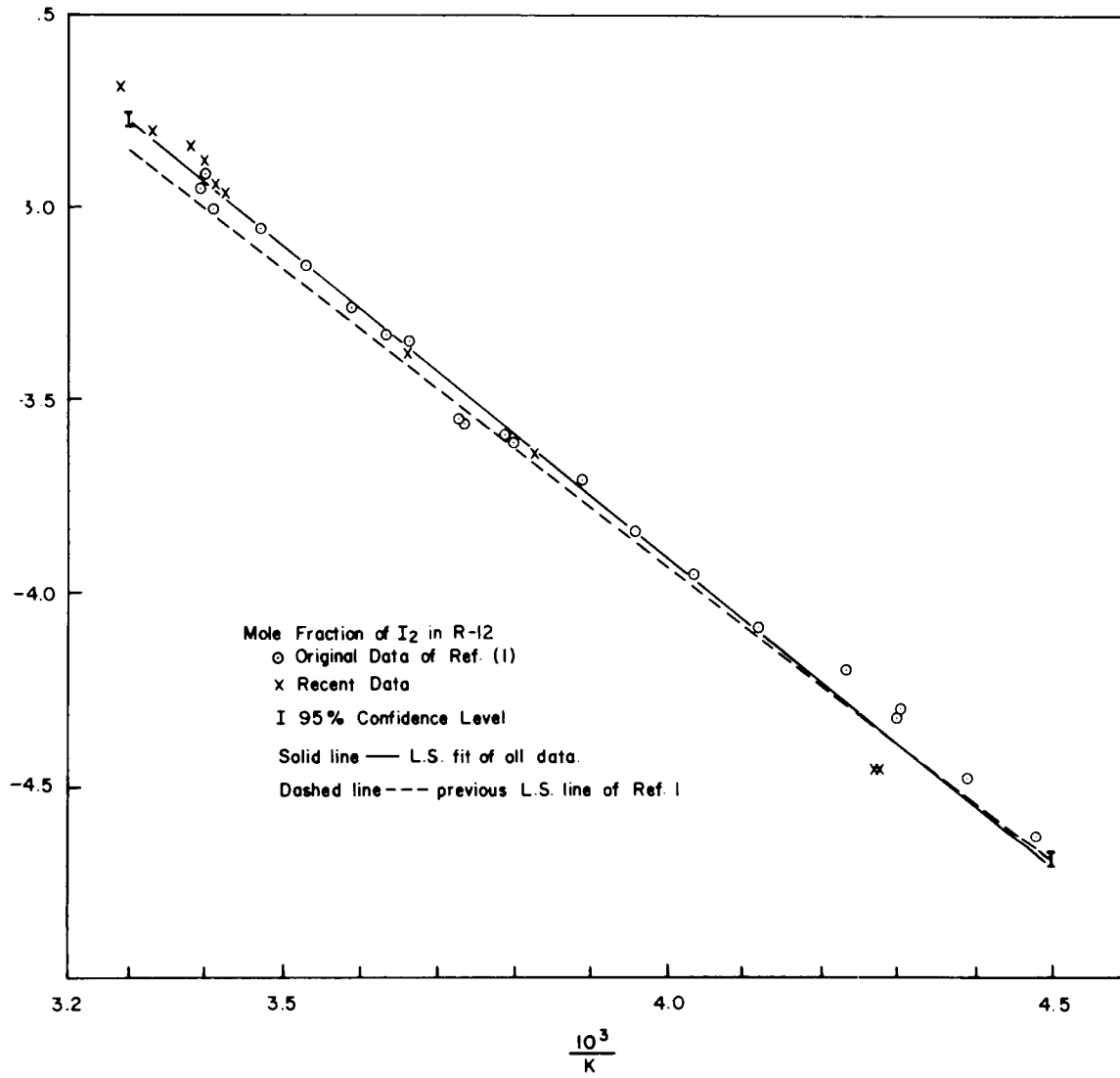


Fig. 3.4. CO₂ distribution coefficients.

With the installation of a new high-pressure spectrophotometric cell and improved rocker system, we have returned to the I_2 - H_2O -304 stainless steel corrosion studies discussed earlier.¹ A principal point we wished to investigate was the possibility that the corrosion loss of I_2 from liquid R-12 was a first-order reaction rate process, independent of the added water as long as the R-12 remained saturated, that is, there was a constant activity of water in solution. We have recently found that the I_2 loss rate at 0°C decreases with the amount of added water for water concentration equivalent to 50 to 100 ppm. This decrease suggests that the corrosion rate is determined instead by the rate of water dissolution in R-12. Other aspects of the corrosion mechanism to be sought in the near future will be: (1) the difference in the corrosion rate and mechanism caused by temperature changes and (2) the maximum acceptable concentration limits of water in the system.

Further aspects of the I_2 solubility have been considered in view of comments from J. R. Merriman² suggesting that our entropies of solution for I_2 in R-12 deviated from similar entropies derived by Hildebrand et al.³ These entropies can be derived from the solubility data, realizing that the entropy of solution is given by $R d(\ln X^I)/d(\ln T)$. Therefore, by differentiating our expression² for the I_2 solubility, we obtain a value of 23.7 eu at 298 K where a value approximately 2 eu higher is expected. The major source of error in our measurement of I_2 solubility rested with the determination of the molar extinction coefficient, ϵ , for the 520-nm band of I_2 . We had previously used a value of 832 liters mole⁻¹ cm⁻¹, which was suspiciously about 10% high in comparison with I_2 in other solvent systems. Recalibration led to an improved

Fig. 3.5. Mole fraction of I₂ in R-12.

value of $\epsilon = 759 \text{ liters mole}^{-1} \text{ cm}^{-1}$. When this value was used to correct the data given earlier, a proportional increase in the I_2 solubility was obtained. These corrected data are shown in Fig. 3.5 plotted as open circles along with the least-squares line (dashed) from the original solubility expression.¹ A repeat of the solubility measurements with the improved spectrophotometric cell and rocker system produced essentially the same results (shown as crosses in Fig. 3.5) as found earlier. A least-squares fit of all these data yields

$$\log_{10}(I_2) = 2.575 - 1620/T \quad (3.2)$$

The 95% confidence limits on these data are shown as bars in Fig. 3.5 at each limit of the data. Within the error in the measurements, we find no serious disagreement in the measured and predicted entropies of solution. It is probable that further repetition of these measurements could reduce the error still further if greater precision were necessary. Because the molar extinction coefficients cancel out of the distribution coefficient expression (assuming $\epsilon_L = \epsilon_V$), no change in the distribution coefficient data is warranted.

REFERENCES FOR SECTION 3

1. L. M. Toth, D. W. Fuller, and J. T. Bell, "Chemical Studies of Contaminants in LWR Off-Gas Processing," in LWR Fuel Reprocessing and Recycle Program Quarterly Report for Period April 1 to June 30, 1976, ORNL/TM-5547 (August 1976).
2. Personal communication with J. R. Merriman, Paducah Gaseous Diffusion Plant. See for example J. R. Merriman "The Solubility of Gases in CCl_2F_2 . A Critical Review," KY-G-400 (March 1977).

3. J. H. Hildebrand, J. M. Prausnitz, and R. L. Scott, "Regular and Related Solutions," Van Nostrand Reinhold, New York (1970), p. 145.

4. PUREX PROCESS STUDIES (SOLVENT EXTRACTION)

B. L. Vondra (Chemical Technology Division, ORNL)

This program involves the integration of laboratory development studies, flowsheet tests employing synthetic solutions, and confirmatory investigations in a hot-cell system using irradiated LWR fuels.

The design and procurement of equipment for the larger-scale Purex facility is proceeding. Hot cell 4 in Building 4507 has been committed to hot operation for head-end studies using typical LWR irradiated fuel. Specific results are reported in the following sections.

4.1 Laboratory Studies

J. C. Mailen (Chemical Technology Division, ORNL)

4.1.1 Solvent cleanup

O. K. Tallent and Karen Williams (Chemical Technology Division, ORNL)

Introduction. The objective of this work is to evaluate and develop new and improved Purex solvent cleanup methods. Results were previously reported from tests that used macroreticular resins to remove solvent degradation products and various actinide and lanthanide ions from both unirradiated¹ and irradiated² solvents. Both cation and anion macroreticular resins have been shown to be highly effective in adsorbing impurities from the solvents. Thus the macroreticular resin method, based on batch equilibration tests and distribution coefficient data, appeared until recently to be a highly promising method.

More recent tests with the resins, however, have indicated two potential problem areas: (1) While the resins load well, they do not consistently elute well. We are investigating the possibility that two

types of substances load onto the resins: precipitated substances that elute poorly and ionic substances in solutions that elute well. We expect to report further on this aspect of the work later. (2) A second, and possibly more serious, problem is that the resins appear to be physically and chemically degraded in the TBP-dodecane solvent. A typical example of results from resin degradation tests is reported and discussed below.

Experimental conditions. Four 1.0-g samples of 20 to 50 mesh, A-29, macroreticular, strongly basic, anion resin were each contacted with 10 ml of 30% TBP-70% dodecane solvent at room temperature for contact times of 1 or 5 hr. Two of the resin samples were stirred in the solvent with a Teflon-coated stirring bar at a rate of about 30 rpm. The other two samples were allowed to stand in contact with the solvent without stirring for the same 1- and 5-hr contact times. The resins, after being contacted, were filtered from the solvent with a coarse glass frit and washed with dodecane. Samples of the resin were then air dried and inspected, using an optical microscope. Infrared spectra of the TBP-dodecane filtrates were recorded and analyzed by J. R. Lund, Analytical Chemistry Division.

The A-29 resin used in the tests was converted from the Cl^- to the OH^- form prior to the tests.

Results. After contact with the solvent, the samples of resin were in most instances physically and chemically degraded. Microscopic examinations of the samples revealed that many of the resin beads were pitted and flawed and that the samples contained significant amounts of powder and chips. Microphotographs (a), (b), (c), and (d) in Fig. 4.1 are of the original resin, resin after 5 hr of unstirred contact, resin after 1 hr of stirred contact, and resin after 5 hr of stirred contact respectively.

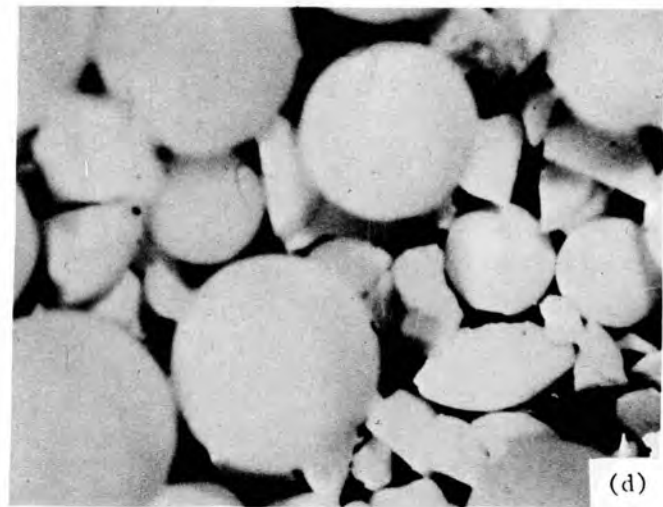
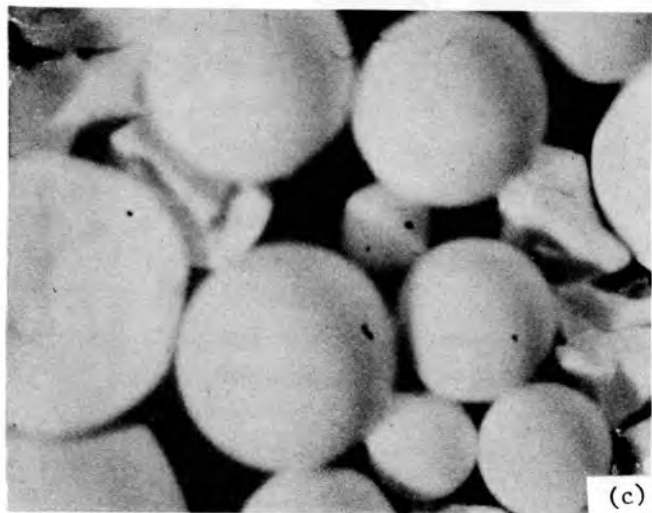
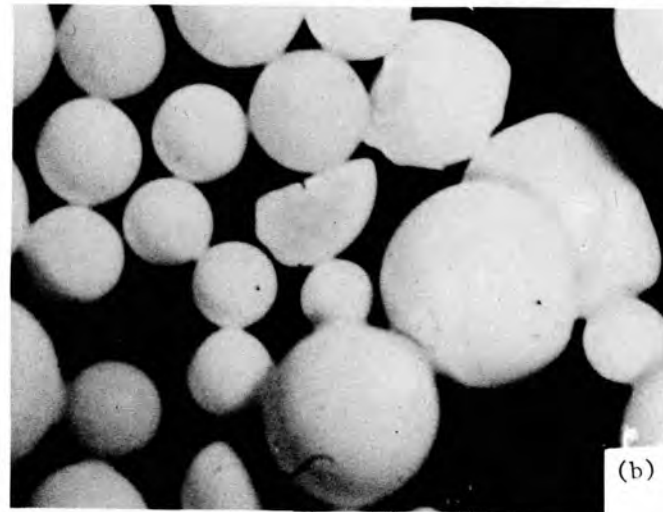
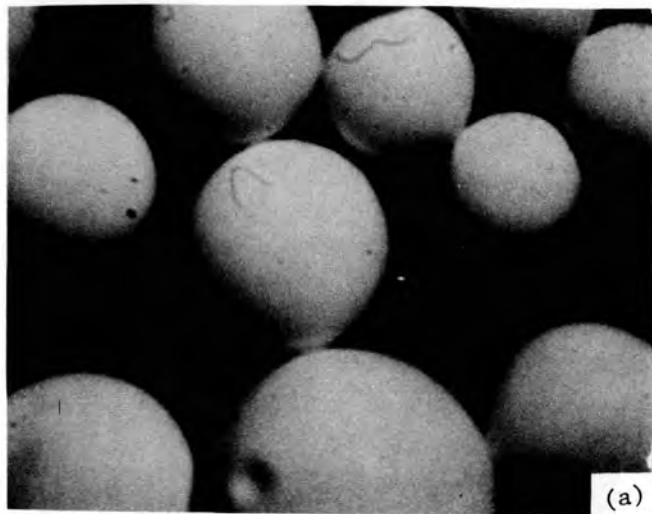


Fig. 4.1. Degradation of A-29 macroreticular resin in 30% TBP-70% dodecane: (a) original, unstirred 5 hr, (c) stirred 1 hr, and (d) stirred 5 hr.

While the chipping and breaking apart is much worse in the stirred samples, the microphotographs show that the effect can also be seen in the unstirred samples.

Evidence for chemical degradation of the resin samples is shown by the infrared spectra in Fig. 4.2. Spectrum (a) is of pure 30% TBP-70% dodecane solvent that is uncontacted with resin, spectrum (b) is of solvent after 5 hr of unstirred contact with the resin, and spectrum (c) is of solvent after 5 hr of stirred contact with the resin. The bands in spectra (b) and (c) at about 1650 and about 1800/cm for the solvents contacted with the resin are characteristic of infrared spectra for aromatic substances.³ Dissolved styrylbenzene-like substances from the resin would be expected to show a strong band at about 1650/cm and weak bands at about 1800/cm and about 3030/cm in their spectra.⁴ The band at 3030/cm does not show in spectra (b) and (c), probably because of the proximity of the strong aliphatic band at 3000/cm. Bands at approximately 850, 1175, 1350, and 1430/cm in spectra (b) and (c) are thought to indicate other dissolved impurities, possibly amines dissolved from the resin; however, these impurities have not been identified at the present time.

Discussion. The stabilities of a number of macroreticular resins in 30% TBP-70% dodecane are being tested in the current investigation. The A-29 resin was chosen for this preliminary report because it has previously been used by other investigators⁵ in solvent cleanup experiments. This resin, which is a strongly basic macroreticular anion resin, was formerly manufactured by the Rohm and Haas Company. At the present time, the resin is not commercially available. The physical and chemical instability of this resin, in and of itself, in TBP-dodecane solvent is not particularly

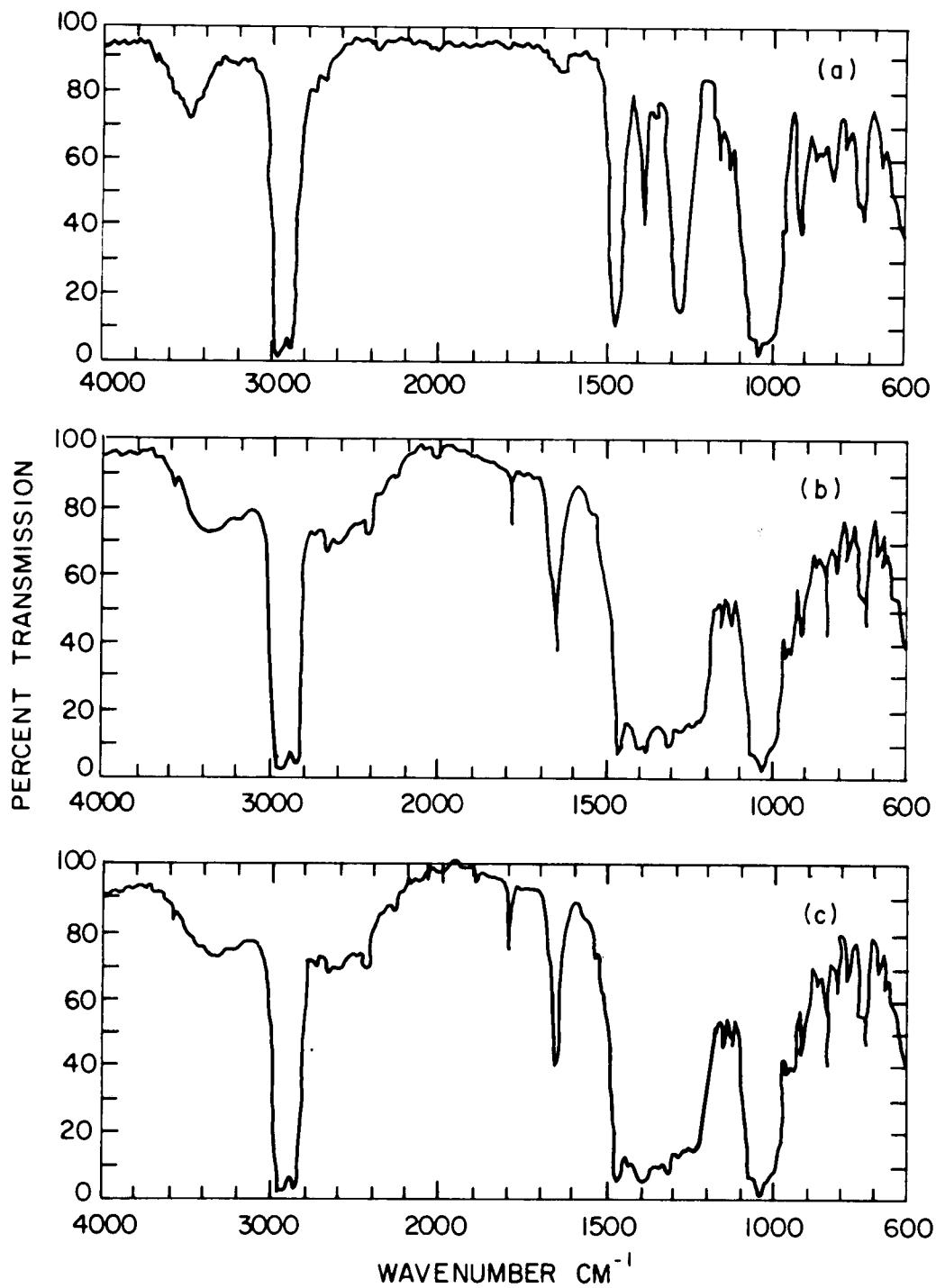


Fig. 4.2. Effect of A-29 macroreticular resin on 30% TBP-70% dodecane IR spectra: (a) uncontacted solvent, (b) after 5-hr contact with unstirred resin, (c) after 5-hr contact with stirred resin.

significant. Other similar results that we are experiencing with other macroreticular resins indicate the possibility that instability in TBP-dodecane solvents is a general problem with macroreticular resins. If these results continue in future tests, it may be necessary to recommend against the use of these resins for irradiated Purex solvent cleanup processes.

4.1.2 Ruthenium chemistry

L. Maya (Chemistry Division, ORNL)

New information developed during this quarter and consideration of the extensive literature on ruthenium chemistry in the Purex process (Fontaine and Berger⁶) have led to a general understanding of the chemistry of ruthenium in nitric acid solutions and to new reactions of potential application in Purex processing. The complexity of ruthenium chemistry in nitric acid stems from the large number of species that may coexist under a given set of conditions. Most of these species are closely related and differ only by the type of number of ligands around the RuNO^{3+} entity. It has proven worthwhile to undertake a broader investigation of the chemistry of ruthenium in nitric acid - one that covers the different oxidation states - so that the relative stabilities of widely different species can be ascertained. This investigation has produced a better understanding of the conditions that lead to the formation of extractable ruthenium species and to the design of methods that might prevent their formation. A general description of the chemistry involved is given in Fig. 4.3, which shows the conditions leading to interconversion as well as other reactions that describe the nature of the species. Central to the chemistry of ruthenium in nitric acid, particularly under Purex process

conditions where nitrogen oxides are commonly present, is the formation of nitrosyl ruthenium because of its relatively high stability under a wide range of pH and redox conditions. Nitrosyl ruthenium thus acts as a sink for all of the dissolved ruthenium in the system. A significant finding is that RuNO^{3+} is labile toward photolytic degradation, yielding inextractable $\text{Ru}(\text{NO}_3)_n^{4-n}$. Another relevant finding is that $\text{RuO}(\text{OH})_2$, which could be present under fuel dissolution conditions, is insoluble in nitric acid; however, it is readily solubilized by reaction with NO_x . Consequently, minimizing NO_x contact in the dissolver could lead to lower amounts of dissolved ruthenium.

A more detailed description of selected reactions from the inter-conversion scheme (Fig. 4.3), is given below.

A. The reaction $\text{RuNO}(\text{NO}_3)_x^{3-x} \xrightarrow{h\nu} \text{Ru}(\text{NO}_3)_x^{4-x}$. A series of preliminary tests was performed to determine the effect of uv irradiation on the different $\text{RuNO}(\text{NO}_3)_x$ species. These tests showed that nitric acid solutions containing $\text{RuNO}(\text{NO}_3)_x$ species develop a deep red color after uv irradiation. The effect is more pronounced when air or an inert gas is sparged through the solution during the irradiation period. On the other hand, there is no appreciable color change when $\text{RuNO}(\text{NO}_3)_x$ is irradiated in a closed system. These results resemble those obtained by Wallace⁷ on the irradiation behavior of RuNOCl_x and are interpreted as follows: The photoreaction of $\text{RuNO}(\text{NO}_3)_x$ in nitric acid leads to displacement of nitric oxide and the formation of a Ru(III)-transient intermediate that is spontaneously oxidized to Ru(IV). In a closed system, the presence of nitric oxide reverses the reaction, while in a sparged system, the NO is removed and the reaction can proceed to completion.

It was found that light at longer wavelengths, such as the output of an argon ion laser (3.5 W at 488.0 and 514.5 nm), was equally effective in producing the photodecomposition of $\text{RuNO}(\text{NO}_3)_x$.

A 10-cm³ sample of a solution containing 2.5 M LiNO_3 , 3.0 M HNO_3 , and 0.12 M $\text{RuNO}(\text{NO}_3)_x$ was irradiated for 90 min using a high-pressure mercury lamp. A 1-cm³ aliquot of the irradiated solution was separated on a column containing 50% TBP on XAD resin according to a procedure previously described.⁸ The chromatogram was similar to those previously obtained;⁸ in this case, however, the relative proportions of the different fractions had changed (Table 4.1).

Table 4.1. Ruthenium distribution (percent)

	$\text{RuNO}(\text{NO}_3)_1$ and 2	$\text{RuNO}(\text{NO}_3)_3$	$\text{RuNO}(\text{NO}_3)_4$	Dimer
Reference	61.9	29	6.6	2.6
Irradiated	76.2 ^a	17.8	4.5	1.4

^aContains Ru(IV) product.

The results show that uv irradiation is not specific and that all of the higher nitrate species are equally decomposed.

Regarding the mechanism of the photoreaction, the fact that it proceeds with light of relatively long wavelengths indicates that the electronic transition that is excited is not too energetic and apparently involves promotion from a t_2 orbital to an antibonding orbital having a considerable NO character. Partially filling an antibonding orbital has the effect of weakening the Ru-NO bond, which eventually breaks and leads to the observed products.

Three independent analytical methods for the determination of Ru(IV) in the presence of $\text{RuNO}(\text{NO}_3)_x$ were developed by experiments to study the chemical properties of this compound. First, upon neutralization to $\text{pH} \geq 11$, a black precipitate of hydrous ruthenium(IV) oxide forms, which can be separated by centrifugation. The $\text{RuNO}(\text{NO}_3)_x$ species, if present, are converted upon neutralization to soluble $\text{RuNO}(\text{OH})_3$. Therefore, in systems using ^{106}Ru tracer, it is possible to calculate the relative proportions of Ru(IV) and $\text{RuNO}(\text{NO}_3)_x$ by counting equal volumes of the top and bottom fractions after centrifugation. A second method employs paper chromatography by use of a 30% solution of 0.5 N HNO_3 in acetone as the solvent. Under these conditions, Ru(IV) has an R_f of 0.9, while $\text{RuNO}(\text{NO}_3)_x$ moves with the solvent front; cutting the strips and counting provides a means of determining the relative proportions of each component. Finally, the amount of Ru(IV) present can be determined by measuring the absorbance of the solution at 485 nm. At this wavelength, Ru(IV) has an extinction coefficient of 761, while the absorbance of $\text{RuNO}(\text{NO}_3)_x$ is so small that it can be ignored at high conversions.

The kinetics of the photoreaction was investigated. A $\text{RuNO}(\text{NO}_3)_x$ solution was irradiated with a uv lamp while sparging with air. Samples were taken at intervals, and the conversion to Ru(IV) was followed by the amount of $\text{RuO}(\text{OH})_2$ produced upon neutralization. The results (Fig. 4.4) reveal a first-order reaction with a half-life of 35 min. The ruthenium distribution coefficient (E_A^0) for the fully irradiated solution (96% conversion) was 0.0038, or about 100-fold smaller than that for the starting solution. These results suggest the use of uv irradiation to improve ruthenium decontamination in the Purex process.

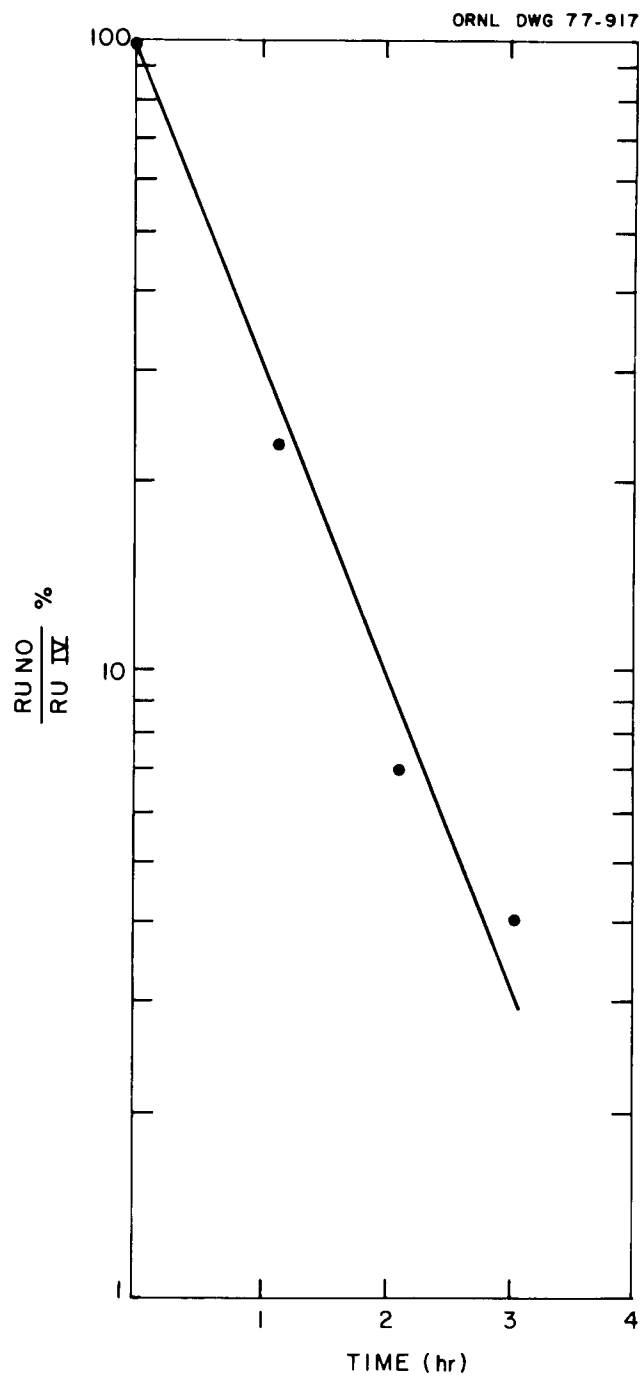


Fig. 4.4. Kinetics of the photodecomposition of $\text{RuNO}(\text{NO}_3)_3$ by uv light.

An experiment was performed to test whether the use of uv irradiation to improve ruthenium decontamination would be feasible under Purex process conditions. A sample of a solution of 1.0 M of $\text{UO}_2(\text{NO}_3)_2$, 3.0 M of HNO_3 , and 0.012 M of $\text{RuNO}(\text{NO}_3)_x$ was irradiated with a uv lamp for 4 hr while sparging with air. Ruthenium and uranium distribution coefficients between 3 N HNO_3 and 30% TBP-kerosene were determined. The uranium distribution was not affected by the irradiation, while the ruthenium K_D decreased from 0.02 to 0.013. The relative limited improvement observed could be because most of the energy available for the photoreaction was absorbed by $\text{UO}_2(\text{NO}_3)_2$. The experiment was repeated at a longer wavelength using an argon ion laser, where $\text{UO}_2(\text{NO}_3)_2$ does not absorb as much. In this case, the ruthenium distribution coefficients in the reference and in the treated solutions were 0.02 and 0.006 respectively. These results show the potential of irradiation as a method to improve ruthenium decontamination factors. The results could be further optimized by using better designed cells and irradiation conditions.

Electrochemical means were considered as an alternative method of oxidizing RuNO^{3+} to take advantage of the fact that Ru(IV) is much less extractable than the RuNO^{3+} species. Preliminary tests were performed by F. A. Posey of the Chemistry Division. In a series of voltammograms, an oxidation wave was seen at about 1.2 V from the reference calomel electrode (which could correspond to the initial oxidation of RuNO^{3+}), whereas reduction waves were observed at about 0.5 and -0.3 V. The last wave corresponds to the catalytic hydrogen discharge. An electrochemical cell has been assembled to perform exhaustive oxidation of $\text{RuNO}(\text{NO}_3)_x$ solutions to determine whether the conversion to Ru(IV) is feasible.

B. The reaction of RuO_4 $\xrightarrow[\text{H}_2\text{O}_2]{\text{HNO}_3}$ $\text{Ru(IV)(NO}_3)_x$. This reaction was investigated by Anderson and McConnell.⁹ The description of the chemical properties and spectra of these species suggests that the $\text{Ru(IV)(NO}_3)_x$ species are identical to those obtained by the photodecomposition of $\text{RuNO(NO}_3)_x$ described in the previous section.

The nature of the $\text{Ru(IV)(NO}_3)_x$ species was examined further to complement the work by Anderson and McConnell, whose observations could be summarized as follows: (1) These species are cationic, with a charge per ruthenium of at least +3. (2) Evaporation of solutions of these species leads to hygroscopic residues containing variable N:Ru ratios that fluctuate around a value of 3; successive dissolution and evaporation steps lower the ratio to a limiting value of 1. (3) Ruthenium is present in an oxidation state of +4 as determined by iodometric titration. (4) Total nitrogen determination by nitron precipitation gives the same number of equivalents as the amount of nitrate present. This result reveals that there are no other nitrogen-containing ligands and that the nitrate ion is not tightly bound to ruthenium and is probably present only as a counter-ion. (5) The visible spectrum of solutions of these species show an absorption band at 485 nm with $\epsilon = \sim 700$. This spectrum is also observed for Ru(IV) solutions in noncomplexing acids such as HClO_4 or HI . (6) Neutralization leads to precipitation of hydrous ruthenium oxide, RuO(OH)_2 .

Attempts were made by chromatography on cation exchange resins to determine whether the $\text{Ru(IV)(NO}_3)_x$ species are a mixture or a single compound. The species were tightly absorbed as a narrow band on top of

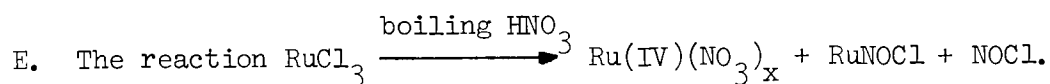
the column (using Dowex 50W-X8) and could not be eluted with nitric acid of as high a concentration as 10 M or with a 2.5 M solution of cerous nitrate. Resins with different particle size and/or degree of cross-linking were tested, but no separation could be obtained. These results indicate that the species are highly charged and possibly polymeric in nature; RuOH^{3+} or RuORu^{6+} are possible forms. On the other hand, paper chromatography of $\text{Ru(IV)(NO}_3)_x$ produced a single band, which suggests that the species could be a single compound.

Attempts to obtain IR spectra of the evaporation residues showed the presence of NO vibrations. Apparently the NO produced in the evaporation of the nitric acid reacted with $\text{Ru(IV)(NO}_3)_x$ to partially regenerate $\text{RuNO(NO}_3)_x$. This would explain why Anderson and McConnell could not lower the N:Ru ratio of evaporation residues below 1.

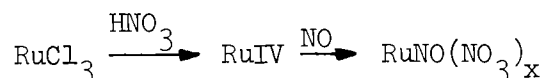
C. The reaction $\text{Ru(IV)(NO}_3)_x \xrightarrow{\text{NO}_x} \text{RuNO(NO}_3)_x$. This reaction proceeds quite easily; the red color of the $\text{Ru(IV)(NO}_3)_x$ solution is discharged after a few minutes of NO_x sparging. The $\text{RuNO(NO}_3)_x$ product was identified by the typical pink color of the resulting solution and the IR spectrum of the evaporation residue, which is identical to that of an authentic sample of $\text{RuNO(NO}_3)_3$.

D. The reaction $\text{Ru(IV)(NO}_3)_x + \text{cation exchange resin} \xrightarrow{\text{HCl}} \text{Ru(OH)}_2\text{Cl}_4^-$. This reaction was investigated to confirm that the NO detected in the evaporation residues is not present in the original dissolved species, but is formed as a result of the evaporation. A sample of a $\text{Ru(IV)(NO}_3)_x$ solution was equilibrated with a cation exchange resin; the species were readily absorbed. The loaded resin was washed with water and contacted with 6 N HCl,

which led to the formation of $\text{Ru}(\text{OH})_2\text{Cl}_4^-$. This species was identified by comparing it with the reported spectrum.¹⁰ That this species was formed proved that ruthenium is actually in the +4 oxidation state and that the NO presence in the residues is only a result of the evaporation process. To further confirm this observation, a solution of $\text{RuNO}(\text{NO}_3)_x$ was treated in a way similar to the Ru(IV) solution; in this case, the product released from the resin was RuNOCl_3 , as identified by its spectrum. This proves that if RuNO^{3+} had been present in the Ru(IV) solution it could have been detected.



We found that Ru(IV) can also be produced by dissolution of RuCl_3 in boiling nitric acid. We hoped that this would provide an alternative for the time-consuming preparation of $\text{RuNO}(\text{NO}_3)_x$ (also described in Fig. 4.3) consisting of the conversion of RuCl_3 to RuNOCl_3 , followed by conversion to $\text{RuNO}(\text{OH})_3$ and finally to $\text{RuNO}(\text{NO}_3)_x$. The alternate route



produces RuNOCl_3 in the first step and does not have preparative value.

F. The reaction $\text{RuO}(\text{OH})_2 \xrightarrow[\text{HNO}_3]{\text{NO}_x} \text{RuNO}(\text{NO}_2)(\text{NO}_3)_2$. Hydrous ruthenium(IV) oxide was suspended in 10 N HNO_3 and sparged with NO_x . A brown solution was produced within a few minutes. The product was evaporated to dryness, and the residue was identified as $\text{RuNO}(\text{NO}_2)(\text{NO}_3)_2$ by comparison with the IR spectrum of this species.¹¹ The dissolution of hydrous ruthenium oxide in the presence of nitrogen oxides could be one of the processes through

which ruthenium can be dissolved in the Purex process. This suggests that sparging the dissolver with an inert gas to minimize NO_x contact with ruthenium solids might reduce the amount of dissolved ruthenium.

G. The reaction $2\text{RuNO}(\text{NO}_3)_x \rightleftharpoons [\text{RuNO}(\text{NO}_3)_x]_2$. This reaction, postulated by Joon¹² as the reaction leading to highly extractable species, is under examination. Previous work⁸ has shown that highly extractable species are present in equilibrium mixtures of $\text{RuNO}(\text{NO}_3)_x$; also, a dimer that proved to be highly extractable was described.⁸ Efforts will be made to isolate these dimers and understand their chemistry.

4.1.3 Solvent extraction kinetics

D. E. Horner (Chemical Technology Division, ORNL)

In recent studies of the kinetics of solvent extraction of uranium and key fission products by the drop technique, the rising drop mode was compared to the previously determined falling drop mode.¹³ The working equations applicable to the rising drop were obtained from the differential equation for organic drops:

$$\frac{dc}{dt} = - \frac{kac - k'ac'}{v}, \quad (4.1)$$

which gives the net transfer between the drops and the bulk phase. In these equations, c is the concentration, v is the drop volume, a is the interfacial area, t is the contact (rise) time, and k' and k are the rates from the aqueous to the organic direction and from the organic to the aqueous direction respectively; the primed symbols refer to the bulk aqueous phase and the unprimed symbols refer to the organic drop phase.

Since the reverse organic to aqueous transfer is negligible, either because $c' \ll c$ (fission products) or $k \ll k'$ (uranium), a reduced equation is obtained by deleting this term in Eq. (4.1). Thus,

$$\frac{dc}{dt} = \frac{k'ac'}{v} \quad (4.2)$$

Integration of Eq. (4.2) between $c = 0$ and c at time t result in

$$\frac{k'ac't}{v} = c \quad (4.3)$$

for aqueous to organic transfer.

Integration of Eq. (4.1) between $c \neq 0$ and c at time t results in

$$-\frac{akt}{v} = \ln \frac{c}{c_0} \quad (4.4)$$

for organic to aqueous transfer. The assumption that the aqueous to organic transfer should be the same for both rising organic drops and falling aqueous drops was confirmed experimentally by values of k' for uranium of 5.69×10^{-3} cm/sec and 7.05×10^{-3} cm/sec respectively. Within experimental error, these can be considered approximately equal. The backward organic to aqueous extractions by the rising and falling modes are also probably the same, but analytical limitations precluded getting a reliable value of k for the rising drop mode.

A major objective in this work is to determine if there are any differences between the extraction rates for uranium and the key fission products, and if so, whether they could be exploited to improve uranium decontamination by using fast contactors. This possibility looks promising, because all the key fission products were shown to extract slower than uranium from aqueous to organic and faster than uranium from organic to aqueous. For example, the ratios of rate constants (U:FP) in the aqueous

to organic direction at 40°C were 13 for Zr, 150 for Nb, 450 for Ce, and 106 for Ru; the ratios (FP:U) in the organic to aqueous direction were 19 for Zr, 80 for Ce, and 65 for Ru. In the latter case, the fission product extractions were determined by the rising drop modes, while uranium extractions were by the falling drop mode.

In other tests, the extraction rate constants for uranium and the key fission products at 40°C were shown to be greater by a factor of about 1.5 than those at 20°C, except for ruthenium, which was shown to be smaller by a factor of about 3. In this case, the lower rate at the higher temperature is probably a result of the formation of less extractable ruthenium species known to form at elevated temperatures.¹⁴

Studies were also made to determine the effect of initial TBP concentration on aqueous to organic uranium extractions. Results for extractions with 2, 15, and 30% TBP show that the extraction rate constant increases regularly with increasing TBP concentration, ranging between 2×10^{-3} and 7×10^{-3} cm/sec over this concentration range.

During the next quarter, we plan to determine the rates of fission product extractions from dilute (0.3 M) HNO_3 . Technetium will be studied to determine if it coextracts with uranium as previous studies have indicated,¹⁵ and if so, to determine the effects of extraction variables on the rate of technetium extraction.

An experimental fast centrifugal contactor has been ordered. When the contactor is available, tests will be made to confirm that uranium decontamination from fission products can be improved by the use of contact times.

4.1.4 Plutonium extraction studies

M. H. Lloyd, J. B. Knauer, J. T. Barker, and J. H. Paehler (Chemical Technology Division, ORNL)

Plutonium distribution coefficients are being obtained in the 6% TBP-NDD system as a function of HNO_3 , uranium, and plutonium concentrations. The acid and uranium concentrations in this study will vary from 0.1 to 4.5 M and 0 to 350 mg/ml respectively. Data will be obtained for tracer level plutonium and for plutonium concentrations of 2 and 10 mg/ml.

Results to date demonstrate that Pu(IV) distribution coefficients increase regularly with increasing HNO_3 to a value of 2.1 at 4.5 M HNO_3 and decrease with increasing uranium concentrations.

Low-acid co-stripping experiments were continued in which aqueous feed solutions that contain 0.5 M $\text{UO}_2(\text{NO}_3)_2$ -0.05 M $\text{Pu}(\text{NO}_3)_4$ -0.4 M HNO_3 are equilibrated with 30 vol % TBP-NDD, which is then stripped with dilute HNO_3 .

It was previously reported that plutonium polymerization occurred when a 0.2 M HNO_3 strip solution was used at 25°C. This observation was probably in error; studies to resolve this point are in progress. In current experiments, plutonium recoveries of more than 99.95% were obtained with six equal-volume stripping stages at HNO_3 concentrations as low as 0.02 M at 25°C. This does not, however, preclude the possibility of plutonium hydrolysis or of polymerization.

4.1.5 Analytical chemistry development

D. L. Manning (Analytical Chemistry Division, ORNL)

Analytical development activities for the remainder of this year (until September 30) will, for the most part, consist of installing and

checking out a high-performance liquid chromatograph and a gas chromatograph and with becoming familiar with liquid and gas chromatographic theory and techniques of operation. Our first liquid chromatographic experiments will involve identifying and measuring nitrogen-containing species (nitrates, nitrites, azides, hydrazine, etc.) that are formed from plutonium valence adjustment steps in Purex processing.

Among longer-range activities, we will look at both liquid and gas chromatographic techniques for the identification and measurement of radiolytic degradation products of TBP formed during Purex processing. An analytical capability is also needed for the analysis of nitrogen oxide gases such as NO_2 , NO , N_2O , and, in some cases, N_2 that are generated in denitration steps, waste treatment, and fuel dissolutions. We plan to evaluate gas chromatography as an analytical method in this area.

We also plan to investigate liquid chromatography for fission product characterizations, such as zirconium and niobium species, both in nitric acid solutions and TBP organics. Very little is known about the behavior of such species under existing experimental conditions.

4.2 Cold Studies

4.2.1 Flowsheet studies using mixer-settlers

V. C. A. Vaughen, H. C. Savage, W. D. Bond, and F. A. Kappelmann
(Chemical Technology Division, ORNL)

Eleven experimental Purex runs were made during the period March 17 to April 15, 1977. These runs were carried out in two 16-stage mixer-settler¹⁶ banks. One mixer bank was run for extraction-scrub (A bank)

and the other for stripping (C bank). Allied General Nuclear Services flowsheet flow ratios were maintained in all runs. Flowsheet conditions are given in Table 4.2 and the flowsheet is shown in Fig. 4.5.

Table 4.2. Flowsheet conditions for Purex experiments in 16-stage mixer-settlers

Process stream	Flow ratio	Composition	Reference flow rate (l/hr)
Feed (AF)	1.0	292 g U/liter of 2.50 M HNO ₃	0.50
Solvent (AX)	3.50	30% TBP-NDD	1.75
Scrub (AJ)	0.40	3.00 M HNO ₃	0.20
Strip (CS)	4.0	0.10 M HNO ₃	2.00

The objective of these experimental runs was (1) to determine the effect of agitator speed and total flow rate on the hydraulic performance and overall efficiencies of the mixer-settlers and (2) to establish operating conditions and limits for future runs with reactor fuels in the hot cell facilities at TRU. The turbine agitator in the mixer-settler stages must pump at a rate at least equal to the heavy-phase flow rate and simultaneously provide adequate mixing for intimate contact of the two phases. Thus a mixer-settler is operable over a range of conditions of agitator speed and liquid throughput as shown in Fig. 4.6.¹⁷

The operating parameters for the 11 experimental runs are shown in Table 4.3. Runs were made at three agitator speeds (800, 1100, and 1700 rpm) and three flow rates ("reference", 0.5 x "reference," 1.5 x "reference"). The "reference" flow rates were based on earlier tests in the 16-stage mixer-settlers. Each mixer-settler unit was equipped

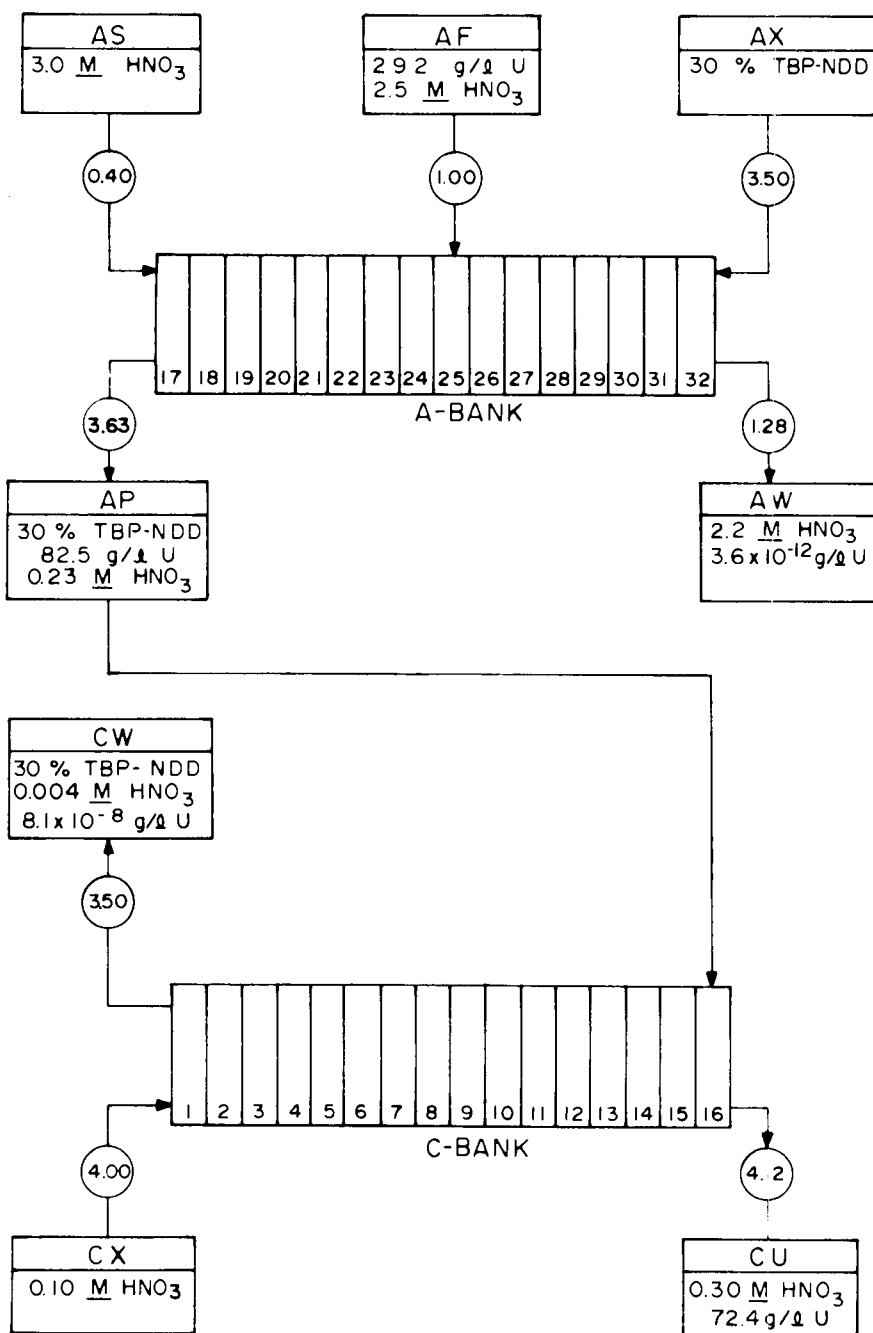


Fig. 4.5. Flowsheet for experimental Purex runs in 16-stage mixer-settlers.

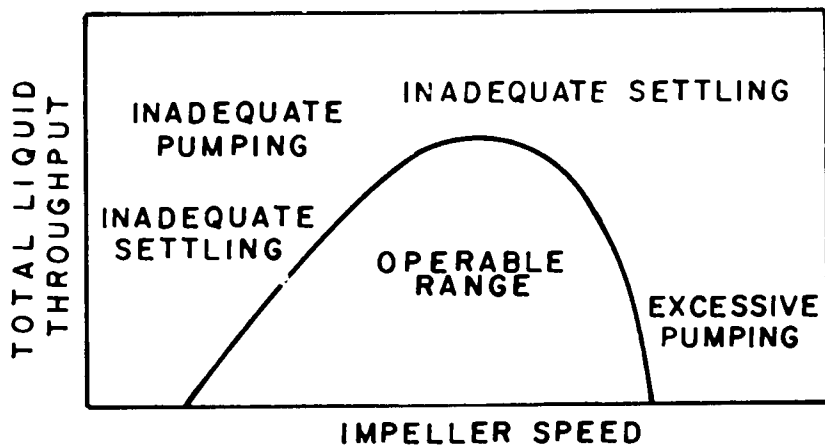


Fig. 4.6. Operating regions of mixer-settlers.

Table 4.3. Operating parameters for Purex experimental runs in 16-stage mixer-settlers

Run	Run time (hr)	Flow rate ^a (l/hr)	Agitator speed (rpm)
1	4	Reference	1100
2	4	Reference	1700
3	4	Reference	800
1R ^b	4	Reference	1100
4	4	1.5 x reference	1100
5	4	1.5 x reference	1700 extraction bank 1300 strip bank
7	6.25	0.5 x reference	1100
8	5	0.5 x reference	1700
9	7	0.5 x reference	800
1A ^c	4.5	Reference	1100
2A ^c	5	Reference	800

^aReference flow rate: Feed (AF) = 0.50 l/hr
Solvent (AX) = 1.75 l/hr
Scrub (AS) = 0.20 l/hr
Strip (CX) = 2.00 l/hr

^bRepeat of run 1.

^cA and B banks reversed to test effect of solid and split agitator blades.

with different types of agitator blades. For runs 1 through 9, the agitator blades in the C bank were 1.25 cm long x 0.56 cm wide x 0.16 cm thick. The blades in the A bank were similar except for a 0.32-cm wide slot at the midpoint of each blade. Figure 4.7 is a photograph of the agitators used in these tests. Runs 1A and 2A were made with the A and B banks reversed to determine the effects, if any, of the two different agitators on operating characteristics of the extraction and strip banks. Run 6, originally scheduled at flow rates of 1.5 x "reference" and agitator speeds of 800 rpm, was deleted because of time limitations and because operating efficiencies were reduced at the higher flow rates.

Run times were those calculated by SEPHIS to reach at least 99% of steady state in both the extraction and strip banks under the run conditions. Times ranged between 4 and 7 hr.

Operating procedures. At the start of each run, the mixer-settler banks contained both solvent and aqueous phases. Each run was initiated by simultaneously starting the agitators and all feed streams, which had previously been adjusted to the desired flow rates. During the run, hourly samples of the product and waste streams were taken until the last hour, when samples were taken every 15 min. Flow rates of all streams were measured every 30 min and adjusted, if required. Solution temperatures were checked periodically with a thermometer. Agitator speeds were continuously monitored by an indicating meter in the speed-control panel and were checked occasionally by means of a stroboscope. Agitator speeds are believed to be within ± 50 rpm of the indicated value.

Each run was terminated by simultaneously stopping the agitators and feed streams (a single switch controlled the power supply to the agitator

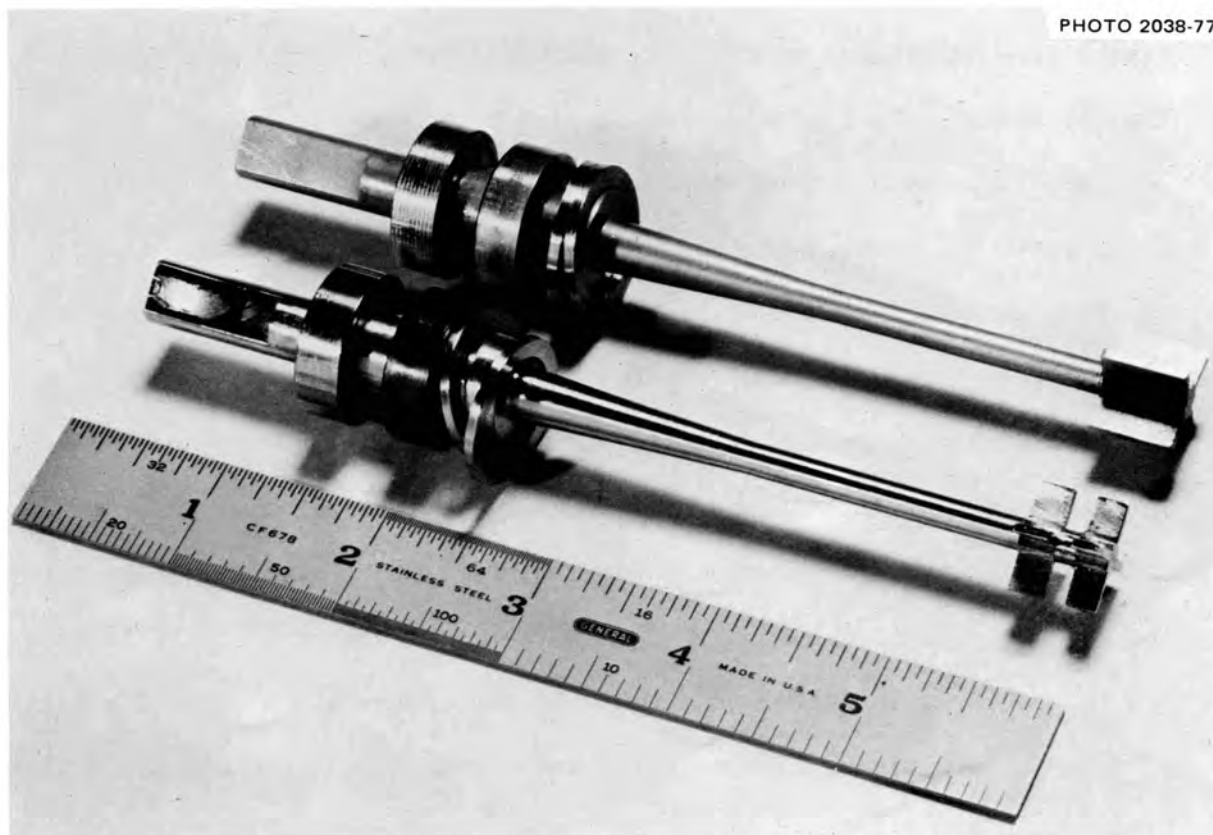


Fig. 4.7. Agitators used in experimental Purex runs.

drive motors and all feed stream supply pumps). Samples were taken of both the organic and aqueous phases from the 32 settling chambers in the A and B banks by using a multiple sampling device that allowed rapid removal of 2.5-ml samples of each phase. The samples were analyzed for uranium and nitric acid concentrations. Distribution coefficients in four selected stages were determined by removing additional samples of the aqueous and organic phases, equilibrating, and analyzing for uranium.

Results. Each experimental run was evaluated by several methods, including: (1) uranium concentration in the product and waste streams, (2) uranium material balance, (3) overall stage efficiencies as determined from McCabe-Thiele diagrams, and (4) visual observation of the settling chambers during operation (flooding, emulsion at the aqueous-organic interface, etc.) Each of the methods used in this series of runs to determine the system performance was insufficient to quantitatively specify the optimum operating conditions. However, the summation of all results and observations indicated qualitatively the system performance for each of the run conditions. The relative value and limitations of each evaluation method are discussed in the following paragraphs and results are summarized in Table 4.4.

Uranium concentrations in the product and waste streams. Final uranium concentrations in the aqueous raffinate from the extraction bank varied from about 2.5×10^{-5} to 3×10^{-3} g of uranium per liter, while that in the organic waste from the strip bank varied from about 1×10^{-5} to 11 g of uranium per liter. The analytical limit for uranium is about 2×10^{-5} g/liter, and significant errors can be expected below about 1×10^{-4} g/liter. Therefore, no significance was attached to variations

Table 4.4. Operating conditions and uranium analyses of product and waste streams for Purex experimental runs in 16-stage mixer-settlers

Run	Run time (hr)	Flow rates ^a	Agitator speed (rpm)	Uranium concentration ^b (g/liter)				Uranium loss (%) ^c	
				AW	AP	CW	CU	AW	CW
1	4	Reference	1100	9.4×10^{-5}	91.4	1.0×10^{-5}	81.3	4.5×10^{-5}	1.2×10^{-5}
2	4	Reference	1700	2.6×10^{-5}	87.1	1.3×10^{-3}	80.1	1.2×10^{-5}	1.6×10^{-3}
3	4	Reference	800	4.0×10^{-5}	92.2	7.0×10^{-5}	80.0	1.9×10^{-5}	8.4×10^{-5}
1R	4	Reference	1100	4.1×10^{-5}	84.9	3.3×10^{-5}	73.7	2.0×10^{-5}	4.0×10^{-5}
4	4	1.5 x reference	1100	2.6×10^{-5}	80.9	1.0×10^{-2}	77.8	1.2×10^{-5}	1.2×10^{-5}
5	4	1.5 x reference	1700 extraction 1300 strip	1.6×10^{-4}	99.2	11.2	89.6	7.7×10^{-5}	13.4
7	6.3	0.5 x reference	1100	3.4×10^{-3}	83.7	4.3×10^{-4}	74.5	1.6×10^{-3}	5.2×10^{-4}
8	5	0.5 x reference	1700	7.6×10^{-4}	81.7	6.3×10^{-2}	67.9	3.6×10^{-4}	7.6×10^{-2}
9	7	0.5 x reference	800	1.1×10^{-4}	79.3	7.1×10^{-5}	72.7	5.3×10^{-5}	8.5×10^{-5}
1A ^d	4.5	Reference	1100	2.8×10^{-4}	85.0	1.4×10^{-4}	73.6	1.3×10^{-4}	1.7×10^{-4}
2A ^d	5	Reference	800	2.2×10^{-4}	85.7	8.4×10^{-4}	73.7	1.1×10^{-5}	1.0×10^{-3}
Uranium concentrations predicted by SEPHIS				3.6×10^{-12}	82.5	8.1×10^{-8}	73.7		

^aReference flow: AF = 0.50 l/hr; AX = 1.75 l/hr; AS = 0.20 l/hr; CX = 2.00 l/hr.

^bFeed (AF) = 292 g U/l.

^cLoss calculated from uranium analyses at the end of run.

^dSplit-bladed agitators in strip bank; solid bladed agitators in extraction bank.

in the uranium concentration in the aqueous raffinate or organic waste unless the value exceeded about 1×10^{-4} g of uranium per liter. (For reference purposes, SEPHIS calculations predict a uranium concentration of about 3×10^{-12} and about 8×10^{-8} g/liter in the aqueous raffinate and organic waste respectively. These values are far below our analytical capability.) Uranium concentrations in the organic- and aqueous-product stream from the extraction and stripping banks ranged from about 68 to 99 g/liter. Uranium concentrations in the product and waste streams leaving the mixer-settler system during each run are shown in Fig. 4.8.

Uranium material balance. Material balances for uranium in the extraction and stripping banks and an overall material balance for both banks are shown in Table 4.5. Since the material balance depends directly on uranium analyses and flow rate, both must be accurately known. The extraction bank product stream (LAP) is the input stream to the stripping bank, and the material balances for each bank depend on this one analysis. The uranium concentration in end streams is based on multiple samples taken during the run and should be considered a good estimate. Thus the overall uranium material balance for both banks probably depends on the accuracy of the flow rate measurements ($\pm 5\%$).

As seen in Table 4.5, the overall uranium material balance ranged from about 97 to 110% with the exception of run 5 (133%) in which flooding was observed in the stripping bank. Uranium losses in the aqueous raffinate and the organic waste streams are shown in Table 4.4.

McCabe-Thiele diagrams. Overall efficiencies of the extraction and stripping banks were estimated from the McCabe-Thiele diagrams, in which the number of actual stages required to produce a given aqueous raffinate

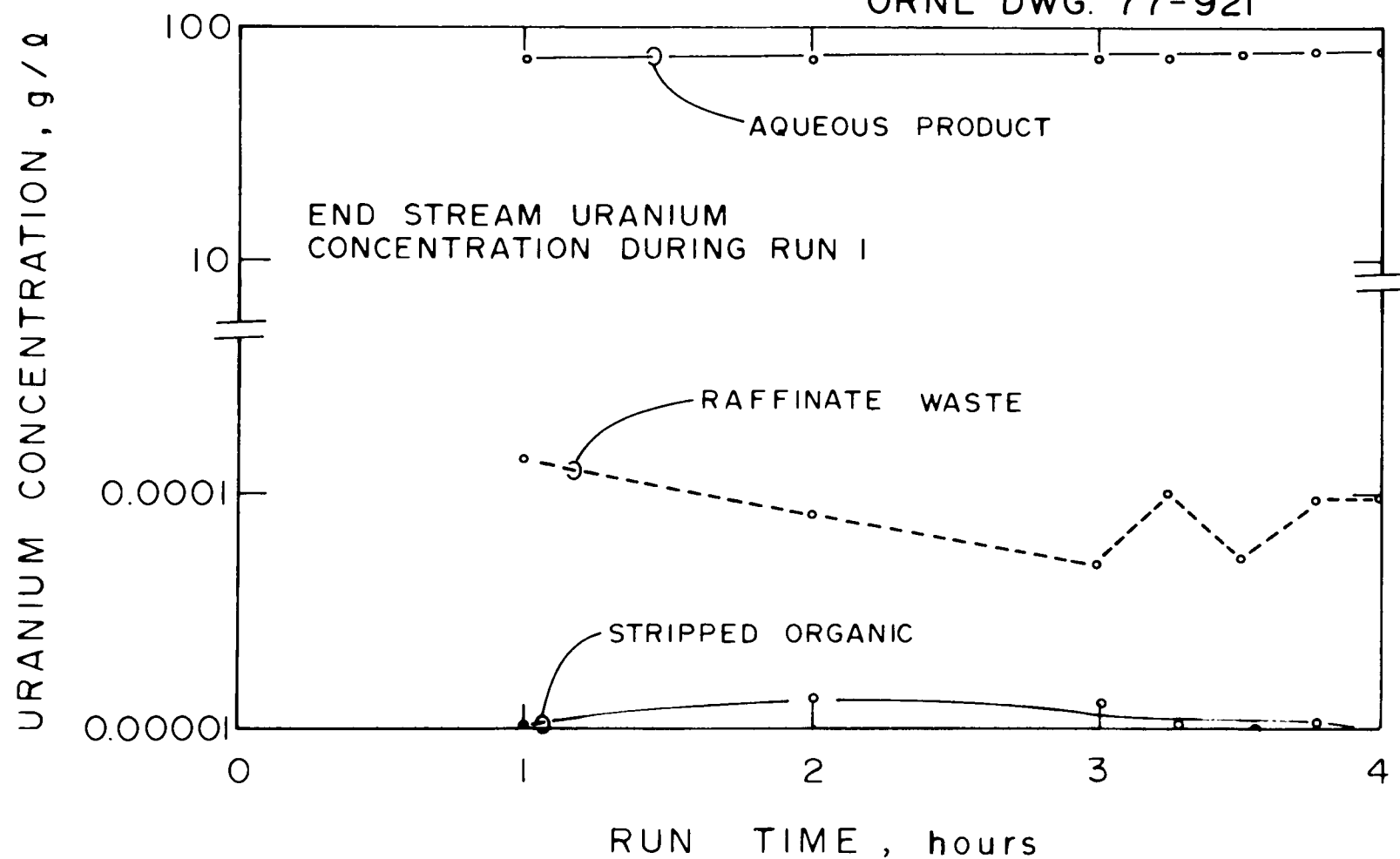


Fig. 4.8. End-stream uranium concentrations vs operating time during run 1.

Table 4.5. Uranium material balance and estimated overall stage efficiencies for Purex experimental runs in 16-stage mixer-settlers

Run No.	Uranium material balance: output-input			Estimated ^a overall stage efficiency (%)		Observations
	Extraction (%)	Strip (%)	Extraction + strip (%)	Ext.	Strip	
1	100	105	106	65	85	Extraction bank organic continuous. Strip bank organic continuous except stages 1 and 3.
2	94	105	99	55	b	Foaming on surface of organic phase - all stages.
3	101	105	106	80	b	All stages organic continuous. Stable operation.
1R ^c	119	87	104	75	b	Same as run 1.
4	93	106	99	55	<<75	Extraction bank same as 1. Strip bank organic continuous except stages 1, 10, and 11.
5	111	120	133	55	b	Strip bank flooding.
7	104	105	109	55	<75	All stages organic continuous. Stable operation.
8	101	96	97	55		Foaming on surface of organic phase - all stages. Stripping poor. Uranium visible at stage 3.
9	98	112	110	55	75	Extraction bank organic continuous. Strip bank organic continuous except stages 1, 3, 9, 11, and 12.
1A ^d	105	99	104	~100	75	Emulsion in strip bank.
2A ^d	113	92	103	80	75	Extraction bank stable. Emulsion in stage 16 with organic loss to product (CU).

^aEstimated from McCabe-Thiele diagrams.

^bAll stages not sampled.

^cUncertainty in organic (AX) feed rate.

^dSplit-bladed agitator in strip bank; solid-bladed agitator in extraction bank.

and organic waste uranium concentration are compared with the number of theoretical stages to produce the same concentration based on SEPHIS calculations. As noted above, analyses could not reliably determine uranium concentrations below about 1×10^{-4} g/liter. For this reason, the number of ideal stages in each bank was compared with the number of actual stages required to reach about 1×10^{-4} g/liter. The number of ideal stages is about 3.5 for the extraction bank and about 12 for the stripping bank. Estimated overall efficiencies for the extraction and stripping banks for those runs for which sufficient data were obtained are shown in Table 4.5. The McCabe-Thiele diagrams for the extraction bank (run 3) and the stripping bank (run 1) are shown in Figs. 4.9 and 4.10 as illustrative examples.

Visual observations. A quartz window allows visual observation of all 32 settling chambers in the mixer-settlers. Abnormal or unsatisfactory operation of a run was easily determined by visual operation (i.e., flooding, condition at the aqueous-organic interface, etc.). Pertinent observations for each run and analytical results are recorded in Table 4.5.

Discussions and conclusions. As discussed in previous sections, the several methods used to determine the optimum operating conditions for the 16-stage mixer-settlers are qualitative. However, summation of all results and observations gave a reasonably good indication of system performance for each of the run conditions. In particular, very poor or very good operation was easily determined. Based on the results summarized in Tables 4.4 and 4.5, the system (extraction-scrub plus stripping) was operable at the reference flow rates and one-half the reference flow

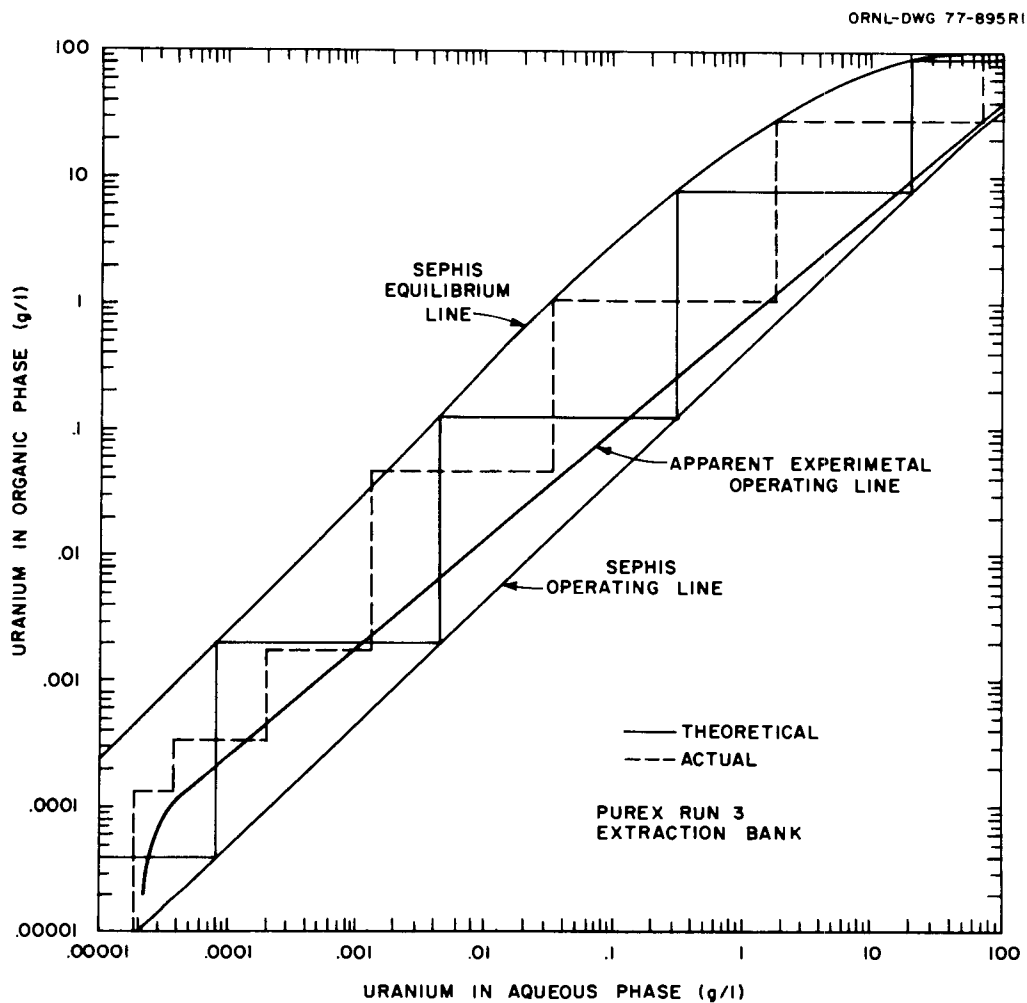


Fig. 4.9. McCabe-Thiele diagram for extraction (stages 25 through 32) section, A bank, Purex experimental run 3.

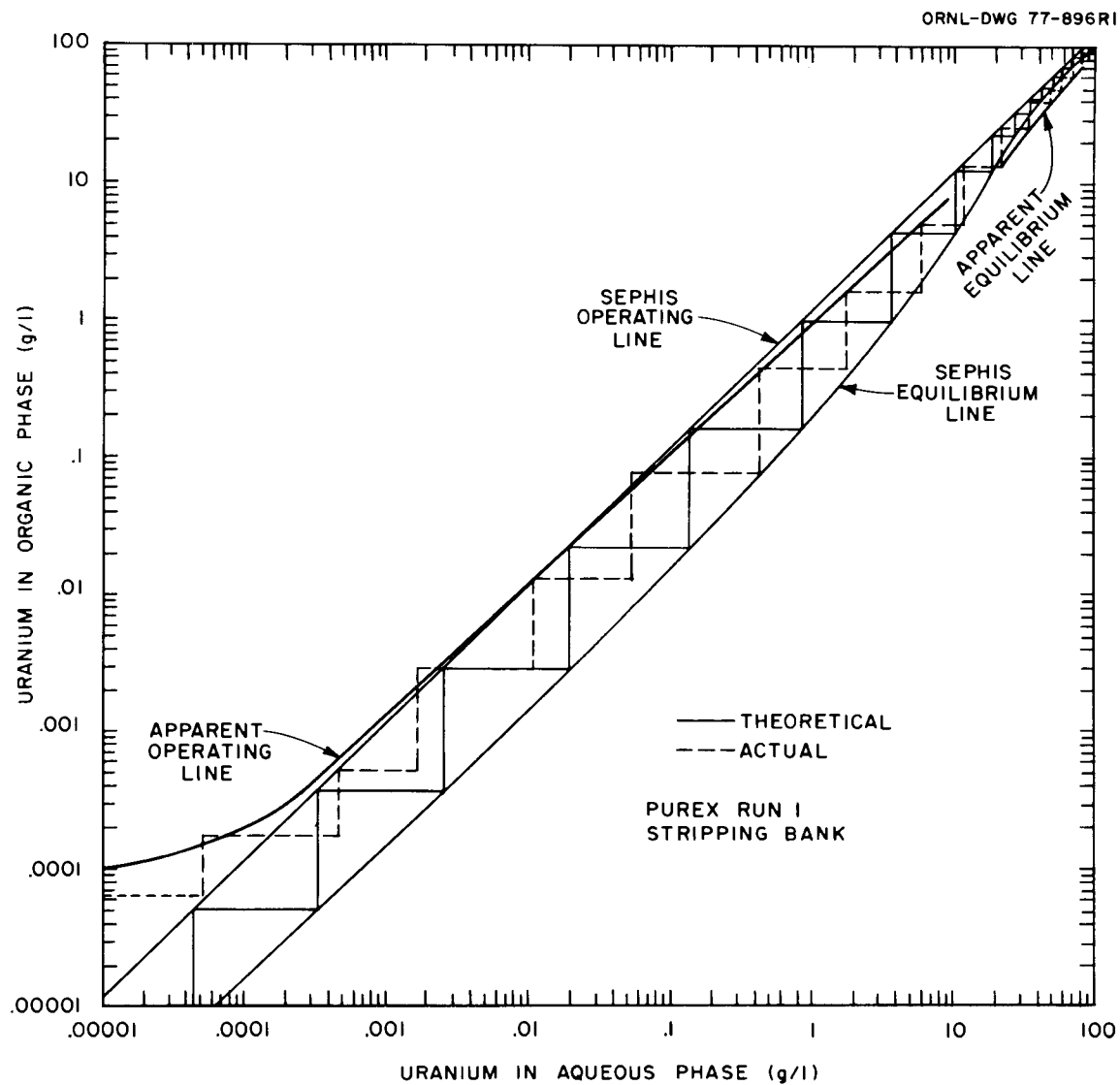


Fig. 4.10. McCabe-Thiele diagram for stripping (stages 1 through 16) in C bank, Purex experimental run 1.

rates at agitator speeds of 800 and 1100 rpm respectively. System performance was unsatisfactory at agitator speeds of 1700 rpm at all of the flow rates tested. At a flow rate of 1.5 times the reference flow rate and 1100 rpm, system performance was poor. The run at agitator speeds of 800 rpm and flow rates 1.5 times the reference flow rate was not made because of time limitations. However, it is believed that system performance would have been less satisfactory than at the lower flow rates. The results are shown diagrammatically in Fig. 4.11.

The performance of the two types of agitators was evaluated by comparing runs 1 and 2 (solid blades in the strip bank, split blades in the extraction-scrub bank) with runs 1A and 2A (split blades in the strip bank, solid blades in the extraction-scrub bank). In run 1A, some emulsion was observed at the aqueous-organic interface in the strip bank. In run 2A, some organic loss to the product stream (CU) was observed. Also, uranium stripping was poorer in run 1A than in run 1 (Fig. 4.12). Thus it is concluded that the solid-bladed agitators performed better in the strip bank. There appeared to be some improvement in the efficiency of the extraction-scrub bank with the split-bladed agitators compared with the solid-bladed agitators (80 to 100% vs 75 to 80%). Since these efficiencies are somewhat qualitative and based on only two runs, a preference for either type of agitator blades in the extraction-scrub bank cannot be made at this time.

The slope of the experimental operating line relative to the SEPHIS operating line (Fig. 4.9) implies some recycle of organics in the extraction bank. A mixer-settler modified to reduce or eliminate organic recycle has been assembled and will be tested.

ORNL DWG. 77-958RI

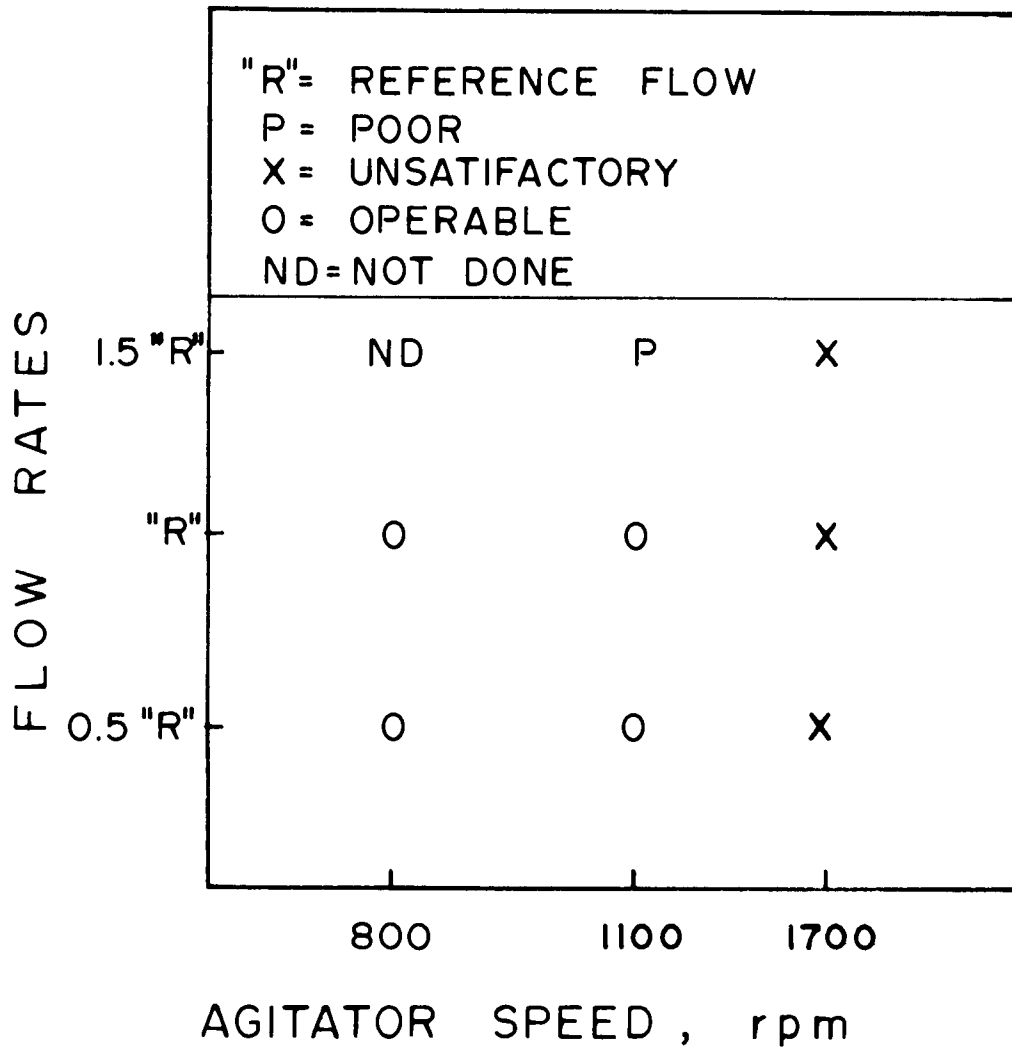


Fig. 4.11. Experimentally determined operating parameters of mixer-settlers.

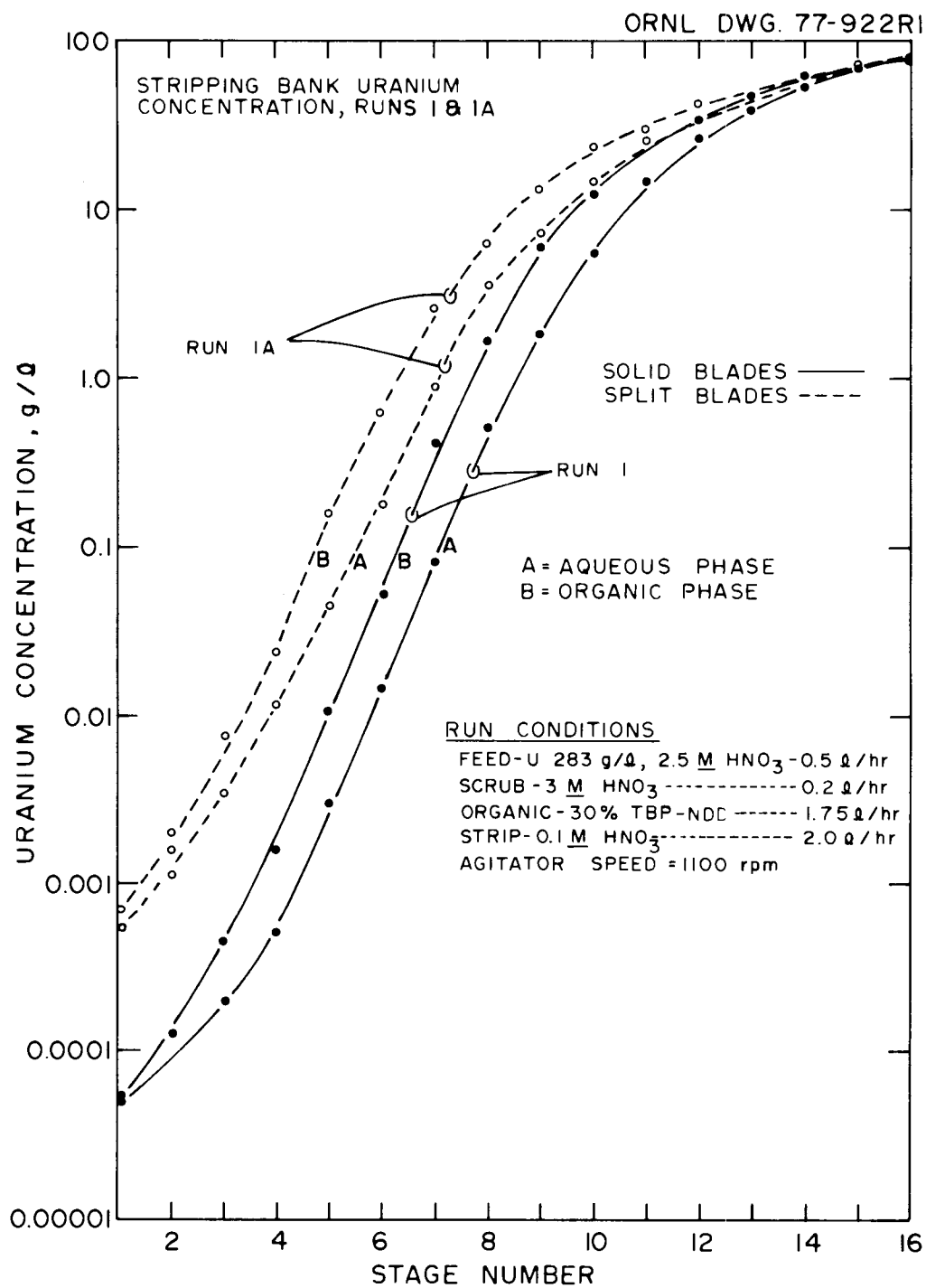


Fig. 4.12. Uranium concentrations in the aqueous and organic phases in the stripping bowls with solid- and split-bladed agitators.

Run times will be increased in the future because the times required to reach steady state (99%) may be longer than the theoretical times calculated by SEPHIS.

4.2.2 Batch countercurrent extractions

W. D. Bond and F. M. Scheitlin (Chemical Technology Division, ORNL)

In cold tests, batch countercurrent extraction showed that plutonium losses to the aqueous raffinate could be reduced to a few thousandths of 1% from feeds containing 1 to 2 g/liter of plutonium (Table 4.6). In these tests, four extraction and four scrubbing stages were employed. The acid concentration of the feed and the scrub were 2 M and 3 M respectively. The presence of cold fission product elements and uranium had little or no effect on plutonium losses to the aqueous raffinate. The distribution coefficients of plutonium appeared to decrease when the plutonium concentrations were reduced to 10^{-6} to 10^{-7} M. The distribution of plutonium in the extraction and scrubbing stages for run X (Fig. 4.13) was typical of the other runs given in Table 4.6.

Table 4.6. Batch countercurrent extraction of plutonium
(feed:scrub:extractant = 1:0.66:3.33)

Run	Plutonium loss (%)	Additives to feed
S(A)	0.003	None
W	<0.01	None
X	0.001	170 g/liter of uranium + FPs ^a
AA	0.003	FPs

^aFission products.

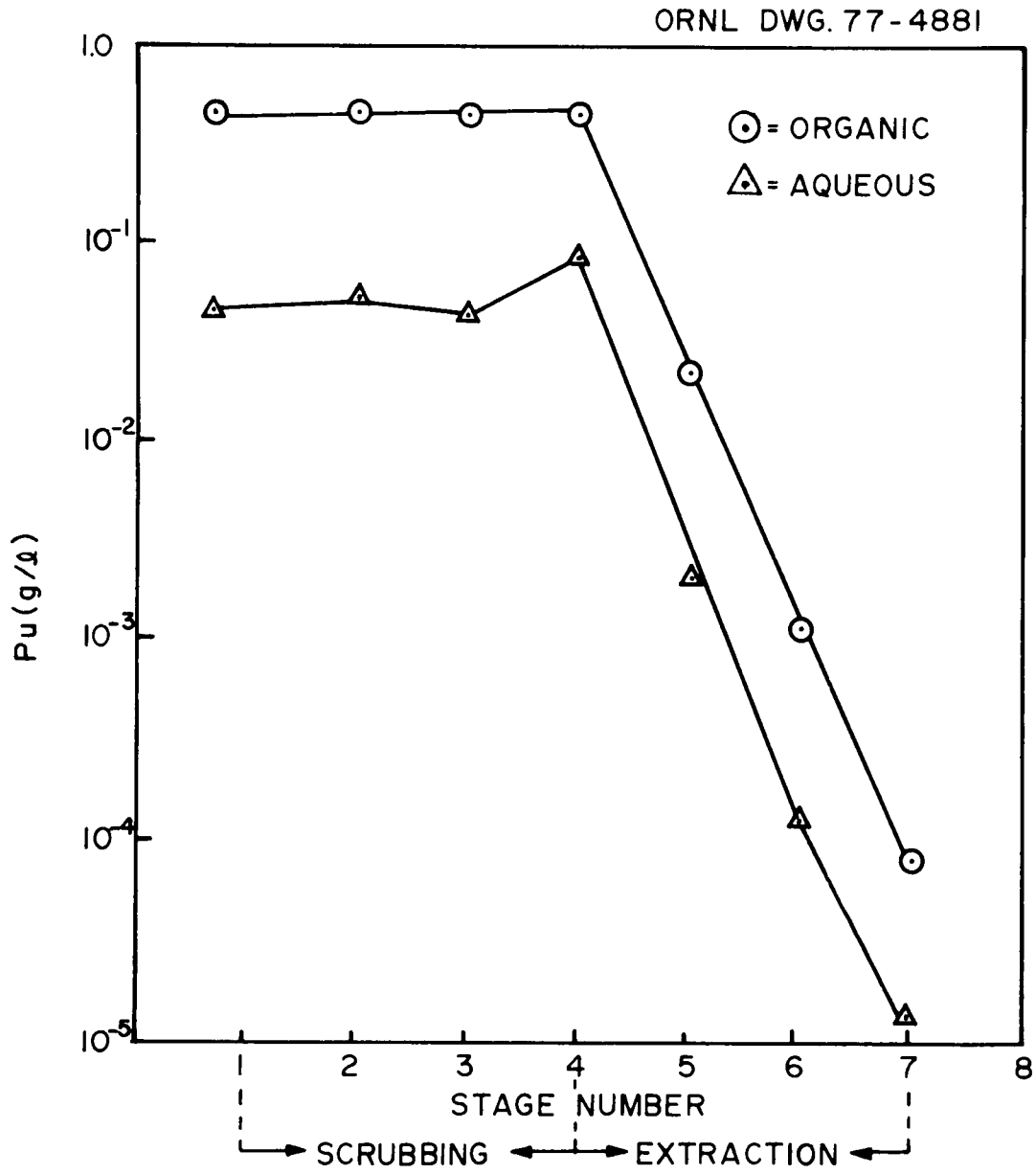


Fig. 4.13. Distribution of plutonium in batch countercurrent extraction run X, Table 4.6.

4.2.3 Component tests

H. C. Savage and V. C. A. Vaughen (Chemical Technology Division, ORNL)

Solution clarification. Feed clarification to remove solid particles immediately prior to solvent extraction is necessary because such particulates could plug liquid flow passages, accumulate in the mixer-settler chambers, and collect at the solvent interface and thereby compound the interfacial crud problem. An etched-disc filter is being evaluated for this application for the proposed TRU hot cell solvent extraction facility.

The filtering efficiencies (amount and size of particles removed) and filtration rates of the etched-disc filter were compared with a 0.1- μm Millipore filter that was used to clarify dissolver solutions from irradiated reactor fuels. These filters will adequately clarify the dissolver solutions, but have unacceptably low filtration rates.

The etched-disc filter element is made up of thin (~ 0.003 in. thick) circular discs chemically etched on one surface to produce a pore size identical to the pore-size rating. Hundreds of identical discs are stacked together and compressed to ensure flow through etched pores only. The filter unit used in these tests was in the form of a cylinder 3.5 cm OD x 14 cm long with an outside surface area of about 154 cm^2 . Construction material is type 316 stainless steel. The Millipore filters were in the form of a circular disc (9.5 cm^2) identified as type VC with a 0.1- μm pore-size rating.

Test procedure. Initially the filtration rates of both the etched-disc filter element and a Millipore filter were measured using demineralized water. Then a series of filtration tests using a synthetic waste solution that contained an unknown amount of small size particles (estimated at

$\sim 1 \mu\text{m}$) was carried out. During each test the differential pressure across the filter was held constant (5 in. of Hg for the etched-disc filter and 20 in. of Hg for the Millipore filters). The weight of the material collected was determined by weighing the filters before and after each test (dry), and the filtration rate was determined by volume-time measurements.

In tests with the Millipore filters, a new filter was used for each test; the etched-disc filter was cleaned by back-flashing before reuse. Only 100 cm^3 of solution was used in all Millipore filter tests because of the small filter area and plugging, but about 7 liters of solution was used in the etched-disc filter tests.

The particulates collected on the filters in all tests were retained and are being examined for size and composition by scanning electron microscopy.

Results. Test results are summarized in Table 4.7. For the initial tests with synthetic waste solution, no plugging of either the etched-disc or Millipore filter was observed, and the filtration rates were similar to those with demineralized water. The etched-disc filter removed 0.676 g of solids from 6.85 liters of solution ($0.010 \text{ g}/100 \text{ cm}^3$); 0.016 g of solids were removed from 100 cm^3 of solution by the Millipore filter (test 4). When 100 cm^3 of the filtrate from the etched-disc filter was refiltered through a Millipore filter, the amount of precipitate collected was more than that from the original solution, and filter plugging occurred. For test 6, part of the filtrate from the etched-disc filter (3.95 liters) was refiltered through the etched-disc filter. No additional precipitate was collected.

Table 4.7. Filtration of synthetic feed solution with a 1- μm , pore-size, etched-disc filter^a and a 0.1- μm Millipore^b filter

Test	Material filtered	Filter element	Wt. of ppt removed (g/100 cm ³)	Filtration rate (cm ³ /min)	Differential pressure (in. of Hg)
1	Demineralized water	A ^a	0.00	240	5
2	Demineralized water	B ^b	0.00	20	20
3	Synthetic feed	A ^a	0.010	200	5
4	Synthetic feed	B ^b	0.016	24	20
5	Filtrate from (3)	B	0.023	6 0.5	20
6	Filtrate from (3)	A	0.00	190	5
7	Filtrate from (6)	B	0.012	6 1	20
8	Filtrate from (7)	B	0.004	15	20

^a1- μm , pore-size, etched-disc filter; 154 cm² surface area. Vacco Industries, 10350 Vacco Street, South El Monte, Calif.

^b0.1- μm Millipore filter; 9.5 cm² area. Millipore Corp., Bedford, Mass.

4-41

In test 7, 100 cm³ of the filtrate from test 6 (twice filtered through the etched-disc filter) was refiltered through a Millipore filter. Results were similar to test 5 in that the filter plugged. However, the amount of precipitate collected was less than that in test 5 (0.012 vs 0.023 g). In the final test in this series, the filtrate from feed solution that had been filtered through a Millipore filter (test 4) was refiltered through another Millipore filter. A small amount of precipitate (0.004 g) was collected, and no filter plugging was observed.

Discussion. As seen in Table 4.7, the 1- μ m etched-disc filter removed about 60% of the amount of solids from the synthetic waste solution as was removed by the 0.1- μ m Millipore filter. No plugging of either filter was observed during filtration of the original solution. Unexpectedly, the weight of precipitate collected on a 0.1- μ m Millipore filter from the filtrate that resulted from the etched-disc filter was greater than that of the original unfiltered solution. This result was observed in two tests (5 and 7). Also severe plugging of the Millipore filter was observed, whereas no plugging was noted when filtering the initial solution. There is no explanation for this anomaly at present. Examination of the filter cakes on the Millipore filters with the scanning electron microscope is in progress.

The clean water filtration rate is about 5 cm⁻³ min⁻¹ cm⁻² for the etched-disc filter and about 2 cm⁻³ min⁻¹ cm⁻² for the Millipore filter to a differential pressure of 20 in. of Hg. These rates did not change appreciably when filtering the waste solution, but as noted above, the Millipore filter was severely plugged by the filtrate from the etched-disc filter. Results of these tests are somewhat inconclusive in determining

whether a 1- μ m etched-disc filter element is suitable for clarification of the dissolver solutions that will be used in our solvent extraction studies. However, further tests using the etched-disc filter to clarify dissolver solution from reactor fuel elements seem warranted to compare this method with clarification by centrifugation and filtration through Millipore filters.

4.3 Solvent Extraction Flowsheet Test Facility

Staff of the Transuranium Processing Plant (Chemical Technology Division, ORNL)

Funds for the TRU Solvent Extraction Flowsheet Test Facility were approved by ERDA. Work orders for equipment design, equipment fabrication and installation, instrument design, and instrument installation have been issued. Quality control documents are being prepared.

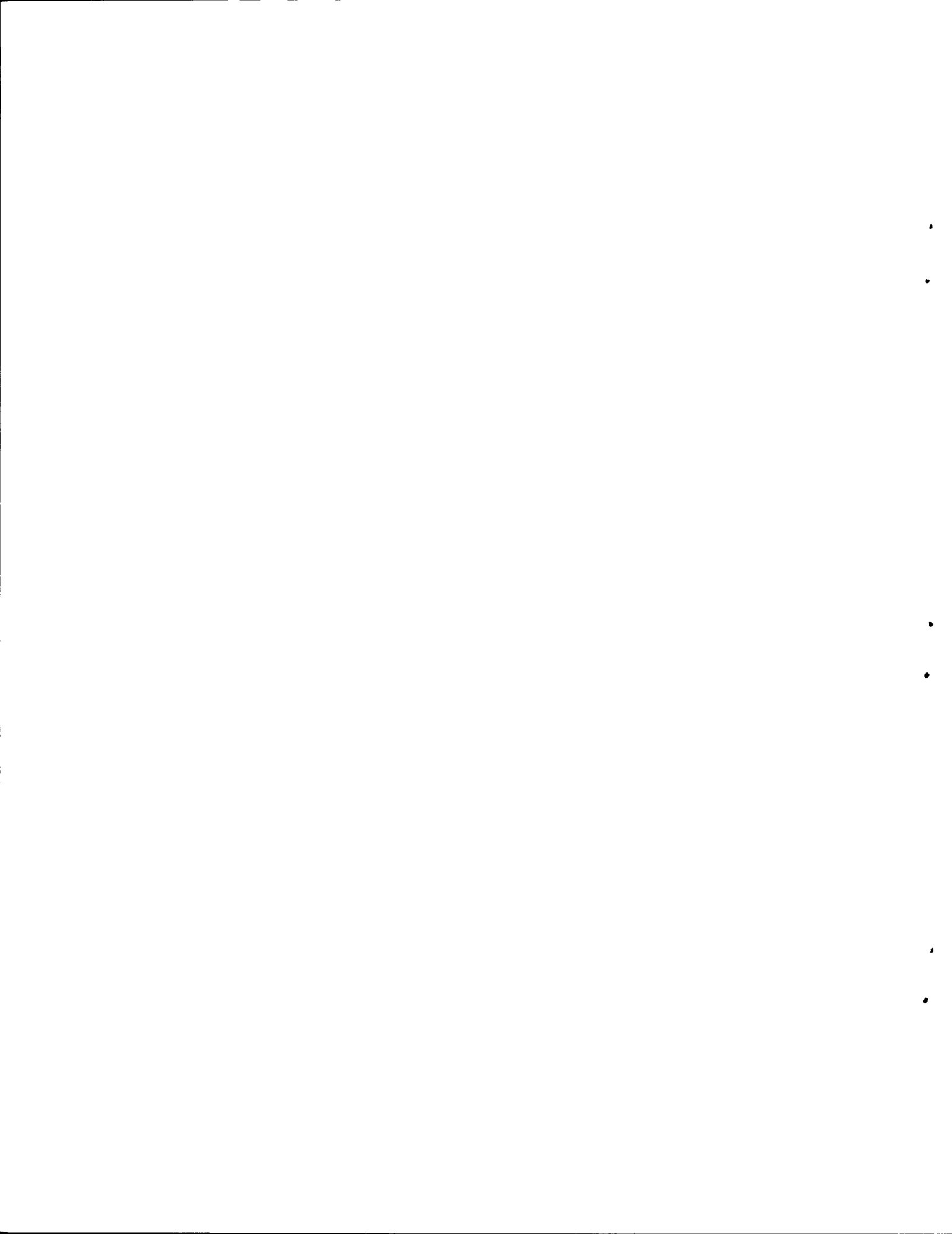
A flowsheet has been approved for tests of the LWR-Purex process, and a flowsheet for fast reactor fuel reprocessing tests is being reviewed. Equipment design is proceeding, based on these flowsheets. Significant portions of the study-and-estimate design are applicable to final design. Thus, design is about 50% complete.

Detailed schedules are being prepared to define manpower requirements and identify critical items.

REFERENCES FOR SECTION 4

1. B. L. Vondra, LWR Fuel Reprocessing and Recycle Program Quarterly Report for Period July 1 to September 30, 1976, ORNL/TM-5660 (November 1976).
2. B. L. Vondra, LWR Fuel Reprocessing and Recycle Program Quarterly Report for Period October 1 to December 31, 1976, ORNL/TM-5760 (February 1977).
3. R. L. Shriner, R. C. Fuson, and D. Y. Curtin, The Systematic Identification of Organic Compounds, Wiley, New York, June 1965, p. 178.
4. Sadtler Research Laboratories, Sadtler Standard Spectra, v. 24, Infrared Spectra 24046 and 24047, Philadelphia, 1964.
5. W. W. Schulz, Macroreticular Anion Exchange Resin Cleanup of TBP Solvents, ARH-SA-129 (May 15, 1972).
6. A. Fontaine and D. Berger, L'Application des Proprietes Chimiques du Ruthenium a des Procedes de Decontamination, Report CEA-R2842 (1965).
7. A. B. Cox and R. M. Wallace, Inorg. Nucl. Chem. Lett. 7: 1191 (1971).
8. L. Maya, LWR Fuel Reprocessing and Recycle Program Quarterly Report for Period January 1 to March 31, 1977, ORNL/TM-5864 (May 1977), pp. 4-18.
9. J. S. Anderson and J. D. M. McConnell, J. Inorg. Nucl. Chem. 1: 371 (1955).
10. P. Wehner and J. C. Hindman, J. Phys. Chem. 56: 10 (1952).
11. P. G. M. Brown, J. Inorg. Nucl. Chem. 13: 73 (1960).
12. K. Joon et al., Highly TBP-Extractable Dimeric and TBP Compounds in the Nitrate and Nitro Series of Aquo-RuNO, KR-143 (1971).

13. B. L. Vondra, LWR Fuel Reprocessing and Recycle Program Quarterly Report for Period January 1 to March 31, 1977, ORNL/TM-5864 (May 1977), pp. 4-23.
14. F. R. Bruce, J. M. Fletcher, and H. H. Hyman, "Progress in Nuclear Energy (Process Chemistry)," Proceedings of the Second International Conference on the Peaceful Uses of Atomic Energy, Geneva, 1958, vol. 3, Pergamon, New York (1961), p. 190.
15. T. H. Siddall III, Behavior of Technetium in the Purex Process, DP-364 (April 1959).
16. B. L. Vondra, LWR Fuel Reprocessing and Recycle Program Quarterly Report for Period April 1 to June 30, 1976, ORNL/TM-5864 (May 1977).
17. J. T. Long, Engineering for Nuclear Fuel Reprocessing, Gordon and Breach Science Publishers, Inc., N. Y (1967), p. 593.



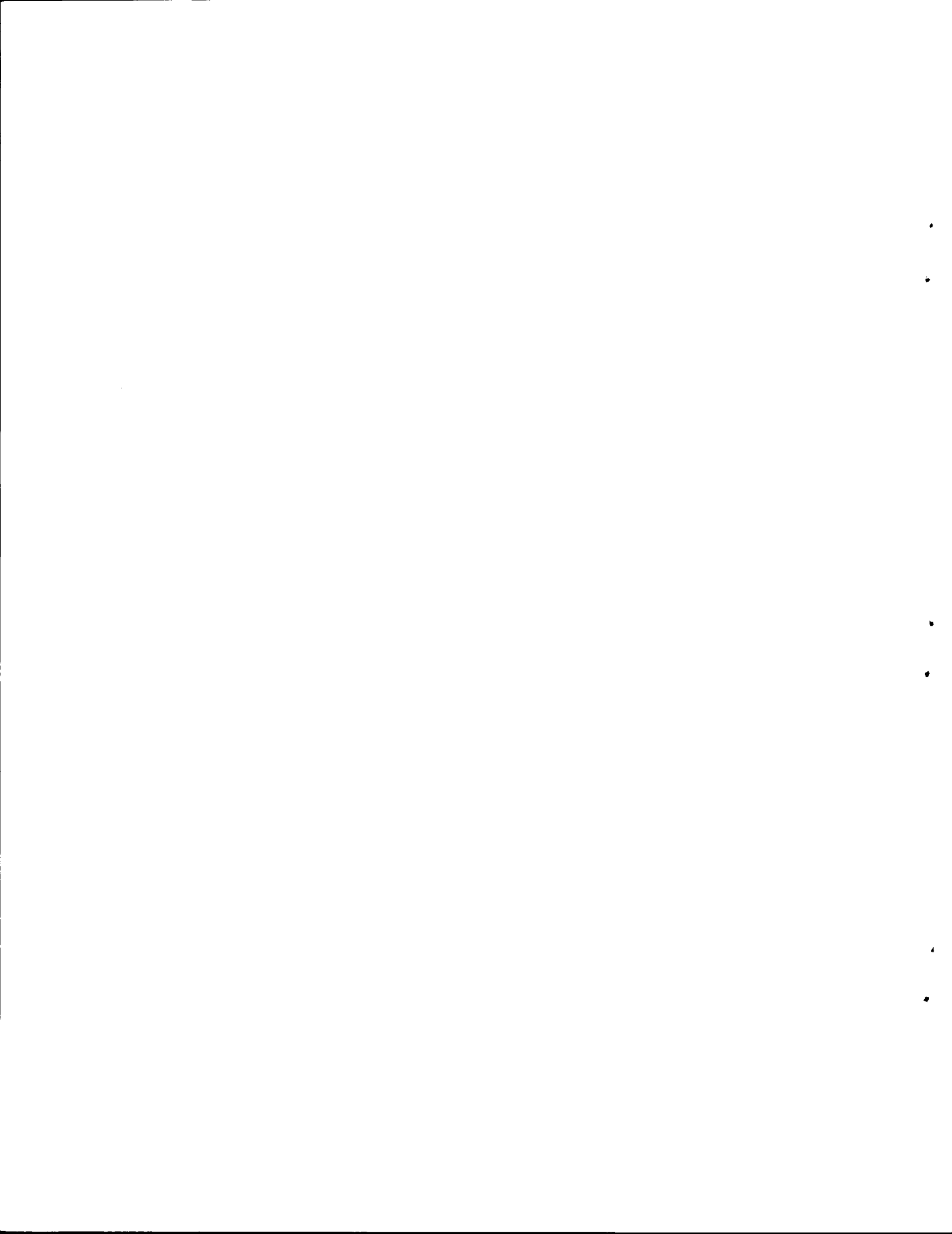
5. URANIUM HEXAFLUORIDE CONVERSION

J. H. Pashley, C. P. McGinnis, and C. C. Littlefield (ORGDP)

A review of process flowsheets was continued, and a flowsheet description was written. A preliminary evaluation of the advantages and problems of the flowsheets was included. Material balance and equipment sizing calculations were continued.

In company with DuPont-Savannah River and Wilmington personnel, the Portsmouth Gaseous Diffusion Plant (operated by Goodyear Atomic Corporation) uranium recovery facility, the Fernald (National Lead) uranium refinery, and the Paducah (UCC-ND) UF_6 production feed plants were visited.

A preliminary series of tests has been made with a magnesium fluoride trap for technetium removal. Data are now being analyzed.



6. RADIOLOGICAL TECHNIQUES FOR ENVIRONMENTAL IMPACT
ASSESSMENTS OF THE LWR FUEL CYCLE

D. C. Kocher (Health and Safety Research Division, ORNL)

Modification of the computer code for calculating the effects of building structures on internal dose from inhaled radionuclides and external photon dose from airborne and surface-deposited radionuclides^{1,2} was conducted and completed. The modification facilitates calculation of dose reduction factors for a large number of radionuclides and for independent variations of the many model input parameters. The modification also provides a more compact summary output of results. A computer listing of dose reduction factors for a wide range of input parameter values for the 40 radionuclides identified as effluents from a fuel reprocessing plant was prepared and transmitted to the Savannah River Laboratory.

The laboratory technical review of the draft manuscript on the building shielding effects model³ was completed, and the final manuscript was prepared and submitted for publication. In addition, a short paper describing the model was submitted to the 1977 Winter Meeting of the American Nuclear Society to be held in San Francisco on November 27 through December 2, 1977.

We have obtained updated dose-rate conversion factors for external exposure to electron and photon radiation from infinite, uniformly distributed sources in air, water, and on a smooth ground surface. A dose-rate conversion factor is defined as the dose rate in millirems per hour resulting from constant exposure to a radionuclide density of 1 $\mu\text{Ci}/\text{cm}^3$ in air and water or 1 $\mu\text{Ci}/\text{cm}^2$ on the ground. The dose-rate

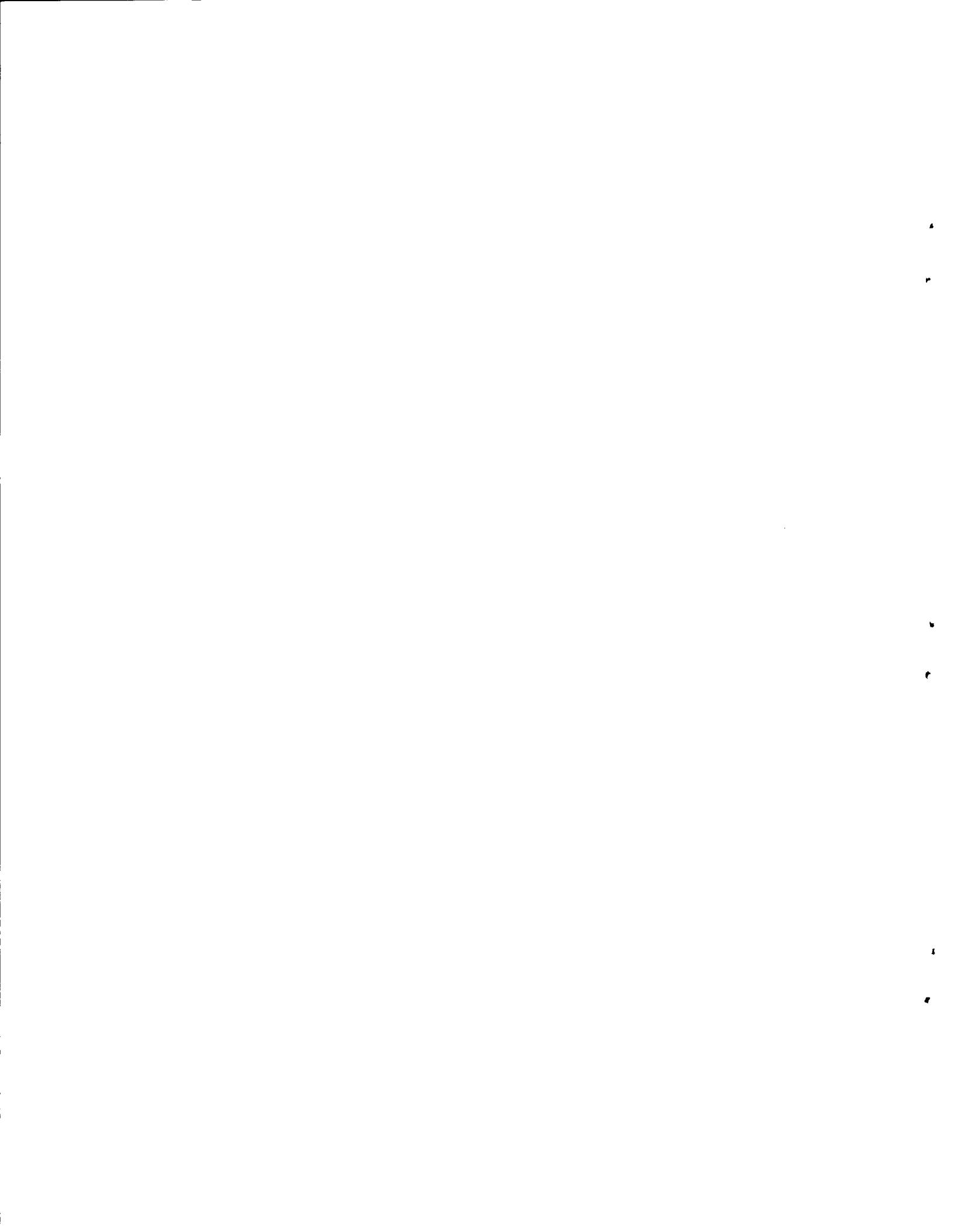
conversion factors for each of the two radiation types and the three exposure pathways are calculated using Eqs. (3-3) through (3-8) of Ref. 4.

A computer listing of the dose-rate conversion factors for the 40 radionuclides from a fuel reprocessing plant was prepared and transmitted to the Savannah River Laboratory. For each radionuclide the energies and intensities of the electron (β^- , β^+ , internal conversion, and Auger) and photon (γ and X ray) radiations were obtained from a recent evaluation of radioactive decay data.⁵ For some radionuclides, the dose-rate conversion factors differ significantly from values obtained previously.⁴ These differences result either from significant changes in the adopted values for the energies and intensities of the various radiations or from the more exact method employed to calculate the average energy for continuous β^- and β^+ radiations.

REFERENCES FOR SECTION 6

1. D. C. Kocher and R. E. Moore, LWR Fuel Reprocessing and Recycle Program Quarterly Report for Period July 1 to September 30, 1976, ORNL/TM-5660 (November 1976).
2. D. C. Kocher, LWR Fuel Reprocessing and Recycle Program Quarterly Report for Period October 1 to December 31, 1976, ORNL/TM-5760 (February 1977).
3. D. C. Kocher, "Effects of Building Structures on Radiation Doses from Routine Releases of Radionuclides to the Atmosphere," to be submitted to Health Physics.

4. G. G. Killough and L. R. McKay, A Methodology for Calculating Radiation Doses From Radioactivity Released to the Environment, ORNL-4992 (March 1976).
5. D. C. Kocher, Nuclear Decay Data for Radionuclides Occurring in Routine Releases From Nuclear Fuel Cycle Facilities, ORNL/NUREG/TM-102, to be published.



7. CO₂ REMOVAL FROM SIMULATED LWR FUEL REPROCESSING OFF-GAS
D. W. Holladay and G. L. Haag (Chemical Technology Division, ORNL)

7.1 Introduction

The primary processes for achieving decontamination factors (DF's) of 10² to 10³ for CO₂ removal from simulated LWR fuel reprocessing off-gases with CO₂ concentration in the 300-ppm range continue to consist of the utilization of agitated gas-slaked lime slurry contactors and 13X molecular sieve beds. As a secondary approach to CO₂ removal, Ba(OH)₂·8H₂O is being studied in both a 27.3-cm-ID, gas-slurry contactor and in gas-solid packed and fluidized beds. While all experimental equipment appears to be functioning as logic dictates, the most vexing experimental problems for all experimental processes (sieves, gas-slurry contactors, gas-solid beds) continue to arise from efforts to accurately determine CO₂ effluent stream concentrations below 10 ppm.

7.2 Studies with 1068 ppm CO₂ Feed

Because the mass transfer driving forces were most likely to be of the same order of magnitude for feeds containing 1068 ppm and 300 ppm CO₂, experiments were conducted with a 1068 ppm CO₂ (balance as N₂) feed in the 1.57 cm x 180 cm molecular sieve column* and in the 27.3-cm-ID agitated contactor. Furthermore, as the lower limit of detectability with then-available infrared (IR) and gas chromatographic (GC) equipment was 10 ppm, a feed of 1068 ppm CO₂ allowed for the determination of DF's of at least 100 with an acceptable degree of accuracy. For gas flow rates of the

*All gas feeds to the molecular sieve columns were bone dry.

1068 ppm CO₂ feed up to 10 standard liters per minute (slm) (retention time of 0.6 sec), DF's >100 were found for the molecular sieve bed. For flow rates of the 1068 ppm CO₂ feed up to 5 slm, DF's >100 were measured for the 27.3-cm-ID contactor (slurry volume 16 liters and agitation speed of 650 rpm).

7.3 CO₂ Removal from Air with the 27.3-cm-ID Contactor

In the 27.3-cm-ID contactor, DF's for removal of CO₂ from air were measured with IR and GC analysis for flow rates from 5 to 22 slm. In all tests the CO₂ concentration in the effluent was below the limit of detection (Table 7.1). More sensitive instrumentation is now being utilized to determine the actual DF's for the contactor.

7.4 Molecular Sieve Studies

In the 1.57 cm x 180 cm 13X molecular sieve column, DF's, dynamic loading capacity, and regeneration characteristics are under investigation. Dynamic loading capacities in the range of 0.5-1.0 g CO₂ per 100 g sieve (temperature = 5 to 10°C) have been obtained for flow rates of 5 slm. Preliminary indications are that the loading capacity (for >90% removal of 300 ppm CO₂) decreases for successive loadings of the regenerated molecular sieves. However, this reduction in loading capacity most likely will be very dependent on the method of regeneration of the molecular sieve beds. Present regeneration is accomplished by applying both heat at 300°C and vacuum to the loaded sieves. There are indications in the literature that regeneration at higher temperatures (>400°C) will prolong the operating life of sieve beds.

For the range of operating conditions we are studying for the 1.57-cm-ID sieve column, and particularly for the superficial velocities, Linde will guarantee a DF of 300 for 13X sieves (personal communication, Dan Kaminsky, South Plainfield, N.J.). For retention times as low as 1.5 sec (based on intersieve particle voids) in the 1.57-cm-ID bed, we have measured DF's in the range of 400 to 800 utilizing liquid scintillation counting of $^{14}\text{CO}_2$ sorbed quantitatively in ethanolamine-ethylene glycol monomethyl ether solvents.

7.5 CO_2 Sorption with Solid $\text{Ba}(\text{OH})_2 \cdot 8\text{H}_2\text{O}$

Due to promising results obtained in reacting CO_2 with $\text{Ba}(\text{OH})_2 \cdot 8\text{H}_2\text{O}$ both as a slurry and as a solid in packed or fluidized beds, inquiries were made to various commercial vendors to determine if a bulk form of $\text{Ba}(\text{OH})_2$ was available that was lower-priced than reagent grade $\text{Ba}(\text{OH})_2$ but was of sufficient purity to produce DF's and conversions similar to the reagent grade material. It was determined from Barium and Chemicals, Inc., of Steubenville, Ohio, that $\text{Ba}(\text{OH})_2 \cdot 8\text{H}_2\text{O}$ at greater than 90% purity could be purchased in truckload quantities for about \$0.50/lb (reagent grade $\text{Ba}(\text{OH})_2 \cdot 8\text{H}_2\text{O}$ is approximately \$3.40/lb). A 100-lb sample of the bulk material has been obtained and will be tested for the DF that can be achieved for CO_2 removal from air.

DF's of the order of 100 have been obtained for CO_2 removal from air in 5.08-cm-ID and 10-cm-long packed columns and in tapered gas-solid fluidized beds (tapering from 2.54 cm to 5.08 cm over 30 cm length) containing solid $\text{Ba}(\text{OH})_2 \cdot 8\text{H}_2\text{O}$ (30-50 mesh). When the fluidized bed was operated with the air stream unsaturated with water, an overall conversion

Table 7.1. Removal of CO₂ from air in the 27.3-cm-ID stirred tank contactor-detection by gas chromatography

Air flow rate, Q_A (slm) ^a	CO ₂ molar flow rate, F_{cd} (g moles/min)	Influent air pressure, P_{in} (psia)	Effluent CO ₂ concentration, Y_{cd} (ppm)	Decontamination factor (DF)	Agitation speed, N_{AG} (rpm)
5.33 ^b	6.7×10^{-5}	15.7	<10 (0.001%)	>30	650
10.45	1.3×10^{-4}	16.2	<10	>30	650
16.36	2.0×10^{-4}	16.7	<10	>30	650
21.67	2.7×10^{-4}	17.2	<10	~30	650

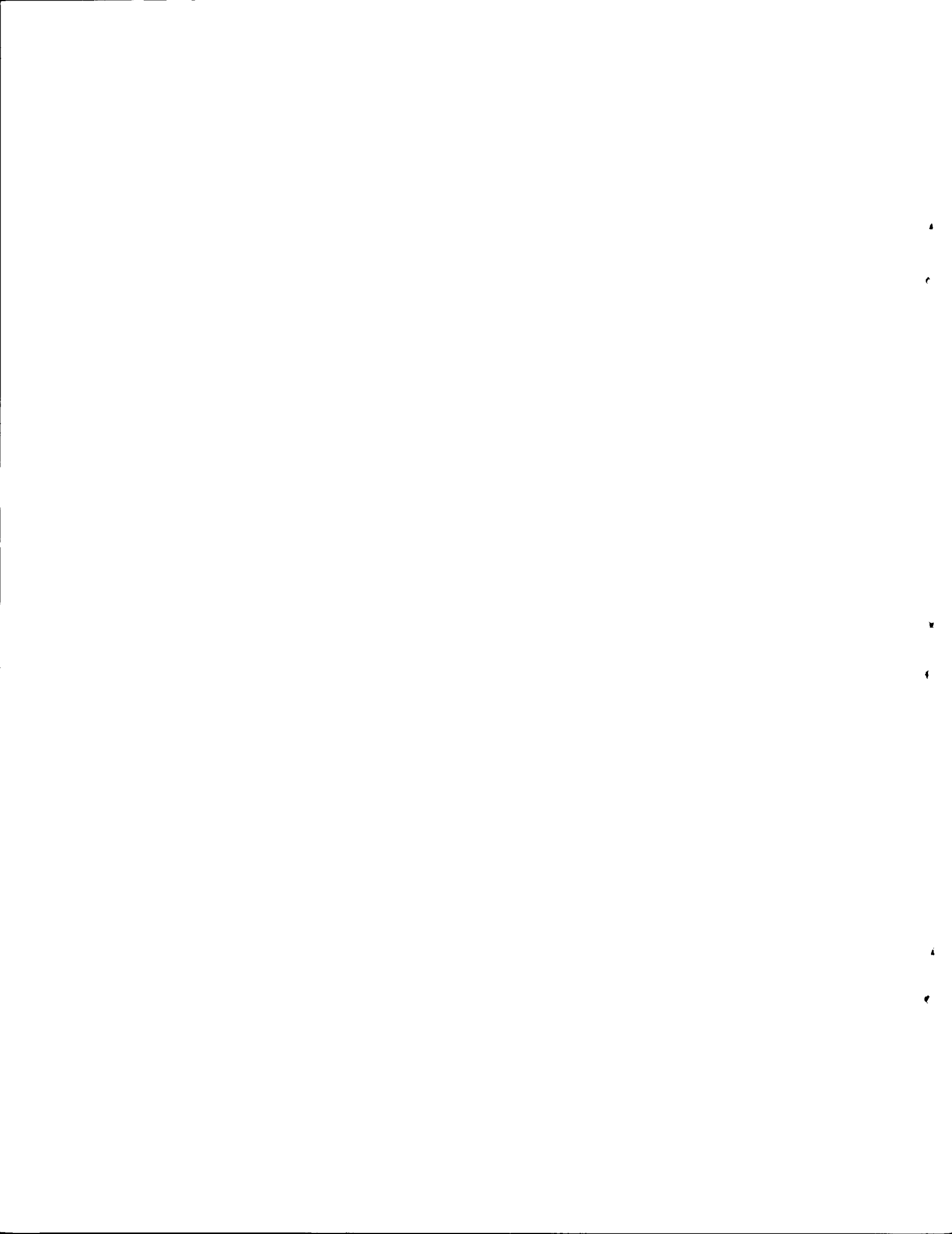
^aStandard temperature and pressure were 21°C and 1 atm respectively.

^bAt 5 slm for 1068 ppm CO₂ feed, DF >100.

of 50% of $\text{Ba}(\text{OH})_2 \cdot 8\text{H}_2\text{O}$ was obtained. Operation of the fluidized bed with a water-saturated air stream resulted in a bed conversion of at least 70%. Contacting was terminated when the effluent CO_2 level exceeded 10 ppm. The highest bed conversion for a solid column was 25% $\text{Ba}(\text{OH})_2 \cdot 8\text{H}_2\text{O}$ depletion.

7.6 Analytical

The development of accurate and reproducible analytical techniques continues to require a large share of laboratory time. The beta-cell radiotracer detector has not shown the sensitivity adequate to determine DF's of 10^2 to 10^3 when the feed level of radiotracer is restricted to 10 mCi, as in our laboratory. The determination of $^{14}\text{CO}_2$ by sorption into organic solutions and then counting of beta emissions in a liquid scintillation system has been successfully used for the determination of DF's up to 10^3 in the $\text{Ba}(\text{OH})_2 \cdot 8\text{H}_2\text{O}$ and molecular sieve beds; however, there is enough uncertainty in the method that an alternate corroborating analytical technique is desirable. Two analytical techniques that have been reported in the literature to be capable of determining CO_2 in the 1.0-ppm range are (1) improved infrared spectroscopy and (2) flame ionization detection of CO_2 after reduction to CH_4 . Instrumentation is available in the Chemical Technology Division that will allow evaluation of the above two analytical techniques in providing CO_2 detection in the 0.1 to 1.0 ppm CO_2 range.

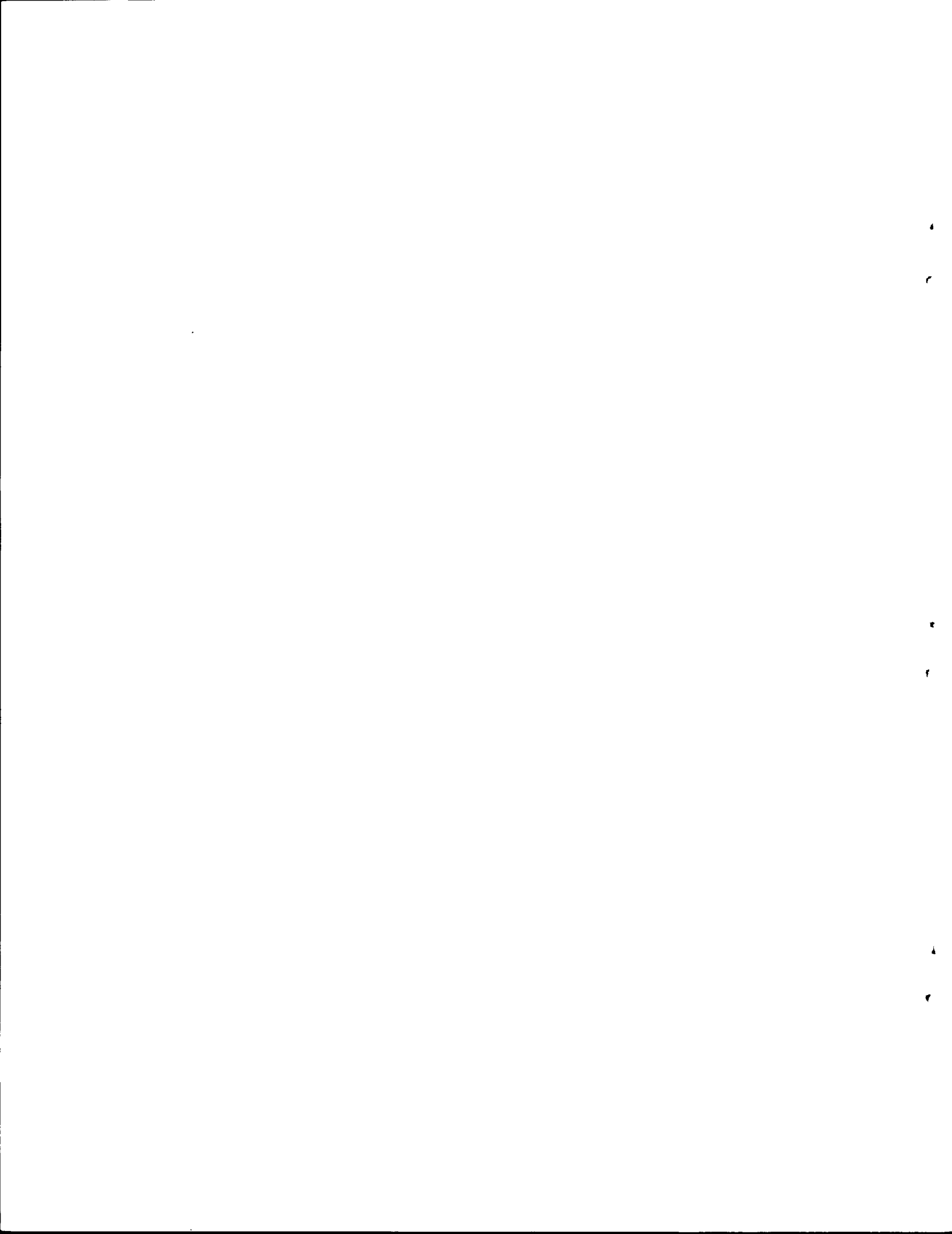


8. LWR SUPPORT/STANDARD DATA INTERCHANGE FORMATS

A. A. Brooks (Computer Sciences Division, ORNL)

The following tasks have been carried out during this period:

1. Control Data Corporation (CDC) software for a level 1 system has been made available for Pacific Northwest Laboratory, Lawrence Livermore Laboratory, Brookhaven National Laboratory (BNL), and Los Alamos Scientific Laboratory (LASL) in both the NOS and SCOPE 34 operating systems and is operational at BNL and LASL.
2. IBM software for a level 1 system has been made available to Argonne National Laboratory, Savannah River Laboratory, and ORNL and is operational at ORNL. The routines have been compiled at SRL.
3. Draft documentation for the CDC software is being adapted for joint CDC/IBM software documentation. Interim operating IBM software instructions have been issued.



INTERNAL DISTRIBUTION

1. S. I. Auerbach
2. J. T. Bell
3. Myer Bender
4. M. R. Bennett
5. J. E. Bigelow
6. R. E. Blanco
7. J. O. Blomeke
8. W. D. Bond
9. B. F. Bottenfield
10. J. T. Bradbury, ORGDP
11. R. E. Brooksbank
- 12-16. W. D. Burch
17. S. R. Buxton
18. D. O. Campbell
19. J. M. Chandler
20. W. E. Clark
21. L. T. Corbin
22. D. A. Costanzo
23. D. J. Crouse
24. F. L. Culler
25. R. G. Donnelly
26. M. J. Feldman
27. D. E. Ferguson
28. L. M. Ferris
29. R. B. Fitts
30. E. L. Gaden, Jr. (Consultant)
31. E. H. Gift, ORGDP
32. J. H. Goode
33. N. R. Grant
34. W. S. Groenier
35. W. R. Hamel
36. D. C. Hampson
37. F. E. Harrington
38. G. S. Hill
39. D. W. Holladay
40. D. E. Horner
41. A. R. Irvine
42. S. V. Kaye
43. A. D. Kelmers
44. L. J. King
45. D. C. Kocher
46. C. E. Lamb
47. R. E. Leuze
48. M. H. Lloyd
49. R. A. Lorenz
50. J. C. Mailen
51. A. P. Malinauskas
52. D. L. Manning
53. Leon Maya
54. W. J. McDowell
55. J. D. McGaugh, ORGDP
56. A. D. Mitchell
57. R. E. Moore
58. J. M. Morrison
59. E. L. Nicholson
60. K. J. Notz
61. A. R. Olsen
62. J. H. Pashley, ORGDP
63. F. L. Peishel
64. Herman Postma
65. R. H. Rainey
66. R. B. Richards (Consultant)
67. C. R. Richmond
68. A. D. Ryon
69. H. C. Savage
70. A. C. Schaffhauser
71. C. D. Scott
72. B. B. Spencer
73. R. G. Stacy
74. M. J. Stephenson, ORGDP
75. W. G. Stockdale
76. O. K. Tallent
77. L. M. Toth
78. H. E. Trammell, ORGDP
79. D. B. Trauger
80. W. E. Unger
81. V. C. A. Vaughen
- 82-96. B. L. Vondra
97. C. D. Watson
98. J. R. Weir, Jr.
99. T. D. Welch
100. M. E. Whatley
101. R. G. Wymer
102. O. O. Yarbro
103. Central Research Library
104. ORNL - Y-12 Technical Library
Document Reference Section
- 105-106. Laboratory Records
107. Laboratory Records, ORNL R. C.
108. ORNL Patent Office
109. Nuclear Safety Information
Center

EXTERNAL DISTRIBUTION

110. R. C. Adkins, Technical Representative, NUSAC, 777 Leesburg Pike, Falls Church, VA 22043
111. Aerojet Nuclear Company, 550 2nd Street, Idaho Falls, ID 83401
112. H. M. Agnew, Director, Los Alamos Scientific Laboratory, P. O. Box 1663, Los Alamos, NM 87545
113. T. W. Ambrose, Director, Pacific Northwest Laboratory, P. O. Box 999, Richland, WA 99352
114. C. K. Anderson, Combustion Engineering Nuclear Power Division, 1000 Prospect Hill Road, Windsor, CT 06095
115. F. H. Anderson, General Manager, Allied Chemical Corporation, 550 Second Street, Idaho Falls, ID 83401
116. Argonne National Laboratory, P. O. Box 2528, Idaho Falls, ID 83401
117. Argonne National Laboratory, 9700 South Cass Avenue, Argonne, IL 60439
118. J. F. Bader, Manager, Plutonium Recycle Fuel Programs, Westinghouse Electric Corporation, Box 355, Pittsburgh, PA 15230
119. R. G. Barnes, Manager, Technical Development, Advance Engineering, General Electric Company, 175 Curtner Avenue, San Jose, CA 95125
120. Battelle-Columbus Laboratories, 505 King Avenue, Columbus, OH 43201
121. R. C. Baxter, President, Allied-General Nuclear Services, P. O. Box 847, Barnwell, SC 29812
122. R. M. Bernero, Chief, Fuel Reprocessing and Recycle Branch, Division of Fuel Cycle and Material Safety, United States Nuclear Regulatory Commission, Washington, DC 20555
123. M. Binstock, Kerr-McGee Nuclear Corporation, Kerr-McGee Building, Oklahoma City, OK 73102
124. K. Bowlman, General Electric Company, 175 Curtner Avenue, San Jose, CA 95125
125. R. G. Bradley, Division of Waste Management, Production and Reprocessing, U. S. Energy Research and Development Administration, Washington, DC 20545
126. M. G. Britton, Manager Technical Liaison, Corning Glass Works, Corning, NY 14830
127. J. Carp, Director for Energy Policy, Edison Electric, 90 Park Avenue, New York, NY 10016
128. W. T. Cave, Director, Monsanto Research Corporation, Mound Laboratory, P. O. Box 32, Miamisburg, OH 45332
129. B. H. Cherry, Manager of Fuel Resources, GPU Services Corporation, 260 Cherry Hill Road, Parisippany, NH 07054
130. R. B. Chitwood, Chief, Industrial Programs Branch, Division of Waste Management, Production, and Reprocessing, U. S. Energy Research and Development Administration, Washington, DC 20545
131. G. R. Corey, Vice Chairman, Commonwealth Edison Company, P. O. Box 767, Chicago, IL 60690
- 132-133. J. L. Crandall, Director, Nuclear Engineering & Materials Section, E. I. du Pont de Nemours & Company, Savannah River Laboratory, Aiken, SC 29801
134. R. G. Cross, DBM Corporation, 1920 Alpine Avenue, Vienna, VA 22180

135. G. W. Cunningham, Director, Division of Waste Management, Production and Reprocessing, U. S. Energy Research and Development Administration, Washington, DC 20545
136. R. Cunningham, Nuclear Materials Safety and Safeguards, Nuclear Regulatory Commission, Washington, DC 20545
137. R. L. Dickeman, President, Exxon Nuclear Company, Inc., 777 - 106th Avenue, NE, Bellevue, WA 98004
138. Electric Power Research Institute, P. O. Box 10055, Palo Alto, CA 94303
139. R. Fullwood, Science Applications, Inc., 2680 Hanover Street, Palo Alto, CA 94303
140. R. L. Grant, Director of Nuclear Projects, Boeing Engineering and Construction Division, P. O. Box 3707, Seattle, WA 98124
- 141-142. H. J. Groh, Jr., Director, Environmental Sciences Section, E. I. du Pont de Nemours & Company, Savannah River Laboratory, Aiken, SC 29801
143. Hanford Engineering Development Laboratory, Associate Lab Director, P. O. Box 1970, Richland, WA 99352
144. T. B. Hindman, Jr., Director, Fuel Cycle Project Office, U. S. Energy Research and Development Administration, Savannah River Operations Office, P. O. Box A, Aiken, SC 29801
145. A. H. Hines, Jr., President, Florida Power Corporation, P. O. Box 14042, St. Petersburg, FL 33733
146. C. A. Hirenda, Director of Marketing, Proposal Management, Inc., 121 N. Orionna Street, Philadelphia, PA 19106
147. P. Hogroian, Division of Waste Management, Production and Reprocessing, U. S. Energy Research and Development Administration, Washington, DC 20545
148. R. Hoskins, Tennessee Valley Authority, 217 Electric Power Board Building, Chattanooga, TN 37401
149. M. L. Hyder, Separations Chemistry & Engineering Section, E. I. du Pont de Nemours & Company, Savannah River Laboratory, Aiken, SC 29801
150. R. H. Ihde, Manager, Contracts and Marketing, Babcock and Wilcox, P. O. Box 1260, Lynchburg, VA 24505
151. A. S. Jennings, Separations Chemistry & Engineering Section, E. I. du Pont de Nemours & Company, Savannah River Laboratory, Aiken, SC 29801
152. W. Johnson, Vice-President, Yankee Atomic Electric Company, 20 Turnpike Road, Westboro, MA 01581
153. W. A. Kalk, Manager, Nuclear Power Systems, Holmes and Narver, Inc., 400 East Orangethorpe Avenue, Anaheim, CA 92801
154. F. J. Kiernan, Eastern Regional Manager, Energy Systems, Aerojet Energy Conversion Company, Suite 1050, 1120 Connecticut Avenue, N. W., Washington, DC 20036
155. K. Killingstad, Cont. Services, Battelle-Human Affairs Research Centers, 4000 N. E. 41st Street, Seattle, WA 98105
156. H. Kouts, Nuclear Regulatory Commission, Washington, DC 20545
157. C. Kuhlman, Division of Waste Management, Production and Reprocessing, U. S. Energy Research and Development Administration, Washington, DC 20545

158. J. A. Kyger, Associate Director, Argonne National Laboratory, 9700 South Cass Avenue, Argonne, IL 60439
159. F. W. Lewis, President, Middle South Utilities, Inc., Box 61005, New Orleans, LA 70161
160. W. H. Lewis, Nuclear Fuel Services, 6000 Executive Blvd., Rockville, MD 20952
161. J. L. Liverman, Division of Biomedical and Environmental Research, U. S. Energy Research and Development Administration, Washington, DC 20545
162. H. E. Lyon, Division of Safeguards and Security, U. S. Energy Research and Development Administration, Washington, DC 20545
163. A. Maimoni, Material Control Group, Lawrence Livermore Laboratory, University of California, P. O. Box 808, Livermore, CA 94550
164. W. H. McVey, Chief, Technology Branch, Division of Waste Management, Production, and Reprocessing, U. S. Energy Research and Development Administration, Washington, DC 20545
165. L. H. Myer, Program Manager, Technical Division, E. I. du Pont de Nemours and Company, Aiken, SC 29801
166. M. I. Naparstek, Manager of Proposals, Burns and Roe, Industrial Services Corporation, P. O. Box 663, Paramus, NJ 07652
167. L. W. Nelms, Chief, Research Branch, Research and Technical Division, Todd Company, P. O. Box 1600, Galveston, TX 77550
168. R. I. Newman, Vice-President, Allied-General Nuclear Services, P. O. Box 847, Barnwell, SC 29812
169. R. D. Oldenkamp, Rockwell International, Atomics International Division, 8900 De Soto Avenue, Canoga Park, CA 91304
170. D. T. Pence, Science Applications, Inc., 1200 Prospect Street, P. O. Box 2351, La Jolla, CA 92038
171. G. B. Pleat, Division of Waste Management, Production, and Reprocessing, U. S. Energy Research and Development Administration, Washington, DC 20545
172. G. K. Rhode, Vice-President-Engineer, Niagara Mohawk Power Corporation, 300 Erie Boulevard, West, Syracuse, NY 13202
173. L. M. Richards, Nuclear Commercial Development Coordinator, Atlantic Richfield Company, Box 2679 - TA, Los Angeles, CA 90071
174. R. W. Roberts, Assistant Administrator for Nuclear Energy, U. S. Energy Research and Development Administration, Washington, DC 20545
175. W. S. Scheib, Jr., Chief, Projects Branch, Division of Waste Management, Production, and Reprocessing, U. S. Energy Research and Development Administration, Washington, DC 20545
176. A. Schneider, Nuclear Engineering Department, Georgia Institute of Technology, Atlanta, GA 30332
177. J. Shefeik, General Atomic Company, P. O. Box 81608, San Diego, CA 92138
178. N. F. Sievering, Jr., Assistant Administrator for International Affairs, U. S. Energy Research and Development Administration, Washington, DC 20545
179. L. E. Smith, Manager-Fuel, Carolina Power and Light Company, P. O. Box 1551, Raleigh, NC 27602
180. D. R. Spurgeon, Acting Assistant Director for Reprocessing, Division of Waste Management, Production, and Reprocessing, U. S. Energy Research and Development Administration, Washington, DC 20545

181. A. Squire, Director, Hanford Engineering Development Laboratory, P. O. Box 1970, Richland, WA 99352
182. C. Stephens, Virginia Electric Power Company, Nuclear Fuel Service Department, 512 Franklin Building, P. O. Box 26666, Richmond, VA 32361
183. N. Stetson, Manager, U. S. Energy Research and Development Administration, Savannah River Operations Office, P. O. Box A, Aiken, SC 29801
184. S. Stoller, Western Reprocessors, The S. M. Stoller Corporation, 1250 Broadway, New York, NY 10001
185. K. Street, Associate Director, Lawrence Radiation Laboratory, P. O. Box 808, Livermore, CA 94550
186. G. Stukenbroeker, NL Industries, P. O. Box 928, Barnwell, SC 29812
187. W. E. Thompson, Technology Assessment Branch, Division of Fuel Cycle and Material Safety, U. S. Nuclear Regulatory Commission, Washington, DC 20555
188. Dr. Uhrig, Florida Power and Light Company, P. O. Box 013100, Miami, FL 33101
189. I. J. Urza, Exxon Nuclear Company, Inc., Oak Ridge National Laboratory, P. O. Box X, Oak Ridge, TN 37830
190. E. J. Wahlquist, Deputy Assistant Director for Terrestrial Programs, U. S. Energy Research and Development Administration, Washington, DC 20545
191. D. S. Webster, Argonne National Laboratory, Building 205, 9700 South Cass Avenue, Argonne, IL 60439
192. A. K. Williams, Director, Nuclear Technology Division, Allied-General Nuclear Services, P. O. Box 847, Barnwell, SC 29812
193. U. S. Energy Research and Development Administration, Chicago Operations Office, Contracts Division, 9800 South Cass Avenue, Argonne, IL 60439
194. U. S. Energy Research and Development Administration, Division of RDD, Energy Systems Analysis, Washington, DC 20545
195. U. S. Energy Research and Development Administration, Division of RDD, Engineering and Technology, Washington, DC 20545
196. U. S. Energy Research and Development Administration, Division of RDD, IMFBR Programs, Washington, DC 20545
197. U. S. Energy Research and Development Administration, Division of RDD, Reactor Safety, Washington, DC 20545
198. U. S. Energy Research and Development Administration, Library, Washington, DC 20545
199. U. S. Energy Research and Development Administration, Research and Technical Support Division, P. O. Box E, Oak Ridge, TN 37830
200. U. S. Energy Research and Development Administration, Oak Ridge Operations Office, Reactor Division, P. O. Box E, Oak Ridge, TN 37830
201. U. S. Energy Research and Development Administration, Patent Office, Washington, DC 20545
202. U. S. Energy Research and Development Administration, Richland Operations Office, P. O. Box 550, Richland, WA 99352
203. U. S. Energy Research and Development Administration, Southern California Energy Program Office, P. O. Box 1446, Canoga Park, CA 91304
204. U. S. Energy Research and Development Administration, Technical Information Center, Oak Ridge, TN 37830

205. U. S. Energy Research and Development Administration, Division of
Reactor Development Demonstration, Washington, DC 20545
206. U. S. Energy Research and Development Administration, Idaho
Operations Office, 550 2nd Street, Idaho Falls, ID 83401
207. U. S. Energy Research and Development Administration, Nevada
Operations Office, P. O. Box 14100, Las Vegas, NV 89114
208. U. S. Energy Research and Development Administration, San Francisco,
Operations Office, 1333 Broadway, Wells Fargo Building, Oakland,
CA 94612